The Effects of α_{2A}-Adrenergic Receptors on Glutamatergic Signaling in the Bed Nucleus of the Stria Terminalis

By

Stephanie A. Flavin

Dissertation

Submitted to the Faculty of the

Graduate School of Vanderbilt University

in partial fulfillment of the requirements

for the degree of

DOCTOR OF PHILOSOPHY

in

Neuroscience

December, 2014

Nashville, TN

Approved:

Sachin Patel, M.D., Ph.D.

Doug McMahon, Ph.D.

Garret Stuber, Ph.D.

Danny G. Winder, Ph.D.

DEDICATION

To Mom and Dad,

Thank you for always being the greatest supporters

of my education and for encouraging me to pursue my dreams.

ACKNOWLEDGEMENTS

I would like to acknowledge the financial support of the National Institute of Drug Abuse award number F30DA034428 that provided financial support for this work. I would also like to thank the Vanderbilt Brain Institute, the Neuroscience Program in Substance Abuse, the Neuroscience Graduate Program, and the Vanderbilt Medical Scientist Training Program for providing educational resources and support throughout my graduate training.

I am grateful for the support of my thesis committee, Dr. Sachin Patel (Chair), Dr. Garret Stuber, Dr. Doug McMahon, and Dr. Danny Winder (mentor) for the guidance and support they provided during the course of this work. I would especially like to thank my mentor Danny Winder for his encouragement and scientific guidance throughout my graduate training. Finally, I would also like to thank my lab mates for creating a supportive, inspiring lab environment during my graduate training.

TABLE OF CONTENTS

LIST OF TABLES

LIST OF FIGURES

LIST OF ABBREVIATIONS

BNST.....Bed Nucleus of the Stria Terminalis

CeA.....Central Nucleus of the Amygdala

AR.....Adrenergic Receptor

NE.....Norepinephrine

ChR2.....Channelrhodopsin

PBN.....Parabrachial Nucleus

BLA.....Basolateral Amygdala

CGRP.....Calcitonin Gene-Related Peptide

PFC.....Prefrontal Cortex

NAc.....Nucleus Accumbens

ACTH.....Adrenocorticotropic hormone

EPSP.....Excitatory Postsynaptic Potential

EPSC.....Excitatory Postsynaptic Current

IPSP.....Inhibitory Postsynaptic Potential

DAB.....Diaminobenzidine

HA.....Hemagluttinin

DREADD.....Designer Receptor Exclusively Activated by Designer Drug

CHAPTER 1

Introduction

The bed nucleus of the stria terminalis (BNST) is a group of inter-connected subnuclei that play critical roles in stress-reward interactions. An interesting feature of this brain region is the massive noradrenergic input that it receives (Phelix et al., 1992; Egli et al., 2005). Important roles for norepinephrine in this region have been documented in a number of stress and reward related behaviors. This work has been paralleled over the last several years by efforts to understand the actions of norepinephrine on neuronal function in the region. In the introduction to this dissertation I will summarize the current state of these research areas.

Norepinephrine (NE) is an often-overlooked neurotransmitter in the field of addiction research, yet over the last decade or so it has become clear that it plays a critical role in key aspects of addiction-related behavior. Extensive evidence supports the role of NE as a mediator of reward in the brain, for a review on this topic see Weinshenker and Schroeder (2007). In particular, NE appears to play a significant role in stress-induced reinstatement of drug-seeking behavior and in negative reinforcement-based behavior. An individual's risk of relapse to drug-seeking remains high even after undergoing addiction treatment (Weiss and Koob, 2001) and exposure to stressful stimuli greatly increases an individual's risk of relapse (Brown et al., 1995; Sinha et al., 1999; Sinha et al., 2011). Recent clinical trials have shown promise for noradrenergic drugs in

attenuating stress-induced drug cravings in humans (Jobes et al., 2011; Sinha et al., 2011; Fox and Sinha, 2014; Fox et al., 2014).

A convergence of animal data indicate that the extended amygdala, which includes structures such as the bed nucleus of the stria terminalis (BNST), the central nucleus of the amygdala (CeA), and the shell of the nucleus accumbens (NAc) (Alheid and Heimer, 1988), is critical in stress-induced reinstatement of drug-seeking behavior (Briand et al., 2010). Not surprisingly, these structures receive some of the densest noradrenergic innervation in the CNS (Brownstein et al., 1974; Phelix et al., 1992; Egli et al., 2005). In particular, the BNST within the extended amygdala is a major site of noradrenergic action in stress-induced reinstatement (Aston-Jones et al., 1999; Shaham et al., 2000; Wang et al., 2001; Leri et al., 2002; Olson et al., 2006). Additionally, there is evidence to suggest that several different types of adrenoreceptors are expressed in the BNST (Rainbow et al., 1984; Scheinin et al., 1994; Day et al., 1997; Shields et al., 2009). Therefore, a better understanding of how NE modulates circuit activity in the extended amygdala may provide insight into the underlying mechanisms of stress-induced relapse of drug- and alcohol-seeking behavior and lead to the identification of new therapies.

This introduction will focus on the mechanisms by which NE regulates signaling within the extended amygdala circuitry, highlighting in particular potential actions that may be of relevance to the addiction field.

The BNST as a nexus for stress-reward interactions

The intrinsic and extrinsic circuitry of the BNST has been extensively studied and is very complex. This dissertation will focus on some of the known extrinsic circuitry of the BNST that is thought to participate in stress and reward behaviors. The complete intrinsic and extrinsic circuitry, however, is beyond the scope of this introduction and the reader is referred to Dong et al. (2001a, 2001b) and Dong and Swanson (2006) for more detailed anatomical discussions.

Current models propose that the BNST is a part of a neuroendocrine striatal-loop (Dong et al., 2001) integrating descending glutamatergic input from prefrontal cortical regions, insular cortex, basolateral amygdala (BLA) and other brain regions with ascending modulatory inputs, such as the parabrachial nucleus (PBN) and then projecting to key midbrain and brainstem homeostatic centers (Weller and Smith, 1982; Shimada et al., 1985; Hurley et al., 1991; McDonald et al., 1999; Chiba et al., 2001; Dong et al., 2001; Shin et al., 2008). For example, the BNST has an inhibitory projection to the paraventricular nucleus (PVN) of the hypothalamus (Cullinan et al., 1993; Herman et al., 1994; Shammah-Lagnado et al., 2000; Choi et al., 2007) that influences the release of ACTH (Herman et al., 1994), which in turn leads to the activation of the hypothalamic stress response (Harris, 1948; Herman et al., 2003). The BNST also projects to the nucleus accumbens (NAc) (Dong et al., 2001) and has excitatory and inhibitory projections to the ventral tegmental area (VTA) (Georges and Aston-Jones, 2001, 2002; Dumont and Williams, 2004; Kudo et al., 2012; Jennings et al., 2013; Kudo et al., 2014). Each of these regions has been

implicated in reinstatement/relapse related behaviors. Thus, it is not surprising that the extended amygdala plays a key role in the integration of stress and reward. A basic, illustrated diagram of this circuitry is shown in Figure 1.

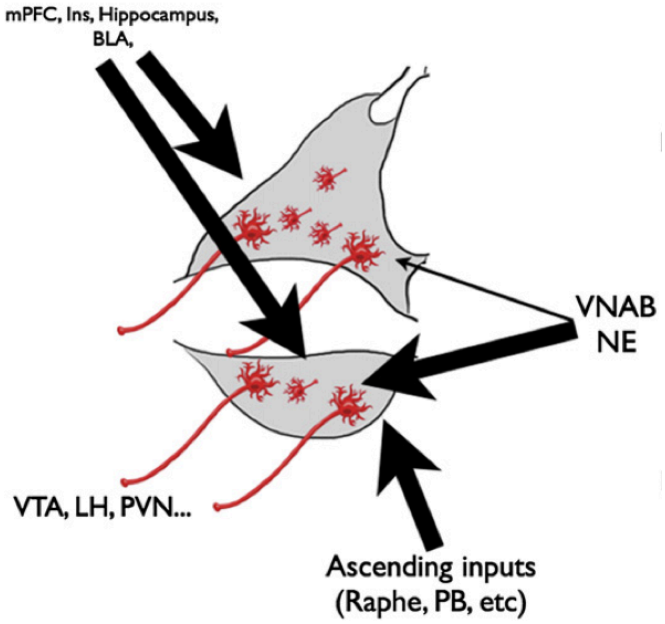

Figure 1. Illustrated diagram of basic extrinsic BNST circuitry. General schematic of the BNST surrounding the anterior commissure, illustrating top-down excitatory input from regions such as the medial prefrontal cortex (mPFC), insular (Ins), hippocampus and basolateral amygdala (BLA). The region integrates this input with ascending inputs from a variety of sources, including the noradrenergic (NE) input from through the ventral noradrenergic bundle (VNAB).

Norepinephrine

The BNST receives very dense noradrenergic innervation through the ventral noradrenergic bundle (VNAB) from the A1 and A2 cell groups in the nucleus of the solitary tract (NTS) (Ricardo and Koh, 1978; Woulfe et al., 1988; Forray and Gysling, 2004; Banihashemi and Rinaman, 2006). The ventral BNST

(vBNST) and the dorsal BNST (dBNST) both receive noradrenergic input (Brownstein et al., 1974; Phelix et al., 1992; Egli et al., 2005). Using microdialysis, extracellular NE has been shown to be elevated in the extended amygdala during both stress and withdrawal (Pacak et al., 1995; Delfs et al., 2000; Cecchi et al., 2002b; Cecchi et al., 2002a). More recently, fast-scan cyclic voltammetry approaches have demonstrated that VNAB stimulation produces elevation of NE in both vBNST and dorsomedial BNST (Park et al., 2009), and that NE levels rapidly rise and fall in the region in response to an aversive tastant (Park et al., 2012).

The Role of Norepinephrine in the Extended Amygdala in Stress-Induced Reinstatement

NE plays a key role in reinstatement of reward seeking (Pacak et al., 1995; Cecchi et al., 2002b; Cecchi et al., 2002a; Ma and Morilak, 2005). Intracerebroventricular (ICV) injection of NE reinstates cocaine-seeking behavior (Brown et al., 2011), and neurons in the BNST and noradrenergic inputs to the BNST are show increased activity during withdrawal from drugs of abuse (Aston-Jones et al., 1999; Delfs et al., 2000), leading to increased levels of NE (Aston-Jones et al., 1999; Delfs et al., 2000; Fuentealba et al., 2000).

The release of NE during times of stress and withdrawal has been shown to impact behavior. Note here that withdrawal refers to the prolonged cessation of chronic drug/alcohol exposure, often accompanied by heightened anxiety responses and other physiologic responses that could drive subsequent negative-reinforcement-based behavior. Rodent behavioral models implicate NE

signaling in the aversive symptoms of withdrawal, as measured by conditioned place aversion and quantification of physiological somatic signs of withdrawal (Aston-Jones et al., 1999; Delfs et al., 2000; Shaham et al., 2000; Wang et al., 2001), as well as in behavioral responses to stressors (Cecchi et al., 2002b; Cecchi et al., 2002a). Mice lacking dopamine-β-hydroxylase (DBH), an enzyme required for NE synthesis, do not demonstrate morphine-induced conditioned place preference (CPP) (Olson et al., 2006). Viral restoration of DBH to the NTS, but not the locus coeruleus (LC), rescues the morphine-induced CPP behavior (Olson et al., 2006). Lesioning of the VNAB blocks stress-induced reinstatement of morphine-seeking (Wang et al., 2001). These studies show an important role for NE from the NTS in stress-induced reinstatement. Subsequent work has focused on the role of particular noradrenergic receptors in stress-induced reinstatement.

Multiple Noradrenergic Receptors Modulate Neuronal Signaling

There are nine different adrenergic receptors (ARs) (Bylund et al., 1994) divided into three major classes: α_1-, α_2-, and β-ARs (Bylund et al., 1994). Each type of receptor has three subtypes: α_1-ARs include α_{1a}, α_{1b}, and α_{1d}; the α_2-ARs are α_{2a}, α_{2b}, and α_{2c}; and the β-ARs are β_1, β_2 and β_3 (Bylund et al., 1994). ARs are G-protein coupled receptors that can modulate synaptic transmission through both pre- and post-synaptic mechanisms. α_1-ARs are linked to G_q signaling, α_2-ARs are linked to $G_{i/o}$ signaling, and β-ARs are linked to G_s signaling (Hein, 2006). Of these adrenergic receptors, immunohistochemical studies have shown

widespread expression of α_{2a}-ARs in the BNST (Shields et al., 2009). Other labeling studies have shown expression of α_{1a}, α_{1b}, α_{2c}, β_1, and β_2 –AR in the BNST (Rainbow et al., 1984; Scheinin et al., 1994; Day et al., 1997).

α_1- and β-AR Antagonists Block Stress-Induced Reinstatement of Drug-Seeking

β-ARs and α_1-ARs play a role in initiating stress-induced reinstatement. Administration of β_1-AR and β_2-AR antagonists peripherally or directly into the CeA or BNST blocks stress-induced reinstatement of cocaine-seeking in rodents (Leri et al., 2002; Mantsch et al., 2010; Vranjkovic et al., 2012). Treatment with either a non-specific β-AR agonist or a selective β_2-AR agonist will induce reinstatement of drug-seeking (Vranjkovic et al., 2012). Peripheral administration of an α_1-AR antagonist, prazosin, blocks footshock-induced reinstatement of alcohol-seeking (Le et al., 2011). These data suggest that these two populations of receptors, β-ARs and α_1-ARs, are the predominant receptor classes responsible for initiating NE-induced reinstatement behavior.

Interestingly, while α_1-ARs in the BNST have been shown to modulate the hypothalamic stress response, β-ARs have not (Cecchi et al., 2002b). For example, while injection of α_1-AR antagonists or β_1- and β_2-AR antagonists into the BNST reduced anxiety after stress (Cecchi et al., 2002b), only the α_1-AR antagonist reduced plasma ACTH levels following stress (Cecchi et al., 2002b). Both α_1-AR antagonists and β-AR antagonists are capable of blocking stress-induced reinstatement of drug seeking, yet only α_1-AR antagonists reduce plasma ACTH levels. Therefore, α_1-AR modulation of the hypothalamic stress

response likely does not contribute to the ability of α_1-AR antagonists to attenuate stress-induced reinstatement.

α_2-AR Agonists Block Stress-Induced Reinstatement of Drug-Seeking

α_2-ARs are commonly thought to act as autoreceptors and also to heterosynaptically oppose the actions of α_1- and β-ARs. Consistent with this idea, activation of α_2-ARs has repeatedly been shown to block stress-induced reinstatement (Erb et al., 2000; Highfield et al., 2001; Wang et al., 2001; Mantsch et al., 2010). Peripheral administration of α_2-AR agonists blocks stress-induced reinstatement of heroin-seeking (Shaham et al., 2000) and cocaine-seeking (Erb et al., 2000; Highfield et al., 2001; Mantsch et al., 2010). Specifically, in the extended amygdala, α_2-ARs oppose stress-induced reinstatement, as administration of α_2-AR agonist directly into the BNST blocks footshock-induced reinstatement of morphine-seeking (Wang et al., 2001). In addition, the α_{2A}-AR agonist guanfacine is shown to reduce withdrawal-induced anxiety, and this reduction in anxiety attenuates reinstatement behavior (Buffalari et al., 2012). Interestingly, in addition to withdrawal-induced anxiety, α_{2A}-ARs have been linked to other anxiety disorders, such as PTSD. For example, mRNA expression levels of the α_{2A}-AR gene (Adra2a) were significantly downregulated in the BNST of PTSD-like mice (Lebow et al., 2012). Of note, α_2-ARs have been implicated in stress-induced reinstatement in humans. Patients being treated for drug addiction who are given α_2-AR agonists have improved relapse outcomes and

show decreases in stress-induced drug cravings (Sinha et al., 2007; Sallee and Eaton, 2010; Jobes et al., 2011).

In total, the data above suggest that β- and α_1-ARs are activated in response to stressors in the BNST and drive reinstatement behavior, while α_2-ARs can be activated to oppose the effects of α_1- and β-AR activation and block stress-induced drug seeking behavior. This suggests that these groups of receptors may have opposing roles in activating BNST neurons and/or regulate different populations of cells. In the following sections, I will first review the known actions of these receptors in regulating neuronal activity in the BNST and then begin to synthesize these actions in a model. I will also identify some of the gaps in this model that the work of this dissertation will seek to fill. A summary of the effects of pharmacology directed against different classes of adrenergic receptors on stress-induced reinstatement behavior in rodent models is summarized in Table 1.

Pharmacological agent	Specific drugs	Behavioral effect	References
β antagonist	Propranolol, betaxolol (β_1), ICI-118,551 (β_2)	Blocks stress-induced reinstatement; reduces anxiety	Leri et al., 2002; Mantsch et al., 2010; Cecchi et al., 2002a; Vranjkovic et al., 2012
α_1	Prazosin, benoxathian	Blocks stress-induced reinstatement of ethanol seeking; reduces anxiety	Le et al., 2011; Cecchi et al., 2002b
α_2	Clonidine, guanfacine, lofexidine, guanabenz	Blocks stress-induced reinstatement; reduces withdrawal-induced anxiety	Erb et al., 2000; Highfield et al., 2001; Mantsch et al., 2010; Wang et al., 2001; Shaham et al., 2000; Buffalari et al., 2012
β agonist	Isoproterenol, clenbuterol (β_2)	Induces reinstatement of drug-seeking	Vranjkovic et al., 2012

Table 1. Table listing effects of particular adrenergic receptors on rodent models of stress-induced reinstatement of drug-seeking behavior.

Noradrenergic Receptors Modulate Excitatory and Inhibitory Transmission

Evidence suggests that the actions of NE in the extended amygdala influence stress-induced reinstatement of drug-seeking behavior; therefore, it is important to understand how NE modulates synaptic transmission to elucidate underlying mechanisms. There has been substantial evidence to support a heterosynaptic role for ARs in modulating glutamatergic transmission (Delaney et al., 2007; McElligott and Winder, 2008; Shields et al., 2009; Nobis et al., 2011) and inhibitory transmission (Dumont and Williams, 2004; Shields et al., 2009) in the extended amygdala. The effect of NE on synaptic transmission in the BNST appears to depend on duration of NE application (McElligott and Winder, 2008), previous alterations in noradrenergic signaling (McElligott and Winder, 2008; McElligott et al., 2010), and type of adrenergic receptor activated (Egli et al., 2005). Studies have shown α_1-ARs and α_2-ARs depress excitatory synaptic transmission (Dumont and Williams, 2004; Egli et al., 2005; McElligott and Winder, 2008; Shields et al., 2009) as well as inhibitory transmission (Shields et al., 2009), while β-ARs are capable of enhancing both excitatory transmission (Egli et al., 2005; Nobis et al., 2011) and inhibitory transmission (Dumont and Williams, 2004). Work has also suggested that α_2-ARs are able to differentially regulating glutamatergic inputs to the extended amygdala (Delaney et al., 2007). ARs are capable of intricate modulation of synaptic transmission in the extended amygdala in response to diverse stress and reward stimuli and these modulations may underlie stress-induced reinstatement. A graph illustrating

potential time-dependent actions of different adrenergic receptor classes is shown in Figure 2.

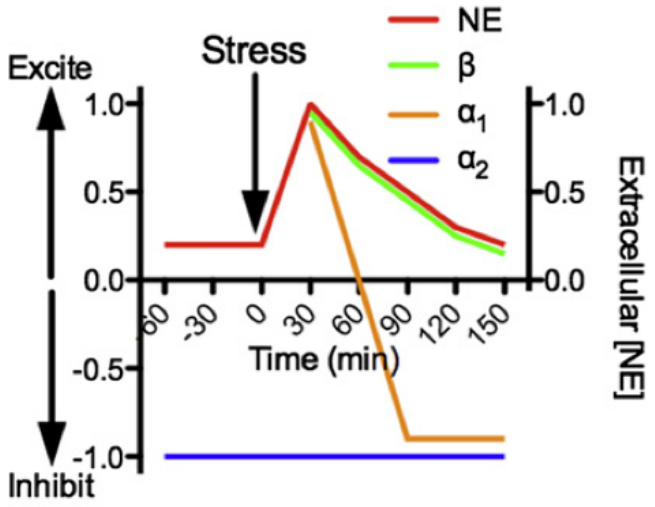

Figure 2. Schematic of the actions of norepinephrine in the BNST. Graph illustrating potential time-dependent overall actions of different NE receptor classes on BNST function. Left axis is the relative excitation or inhibition of BNST function over time, right axis is extracellular NE levels.

β-ARs Enhance Excitatory and Inhibitory Transmission in the BNST

Both β_1- and β_2-ARs regulate synaptic transmission and neuronal excitability in the BNST. Administration of the β-AR agonist isoproterenol enhances both evoked (Egli et al., 2005) and spontaneous excitatory synaptic transmission (Nobis et al., 2011). Noradrenergic enhancement of field potential responses in dBNST, which results from effects on excitatory transmission and/or cellular excitability, is preferentially blocked by a β_2-AR rather than a β_1-AR antagonist (Egli et al., 2005). Isoproterenol effects on spontaneous excitatory

postsynaptic currents (sEPSCs), however, are blocked by β_1-AR antagonists (Nobis et al., 2011). The actions of isoproterenol on sEPSCs are also blocked by a CRFR1 antagonist, and mimicked by CRF and Urocortin (Nobis et al., 2011). These data suggest that NE may act in the BNST in part through the recruitment of endogenous CRF signaling. This is particularly interesting given evidence indicating a serial NE-CRF control of reinstatement behavior (Brown et al., 2011).

α_1-ARs Modulate Excitatory Transmission in a Time-Dependent Manner

Noradrenergic modulation of synaptic transmission in the extended amygdala depends on duration of NE action. With a shorter application of NE, only a transient depression or enhancement is seen (Egli et al., 2005; McElligott and Winder, 2008). Extended application of NE to the BNST produces α_1-AR-dependent long-term depression (LTD) of glutamatergic transmission in the BNST (McElligott and Winder, 2008) through a postsynaptic mechanism (McElligott and Winder, 2008). This LTD is disrupted in mice with chronic alterations in adrenergic signaling, such as α_{2A}-AR-knockout (KO) or NET-KO mice (McElligott and Winder, 2008), or mice that have undergone chronic stress or chronic ethanol exposure (McElligott et al., 2010). The absence of α_1-mediated LTD in the context of chronic disruption of noradrenergic signaling suggests that α_1-ARs may be important for long-term control of excitatory transmission in the extended amygdala. Thus, prolonged dysregulation of noradrenergic signaling interferes with the α_1-ARs' ability to modulate transmission. Further, evidence suggests α_1-ARs dominate regulation of synaptic transmission after prolonged

exposure to NE by ultimately inducing LTD (McElligott and Winder, 2008), regardless of whether the initial response to NE is a β_2-AR-mediated increase in excitatory transmission or an α_2-AR-mediated decrease of excitatory transmission (Egli et al., 2005).

In addition to transient depression in excitatory signaling, acute actions of NE on α_1-ARs causes a transient increase of inhibitory transmission through a presynaptic mechanism (Dumont and Williams, 2004). Initially, NE signaling through α_1-ARs may predominantly activate presynaptic α_1-ARs that enhance inhibitory transmission in the short term. After prolonged stimulation, post-synaptic α_1-ARs may be predominantly activated thus depressing excitatory transmission (McElligott and Winder, 2008; McElligott et al., 2010). α_1-ARs would then have the ability to depress activity in the BNST both short-term, through enhancement of $GABA_A$ inhibitory postsynaptic currents (IPSCs), as well as long term, through long-term depression (LTD). One interesting caveat, however, is that, as with the β_1-AR actions described above, evidence suggests that transient activation of α_1-ARs leads to acute enhancement of spontaneous excitatory transmission in the BNST through recruitment of CRF signaling (McElligott et al., 2010).

The ability of α_1-ARs to induce LTD in the extended amygdala suggests a possible mechanism for α_1-ARs in modulating the hypothalamic stress-response after exposure to a prolonged stressor. As previously discussed, α_1-ARs in the extended amygdala are capable of modulating the stress response, with injection of α_1-AR antagonists into the BNST decreasing levels of plasma ACTH (Cecchi

et al., 2002b). By modulating excitatory or inhibitory transmission in the BNST, α_1-ARs may affect the strength of the BNST's inhibitory projection to the PVN, therefore influencing the downstream hypothalamic stress response.

α_2-ARs Mediate Short-term Depression of Excitatory and Inhibitory Transmission

Early studies indicated an important role for α_2-ARs in mediating inhibitory effects of NE in the BNST (Sawada and Yamamoto, 1981). Like α_1-ARs, α_2-ARs depress synaptic transmission in the BNST through heterosynaptic mechanisms (Delaney et al., 2007; Shields et al., 2009). As previously, there are three types of α_2-ARs expressed in the brain: α_{2A}-ARs, α_{2B}-ARs, and α_{2C}-ARs (Bylund et al., 1994). While expression of α_{2B}-AR mRNA is predominantly limited to the thalamus (Scheinin et al., 1994), expression of α_{2A}-AR and α_{2C}-AR mRNA is widespread in the brain (Scheinin et al., 1994). Expression patterns of α_{2A}-AR mRNA and α_{2C}-AR mRNA are similar and include regions such as the amygdaloid complex, the NTS, and the hypothalamus (Scheinin et al., 1994). Previous work done by our lab suggests that functionally the α_{2A}-ARs are the predominant subtype of α_2-ARs to modulate synaptic transmission in the BNST (Egli et al., 2005). For example, previous studies from our lab show that the effects of the general α_2-AR agonist UK-14,314 on excitatory transmission in the dorsal BNST are nearly absent in α_{2A}-AR-KO mice, thus indicating that α_{2A}-ARs are the primary receptor through which α_2-AR agonists depress excitatory transmission in the dorsal BNST (Egli et al., 2005). Therefore, since α_{2A}-ARs have widespread expression in the dorsal BNST (Scheinin et al., 1994; Shields et

al., 2009) and appear to be the primary α_2-AR subtypes responsible for modulation of synaptic transmission in the dorsal BNST (Egli et al., 2005), this dissertation will focus specifically on the actions of α_{2A}-ARs in the BNST.

The distribution of α_{2A}-ARs in the BNST suggests a prominent role for α_{2A}-ARs in modulating glutamatergic transmission. Immunohistochemical studies reveal that α_{2A}-ARs in the BNST are more broadly distributed than noradrenergic terminals and instead closely resemble distribution of glutamatergic terminals (Shields et al., 2009). Functionally, activation of α_2-ARs in the BNST leads to a decrease in excitatory transmission (Egli et al., 2005; Shields et al., 2009; Krawczyk et al., 2011). Recent studies have shown that application of the selective α_{2A}-AR agonist, guanfacine, leads to a decrease in both excitatory and inhibitory synaptic transmission in the BNST (Shields et al., 2009). Unlike α_1-ARs, the depression of synaptic transmission by α_2-ARs occurs through a presynaptic mechanism (Shields et al., 2009; Krawczyk et al., 2011). Also in contrast to α_1-ARs, α_2-ARs may play a greater role in short-term depression of synaptic transmission (Egli et al., 2005).

Norepinephrine integration of AR actions

Prior alterations in noradrenergic signaling can influence which ARs are recruited by NE. For example, with brief application of NE, α_1-ARs have been shown to enhance IPSC frequency in the BNST (Dumont and Williams, 2004). However, during acute withdrawal from morphine, NE-treated slices also demonstrate increased IPSC frequency but instead through a β-AR-dependent

mechanism (Dumont and Williams, 2004). Therefore, although the overall outcome of enhanced inhibitory transmission is the same whether through α_1- or β-ARs, the physiological circumstances under which NE is released in the extended amygdala seems to influence which receptors regulate synaptic transmission.

While brief application of NE to a slice might mimic a brief stressor, withdrawal may lead to long-term changes in NE signaling that affect the basal activity of ARs and thus their likelihood of recruitment by subsequent NE signaling. Evidence suggests that the recruitment of β-ARs by NE depends on their initial state of activity before NE application (Egli et al., 2005). If enhanced excitatory transmission does not occur with initial slice application of NE, subsequent treatment with β-AR agonists will not lead to β-AR-mediated enhancement of excitatory transmission (Egli et al., 2005). However, if excitatory transmission is enhanced by initial NE application, subsequent β-AR agonists will cause a similar enhancement of excitatory transmission (Egli et al., 2005). Withdrawal may therefore influence the initial state of β-ARs, increasing their likelihood of recruitment by NE signaling. In other studies, β-ARs have been shown to enhance excitatory synaptic transmission through processes that rely on concurrent activation of other receptors, such as α_2-ARs (Egli et al., 2005) and CRFR1 receptors (Nobis et al., 2011). Therefore, the initial state of the β-ARs may also rely on signaling through other receptors. As a result, β-ARs may be poised to integrate stress and reward information received from inputs that signal through different neurotransmitters, for example integrating NE

neurotransmission with CRF neurotransmission. The ability of β-ARs to enhance synaptic transmission in the extended amygdala may rely on both prior noradrenergic signaling and on activation of other receptors.

α_2-ARs Differentially Modulate Individual Inputs to the Extended Amygdala

α_2-ARs appear to differentially regulate synaptic transmission from individual inputs to the extended amygdala (Delaney et al., 2007; Savchenko and Boughter, 2011; Flavin et al., 2014). As in the BNST, NE signaling in the CeA has been shown to heterosynaptically depress glutamatergic transmission through α_2-ARs (Delaney et al., 2007). Further, NE has differential effects on the modulation of the glutamatergic inputs to the CeA from the PBN and the BLA (Delaney et al., 2007). One of the goals of the work in this dissertation will be to determine is glutamatergic inputs to the BNST are also specifically regulated by α_{2A}-ARs.

The BNST receives many glutamatergic inputs that are involved in processing stress stimuli, including the basolateral amygdala (BLA), the insular cortex, the infralimbic cortex, the PBN, and the hippocampus (Weller and Smith, 1982; Shimada et al., 1985; Hurley et al., 1991; McDonald et al., 1999; Chiba et al., 2001; Dong et al., 2001; Shin et al., 2008). The PBN is one of the more prominent glutamatergic inputs to the BNST and is an ascending input (Shimada et al., 1985; Dobolyi et al., 2005) that forms characteristic axosomatic synapses onto dorsal BNST neurons (Shimada et al., 1989). The PBN input to the extended amygdala has been implicated in a wide range of behaviors including

pain sensitization (Han et al., 2005; Han et al., 2010), fear conditioning (Sink et al., 2013a), and feeding (Carter et al., 2013). The PBN has also been implicated in behaviors such as taste aversion (Mungarndee et al., 2006) and hypercapnic arousal (Kaur et al., 2013). The BLA has been implicated in fear conditioning and cue-induced reinstatement of drug-seeking (Rosenkranz et al., 2006; Onur et al., 2009; Buffalari and See, 2010). It may be interesting to compare what factors regulate glutamatergic transmission from each of these inputs to the BNST as it may reveal mechanisms underlying stress and relapse behaviors.

The PBN is a unique input to the BNST in that it forms axosomatic synaptic contacts in the BNST, particularly in the dorsal BNST (Shimada et al., 1989; Dobolyi et al., 2005). These axosomatic contacts formed by the PBN input to the dorsal BNST resemble the axosomatic contacts formed by purkinje fibers in the cerebellum (Eccles et al., 1966). Further, the PBN input to the BNST contains calcitonin gene-related peptide (CGRP), a high-fidelity marker of PBN inputs within the BNST (Shimada et al., 1985; Shimada et al., 1989; Dobolyi et al., 2005). Projections from the PBN to the BNST are believed to be the only source of CGRP within the BNST (Shimada et al., 1985). CGRP immunoreactivity from the PBN is densest in the dorsal anterolateral portions of the BNST (Dobolyi et al., 2005; Gungor and Pare, 2014). Therefore, we are able to use CGRP as a marker of PBN terminals in the BNST, though one cannot exclude the possibility that there may be other PBN inputs to the BNST that are not CGRP-containing. In the work done in the dissertation, I use CGRP as a marker to the PBN input to the BNST. Finally, the PBN has previously been

demonstrated to contain vGluT2-containing projection neurons (Niu et al., 2010; Kaur et al., 2013). Therefore, I am able to target the PBN projection to the BNST with channelrhodopsin (ChR2) by expressing ChR2 under a CaMKIIα promoter that directs ChR2 expression to glutamate neurons of the PBN.

Previous studies using electrical stimulation to isolate glutamatergic inputs suggest that α_2-ARs may differentially modulate the PBN and the BLA inputs to the CeA (Delaney et al., 2007). Therefore, we hypothesize that the PBN and BLA inputs to the BNST are specifically modulated by α_{2A}-ARs and we will investigate this hypothesis in Chapter 1 of this dissertation. Differential modulation could have important implications for understanding the circuitry underlying the relationship between stress and reward-seeking, as specific glutamatergic inputs could have a stronger influence on synaptic transmission in the extended amygdala, contingent on activation of α_2-ARs.

Further evidence of differential regulation of glutamatergic inputs to the extended amygdala through α_2-ARs has been shown by increased c-fos expression, indicating activation of BNST and CeA neurons, after treatment with an α_{2A}-AR agonist (Savchenko and Boughter, 2011). The c-fos expression following treatment with an α_{2A}-AR agonist could indicate α_{2A}-AR-mediated enhancement of excitatory synaptic transmission for some inputs to the CeA and BNST, which would contrast with previous work showing α_{2A}-ARs depress excitatory transmission (Egli et al., 2005; Shields et al., 2009; Flavin et al., 2014). Alternatively, these fos data may reflect direct α_{2A}-AR actions on a subpopulation of BNST neurons or on inhibitory transmission onto those neurons. We will

further investigate this population of c-fos expressing neurons in Chapter 2 of this dissertation.

Summary

Evidence implicates ARs in the extended amygdala in stress-induced reinstatement of drug-seeking behavior. In the BNST, β- and α_2-ARs may be critical in integrating information from different inputs to the extended amygdala. β-ARs may integrate signals from different neurotransmitters, such as α_2-ARs (Egli et al., 2005) and CRFR1 (Nobis et al., 2011). Activation of these receptors may help to determine the initial state of β-AR responsiveness to NE, thus determining subsequent response to β-AR agonists (Egli et al., 2005).

α_2-ARs play a role in transient depression of excitatory transmission and may differentially modulate excitatory inputs to the extended amygdala. Differential modulation would allow for certain inputs to dominate regulation of synaptic transmission in the extended amygdala depending on the neural context of information reaching the BNST. Integration of inputs to the extended amygdala and modulation of neural activity within the region allow ARs to regulate stress-induced reinstatement of drug-seeking.

While some of the key ARs underlying stress-induced relapse of drug-seeking behavior have been identified, there is still work to be done in understanding the specific mechanisms of stress-induced relapse. In particular, there is a need for an understanding of the particular afferent and efferent connections of the BNST that may be modulated by specific ARs. Delaney et al.,

2007 have shown that the PBN and BLA inputs to the CeA appear to be differentially modulated by α_2-ARs. It is quite possible that many of the extended amygdala's inputs and outputs are differentially modulated by ARs. An understanding of such differential modulation would further elucidate the specific neural circuitry underlying stress-induced relapse.

Additionally, the BNST is composed of a heterogenous population of cells, including interneurons and projection neurons. Various types of ARs may differentially modulate excitability of these various cell types within the BNST. Both differential modulation of afferents to the BNST and differential changes in excitability of various cell types within the BNST may influence the excitability of the BNST's projections neurons. A deeper understanding of how various ARs modulate the strength of the BNST's downstream projections would elucidate some of the key components of the neural circuitry that are engaged during stress-induced reinstatement of drug-seeking. Thus, investigation of how ARs regulate synaptic transmission in the extended amygdala may also shed light on the therapeutic potential for α_1- and β-antagonists and α_2-agonists in preventing stress-induced relapse of drug-seeking.

The relatively recent emergence of both *in vivo* and *ex vivo* optogenetic approaches will be a very powerful tool in dissecting the neural circuitry underlying stress induced reinstatement and in dissecting the regulation of this circuitry by ARs. In this dissertation, we will use *ex vivo* optogenetic approaches to investigate the specific regulation of glutamatergic transmission from the PBN and the BLA to the BNST in hopes of better understanding some of the neural

circuitry that allows α_2-AR agonists to block stress-induced reinstatement of drug-seeking in mice. We will also investigate a population of neurons in the BNST that expresses c-fos in response to *in vivo* guanfacine treatment in an effort to understand if α_{2A}-ARs have more than one effect on synaptic transmission and/or neuronal activation in the BNST.

Overall, the work in this dissertation will address:

Hypothesis: α_{2A}-receptors differentially regulate glutamatergic transmission in the BNST.

Aim 1: Test the hypothesis that the inputs from the BLA, the insular cortex, and the parabrachial nucleus to the BNST are differentially regulated by α_{2A}-ARs.

Aim 2: Test the hypothesis that a population of BNST neurons is activated by α_{2A}-ARs, and explore the properties of this neuronal population.

CHAPTER II

α_{2A}-Adrenergic Receptors Filter Parabrachial Inputs to the Bed Nucleus of the Stria Terminalis

α_2-adrenergic receptors (AR) within the bed nucleus of the stria terminalis (BNST) reduce stress and reward interactions in rodent models. In addition to their roles as autoreceptors, BNST α_{2A}-ARs suppress glutamatergic transmission. One prominent glutamatergic input to the BNST originates from the parabrachial nucleus (PBN) and consists of asymmetric axosomatic synapses containing CGRP and vGluT2. Here we provide immunoelectron microscopic data showing that many asymmetric axosomatic synapses in the BNST contain α_{2A}-ARs. Further, I examined optically-evoked glutamate release *ex vivo* in BNST from mice with virally-delivered channelrhodopsin2 (ChR2) expression in PBN. In BNST from these animals, ChR2 partially colocalized with CGRP, and activation generated excitatory postsynaptic currents (EPSCs) in dorsal anterolateral BNST neurons that elicited two cell-type specific outcomes; 1) feed-forward inhibition or 2) an EPSP that elicited firing. I found that the α_{2A}-AR agonist guanfacine selectively inhibited this PBN input to the BNST; preferentially reducing the excitatory response in *ex vivo* mouse brain slices. To begin to assess the overall impact of α_{2A}-AR control of this PBN input on BNST excitatory transmission, I used a Thy1-COP4 mouse line with little postsynaptic ChR2 expression nor colocalization of ChR2 with CGRP in the BNST. In slices from these mice, I found that guanfacine enhanced, rather than suppressed,

optogenetically-initiated excitatory drive in BNST. Thus, our study reveals distinct actions of PBN afferents within the BNST and suggests that α_{2A}-AR agonists may filter excitatory transmission in the BNST by inhibiting a component of the PBN input while enhancing the actions of other inputs.

Introduction

Risk of relapse to drug-seeking behavior in addicts remains high even after treatment (Weiss and Koob, 2001) and stress increases relapse risk (Brown et al., 1995; Sinha et al., 1999; Sinha et al., 2011). In recent studies, α_2-AR agonists have shown promise in curbing cravings in drug-addicted individuals (Sinha et al., 2007; Jobes et al., 2011; Fox and Sinha, 2014; Fox et al., 2014). These clinical data are supported by rodent data demonstrating that α_2-AR agonists reduce stress-induced reinstatement of drug-seeking behavior in rats (Erb et al., 2000; Shaham et al., 2000; Highfield et al., 2001; Mantsch et al., 2010).

Noradrenergic signaling in the bed nucleus of the stria terminalis (BNST) plays an important role in stress-induced relapse to drug-seeking behavior (Aston-Jones et al., 1999; Erb et al., 2001; Briand et al., 2010; Flavin and Winder, 2013). Direct administration of α_2-AR agonists into the BNST reduces stress-induced reinstatement of drug-seeking behavior (Wang et al., 2001), as well as conditioned place aversion from morphine withdrawal (Delfs et al., 2000). α_{2A}-ARs are widely expressed in the BNST (Shields et al., 2009). In addition to their autoreceptor function, α_{2A}-ARs in the BNST can heterosynaptically modulate excitatory transmission (Shields et al., 2009; Krawczyk et al., 2011).

The BNST receives many glutamatergic inputs from which α_{2A}-ARs may modulate excitatory transmission. A better understanding of which excitatory inputs to the BNST are selectively modulated by α_{2A}-ARs may help elucidate neural circuitry underlying the ability of α_2-ARs agonists to block stress-induced reinstatement of drug-seeking in rodent models.

One of the more prominent glutamatergic inputs to the BNST is an ascending input from the parabrachial nucleus (PBN) (Shimada et al., 1985; Shimada et al., 1989; Dobolyi et al., 2005) that forms axosomatic synapses onto dorsal BNST neurons (Shimada et al., 1989; Dobolyi et al., 2005). These axosomatic inputs contain both the neuropeptide CGRP as well as vGluT2 (Shimada et al., 1985; Shimada et al., 1989; Dobolyi et al., 2005; Niu et al., 2010; Kaur et al., 2013). The PBN input to the extended amygdala, which includes both the BNST and the central nucleus of the amygdala (CeA), has been implicated in a wide range of behaviors including pain sensitization (Han et al., 2005; Han et al., 2010), taste aversion (Mungarndee et al., 2006), fear conditioning (Sink et al., 2013a), hypercapnic arousal (Kaur et al., 2013), and feeding (Carter et al., 2013). Previous studies using electrical stimulation to target glutamatergic inputs suggest that α_2-ARs may differentially modulate the PBN and basolateral amygdala (BLA) inputs to the CeA (Delaney et al., 2007).

Here I demonstrate that the α_{2A}-AR agonist guanfacine selectively regulates a PBN input to the BNST. I also show that optical PBN afferent stimulation in the BNST generates two different responses and that these responses are differentially inhibited by guanfacine. Conversely, we show that in a mouse line

where ChR2 is widely expressed, but not colocalized with BNST CGRP, α_{2A}-AR activation enhances the response to other inputs, suggesting a role in filtering information.

Methods

Microinjection surgeries

5-10 week old male C57Bl/6J mice (Jackson Laboratory) were used. All mice were group-housed and on a 12-h light/dark cycle. Mice were given access to food and water ad libitum. During surgeries, mice were anesthetized with isoflurane and injected intracranially with an adeno-associated virus (AAV5) encoding channelrhodopsin (ChR2) fused to YFP, under the control of a CaMKIIα promoter (AAV-CaMKIIα-ChR2:YFP; University of North Carolina Vector Core). A targeted microinjection of the virus (100-150 nl) was made into one of the following sites according to the Franklin and Paxinos mouse brain atlas: the BLA (AP: -1.58, ML: +/-2.90, DV: -5.11) or the PBN (AP: -5.34, ML: +/-1.26, DV: -3.64). Mice were treated with 1 mg/kg injections of ketoprofen for 72 hours following surgery. Virally injected mice were killed 6 to 12 weeks after surgery for anatomical and electrophysiological analysis.

To confirm specificity of injection into the PBN, 7 male C57Bl/6J mice (Jackson Laboratory) 7-10 weeks old were injected with 150 µl of AAV5-CaMKIIα-ChR2:YFP virus unilaterally into the hindbrain, targeted to the PBN. After 6 weeks survival, brains were removed under deep Nembutal anesthesia and immersion fixed in 4% paraformaldehyde. Frozen sections were cut on a

cryostat and the locations of injection sites were compared to fiber densities in the ipsilateral BNST by imaging for ChR2-YFP fluorescence. Few or no fibers were seen in the BNST when injection sites were lateral, rostral or caudal to the PBN (n=1 each). Injections medial to the PBN were avoided because of the known projections of the locus coeruleus to the BNST (Aston-Jones et al., 1999). In two mice, virus injections appeared to be confined to the dorsal PBN and only a few ChR2-YFP positive fibers were visible in each 40 µm section of the BNST. In two other mice, the injection site included both dorsal and ventral parts of the PBN and a moderate density of ChR2-YFP fibers was seen in the BNST (Figure 3 D1). Henceforth, viral injections were targeted to both dorsal and ventral PBN. When the viral injection site was confined to the PBN, ChR2-YFP fibers in the BNST were tyrosine hydroxylase negative (n=2), suggesting that afferents from the locus coeruleus were not part of the ChR2-YFP positive fiber population imaged and light activated in this study (data not shown).

Fluorescent Immunohistochemistry

For immunohistochemical colocalization studies, 6 additional male C57Bl/6J mice that had the AAV5-CaMKIIα-ChR2:YFP virus injected into the PBN six weeks earlier, and three B6.Cg-Tg(Thy1-COP4/EYFP)9Gfng (Thy1-COP4) transgenic mice (Jackson Laboratory, strain ID 007615), were transcardially perfused with 10 mL of ice-cold phosphate-buffered saline (PBS), followed by 20 mL of ice-cold 4% paraformaldehyde in PBS. Thy1-COP4 transgenic mice express ChR2-YFP widely in the brain under the direction of the

pan-neuronal Thy1 promoter. Multiple founder lines exist with variations in overall expression pattern, likely due to differences in copy number and insertion site of the transgene (Arenkiel et al., 2007). Brains were post-fixed in 4% paraformaldehyde overnight at 4°C and were then transferred into 30% sucrose and stored for 2 to 10 days at 4°C. Coronal sections of were cut on a cryostat (Leica, CM3050S) at a thickness of 40 μM. Sections containing the BNST were free-floated in PBS for immuno-labeling. Sections were permeabilized for 30 minutes with 0.5% Triton-X 100 in PBS at room temperature (RT). Next, non-specific binding was blocked with 10% normal donkey serum in PBS containing 0.1% Triton-X-100 for one hour at RT. Sections were then incubated in primary antibody in PBS containing 0.1% Triton-X-100 for 2 days at 4°C, followed by 4 x 10 minute PBS washes. Sections were then incubated overnight at 4°C with secondary antibodies in PBS containing 0.1% Triton-X-100. Finally, sections were washed with PBS (4 x 10 minutes), mounted on Fisher + slides (Fisher Scientific) and coverslipped with PolyAquamount (Polysciences).

Images of fluorescent marker-labeled brain sections and viral vector injection sites were taken with a Zeiss 710 confocal microscope. Lenses used included a 20X/0.80 N.A. Plan-Apochromat and a 63X/1.4 N.A. Plan Apochromat oil. Excitation/emission wavelengths (nm) for each fluorophor were; Dylight 405, 405/410-505; YFP, 512/519-553; cy3, 561/566-600; cy5, 633/638-759. Mosaic image stitching was done with Zeiss ZEN software.

Image Analysis

The neuropeptide CGRP is a marker of the PBN input to the BNST (Shimada et al., 1985; Shimada et al., 1989; Dobolyi et al., 2005). I sought to further illustrate the level of colocalization of CGRP immunofluorescence with ChR2-YFP fluorescence in the BNST of both Thy1-COP4 mice and mice that had PBN injections of AAV5-CaMKIIα-ChR2:YFP. I did this as a means of assessing the relative expression of ChR2 on PBN terminals in the BNST of these two types of mice. I used ImageJ (Fiji) software to visualize the colocalization of CGRP immunohistochemistry fluorescence with ChR2-YFP fluorescence in the BNST. From each of these types of mice, I selected images (63x) of BNST cells that had an observed CGRP-containing axosomatic contact, as CGRP-containing axosomatic synapses are found in projections from the PBN to the dorsal BNST (Dobolyi et al., 2005). I then drew a line through the selected cell body as well as the neuropil immediately surrounding the soma. I next individually plotted the Gray Value (y-axis) versus distance (μm) for each of the different fluorescent markers (CGRP, ChR2, or NeuN) along the line that we drew through the soma and the immediately-surrounding neuropil. Next, I overlaid each of the fluorescent profiles using PRISM software to visualize the level of overlap in the localization of CGRP, ChR2-YFP or NeuN.

Electron Microscopy

For immunoelectron microscopy, mice were sacrificed and perfused with 4% paraformaldehyde, 0.2% glutaraldehyde and 0.2% picric acid in PBS. We

perfused hemagglutinin (HA) α_{2A}-AR knock-in (HA α_{2A}-AR KI) mice that label the N-terminus of the α_{2A}-AR with an HA tag. This mouse line was developed by Qin Wang. The HA-tag on the α_{2A}-AR allows us to use HA antibodies to more easily visualize α_{2A}-AR expression, as α_{2A}-AR antibodies show poor specificity.

In some cases the mice were pretreated with the α_2-AR agonist clonidine to induce internalization of the hemagglutinin (HA)-tagged α_{2A}-AR. Animals were given intraperitoneal (i.p.) clonidine (1 mg/kg) 30 minutes prior to sacrifice. The brains were blocked and postfixed in 4% paraformaldehyde for 4 hours. Coronal, 50 µm thick vibratome sections of the brain were cut and stored frozen at -80^{o}C in 15% sucrose until immunohistochemical experiments were performed. The care of the animals and all anesthesia and sacrifice procedures in this study were performed according to the National Institutes for Health Guide for the Care and Use of Laboratory Animals and were approved by the Institutional Animal Care and Use Committee of Emory University.

Single-label immunoperoxidase labeling was performed using a mouse monoclonal antibody against the HA tag at a 1:500 dilution (Covance, clone 16B12). The single-label immunoperoxidase labeling was performed as described previously (Muly et al., 2003). Briefly, sections were thawed, incubated in blocking serum (3% normal goat serum, 1% bovine serum albumin, 0.1% glycine, 0.1% lysine in 0.01 M phosphate buffered saline, pH 7.4) for one hour and then placed in primary antiserum diluted in blocking serum. After 36 hours at 4^{o}C, the sections were rinsed and placed in a 1:200 dilution of biotinylated horse anti-mouse IgG (Vector) for one hour at RT. The sections

were then rinsed, placed in avidin-biotinylated peroxidase complex (ABC Elite, Vector, Burlingame, CA) for one hour at RT, and then processed to reveal peroxidase using 3,3'-diaminobenzidine (DAB) as the chromagen. Sections were then post-fixed in osmium tetroxide, stained en bloc with uranyl acetate, dehydrated, and embedded in Durcupan resin (Electron Microscopy Sciences, Fort Washington, PA). Selected regions of the BNST were mounted on blocks, and ultrathin sections were collected onto pioloform-coated slot grids and counterstained with lead citrate. Control sections processed as above except for the omission of the primary immunoreagent, did not contain DAB label upon electron microscopic examination.

Ultrathin sections were examined with a Zeiss EM10C electron microscope and immunoreactive elements were imaged using a Dualvision cooled CCD camera (1300 x 1030 pixels) and Digital Micrograph software (version 3.7.4, Gatan, Inc., Pleasanton, CA). Images selected for publication were saved in TIFF format and imported into an image processing program (Canvas 8; Deneba Software, Miami, FL). The contrast was adjusted, and the images were cropped to meet size requirements.

In considering the results of our immunoelectron microscopic examination of α_{2A}-AR there are several caveats. First, it is possible that the presence of the HA tag on the knock-in transgenic mouse resulted in an alteration in the subcellular distribution of the receptor. However, other studies of α_{2A}-AR receptor localization have found it is localized in dendritic, axonal and glial compartments in the locus coeruleus (Lee et al., 1998), the ventrolateral medulla

(Milner et al., 1999) and hippocampus (Milner et al., 1998), so if the presence of the HA tag had an effect on localization it appears to have been of a quantitative nature, and not such as to qualitatively change the localization pattern. A second issue was our use of clonidine pretreatment. We found this necessary because the HA tag is located on an extracellular portion of the receptor and in untreated animals the majority of the label appeared to be extracellular, outlining adjacent structures. It is possible that the clonidine-induced internalization also induced transport from axon terminals and dendritic spines to more proximal positions in the dendritic and axonal arbors. In clonidine treated animals, we observed that dendritic shafts and preterminal axons were the most commonly labeled structures; however, it is possible that spines and axon terminals would have been more common without clonidine treatment.

Electrophysiology Recordings in the BNST

Brain slice preparation

Brain slice preparation methods were used as previously described (Grueter and Winder, 2005; Grueter et al., 2006; Shields et al., 2009). Mice were removed from colony and allowed to acclimate for one hour in a Med Associates sound-attenuating chamber. Following the acclimation, mice were anesthetized with isofluorane and then decapitated. Brains were removed quickly and transferred to a 1-4°C oxygenated, low sodium sucrose dissecting solution (in mM: 194 sucrose, 20 NaCl, 4.4 KCl, 2 $CaCl_2$, $MgCl_2$, 1.2 NaH_2PO_4, 10 glucose, 26 $NaHCO_3$). A Leica vibratome was used to prepare coronal brain slices (300

μm) containing the dorsal BNST. Slices were then transferred to either an interface chamber for field potential recordings or to a holding chamber for whole cell recordings. Both the interface chamber and the holding chamber contained heated, oxygenated artificial cerebral spinal fluid (ACSF) that was composed of (in mM): 124 NaCl, 4.4 KCl, 2.5 $CaCl_2$, 1.3 $MgSO_4$, 1 NaH_2PO_4, 10 glucose, 26 $NaHCO_3$.

Field potential recordings

For field potential recordings, Thy1-COP4 transgenic mice of at least 5 weeks in age were used. Slice preparation for field potential recordings in the dlBNST was performed as previously reported (McElligott and Winder, 2008). Picrotoxin (25 μM) was added to all recordings to isolate excitatory transmission. For optical field potential recordings, light stimulation was produced from a Lamba XL light source (Sutter instruments) and shone through a bandpass filter (Semrock, 475 nm wavelength, 20 nm bandwidth). The blue light was guided from the light source through a water-shielded cable that was positioned approximately 5 cm above the surface of the slice, resulting in full-field illumination. The light stimulation produced a shift in potential, the optical field potential (oN) that was shown to be NBQX sensitive (decreased 76% from mean, n=2), similar to the N2 seen in electrical field potential recordings previously described (Weitlauf et al., 2004; Egli et al., 2005; Grueter and Winder, 2005). pClamp software (Axon Instruments) controlled light pulse duration and frequency. For optical field potential recordings, light stimuli were approximately

2 ms in duration and occurred every 20 seconds. All field potential data was collected using Clampex 10.2 (Molecular Devices).

Analysis of field potential recordings

All field potential recordings were analyzed via Clampfit 10.2 (Molecular Devices) as previously described (Shields et al., 2009). All field recordings contain a 20 min baseline prior to agonist application, with the exception of the atipamezole pre-incubated experiments for which atipamezole was present during baseline, and all data points are normalized to the baseline 5 minutes prior to agonist application. Plotted time courses for field experiments are represented as one-minute averages.

Optical whole-cell recordings

Whole-cell voltage-clamp recordings were performed as previously reported (Grueter and Winder, 2005; Grueter et al., 2006; Kash and Winder, 2006; Silberman and Winder, 2013). Briefly, after brain slice preparation, slices recovered for one hour in a submerged holding chamber (25°C) containing oxygenated (95% O_2/5% CO_2) ACSF. After recovery in the holding chamber, slices were transferred to the recording chamber where they were continuously perfused with oxygenated and heated (25°C) ACSF at a rate of 2 mL/min. For optical whole cell recordings, light stimulation was produced from a Lamba XL light source (Sutter instruments) shone through a bandpass filter (Semrock, 475 nm wavelength, 20 nm bandwidth). The blue light was guided from the light

source through the objective lens using a double lamp-housing adapter (Olympus), resulting in illumination of the slice. Light stimuli were approximately 2 ms in duration and occurred every 10-20 seconds. oEPSCs of 100-1000 pA were recorded while voltage-clamped at -70 mV in the presence of picrotoxin (25 μM). While I did not quantify the levels of viral expression for comparison between the BLA and the PBN, I adjusted initial oEPSCs from each of the inputs such that all baseline oEPSCs were between 100-650 pA at the beginning of each experiment. For large starting oEPSCs, neutral density filters and microscope apertures were used to adjust light intensity such that all experiments were recorded on baseline oEPSCs within the defined amplitude range. Evoked oEPSCs were of a short, invariant latency, consistent with monosynaptic excitation. In data analysis, oEPSCs were normalized to the amplitude of the baseline oEPSCs recorded. After achieving whole-cell configuration, cells were allowed to equilibrate for a minimum of 5 minutes before baseline was started. Postsynaptic parameters were monitored continuously throughout the duration of the experiments. Data are represented as an average of the peak amplitude of 3 sweeps. For voltage-clamp recordings, electrodes of 2.5-5.0 MΩ were filled with (in mM): 117 Cs gluconate, 20 Hepes, 0.4 EGTA, 5 TEA, 2 MgCl, 4 Na2ATP, 0.3 NA2GTP (pH 7.2-7.4, osmolarity 290-295). Input resistance, holding current, and series resistance are monitored continuously. Experiments with input resistances that change by 20% or more are excluded from data analysis. All whole cell data were recorded with Clampex version 10.2 and analyzed with pClamp version 10.2 (Molecular Devices).

Whole-cell optical current-clamp oEPSP recordings

Whole-cell current-clamp recordings were performed as previously reported (Grueter and Winder, 2005; Grueter et al., 2006; Kash and Winder, 2006; Silberman et al., 2013). For current-clamp recordings, electrodes of 2.5-5.0 MΩ were filled with (in mM): 135 K+-gluconate, 5 NaCl, 10 Hepes, 0.6 EGTA, 4 Na2GTP (pH 7.2-7.4, osmolarity 290-295). There was no picrotoxin in the ACSF. After brain slice preparation, slices recovered for one hour in a submerged holding chamber (25°C) containing oxygenated (95% O_2/5% CO_2) ACSF. After recovery in the holding chamber, slices were transferred to the recording chamber where they were continuously perfused with oxygenated, RT (25°C) ACSF at a rate of 2 mL/min. For optical whole cell recordings, stimulation was produced from a Lamba XL light source shone through a bandpass filter. The blue light was guided from the light source through the objective lens using a double lamp-housing adapter, resulting in illumination of the slice. Light stimuli were approximately 2 ms in duration and occurred every 10 seconds. oEPSPs of 5-25 mV were recorded. After achieving whole-cell configuration, cells were allowed to equilibrate for a minimum of 5 minutes before baseline was started. Postsynaptic parameters were monitored continuously throughout the duration of the experiments. Data are represented as an average of the peak amplitude of 3 sweeps.

To determine type of current clamp response, I first applied light stimulation to the slice before injecting any current into the cell to establish if the cell was PBN-responsive. Approximately 1 out of 10 cells was either PBN-

unresponsive or the response generated by the light stimulation was too small to be appropriately interpreted and classified. I did not record from cells in which the oEPSC recorded with PBN stimulation was less than 100 pA. The membrane potentials of the cells that we recorded from in the BNST rested between -70 mV and -85 mV prior to any current injection. Once it was determined that a BNST cell was PBN-responsive, I injected current into the cell until its membrane potential was between -45 mV and -60 mV. Within these membrane potentials, the cell would either fire or a feed-forward IPSP would be generated. If the cell fired within these membrane potentials, I classified it as a PBN-excited cell, if an IPSP was observed, I classified the cell as a PBN-inhibited cell. For cell profile recordings, current was injected into cells until their membrane potential was between -50 mV and -60 mV. Progressive 10 pA current steps current were then delivered to the cell from which we determined input resistance. By visual inspection of the responses to hyperpolarizing current injection, I determined whether a cell exhibited I_h current. From the responses to depolarizing steps, I determined if a cell demonstrated fast- or slow-rise action potentials. Fast-rise action potentials had an action potential rise time of approximately 25 ms, while slow-rise action potentials had a rise time of about 40 ms.

For drug application experiments, cell type was determined by injecting current until the cell membrane potential rested between -45 to -60 mV and then cell type was determined by visual inspection as described above. For PBN-inhibited cells, current was injected into the cell so that the IPSP was observed during drug-application recordings. A five-minute baseline of the IPSP was taken

before drug application. For PBN-excited cells, no current was injected into the cell. A five-minute baseline of the EPSP observed at the resting membrane potential of the cell was taken before drug application.

All whole cell data were recorded with Clampex version 10.2 and analyzed with pClamp version 10.2 (Molecular Devices). Recordings contained a 5 to 10 minute baseline recording prior to drug application. All data points were normalized to the first 5 minutes of baseline. Plotted time courses for whole-cell experiments are represented as 30 second averages.

Statistics

Experiments comparing a difference to baseline were analyzed using a student's T-test. Experiments comparing baseline to two consecutive drug treatments were compared using a repeated measures one-way ANOVA and a Tukey's multiple comparisons test for pairwise comparisons of baseline versus guanfacine-treated, baseline versus atipamezole-treated, and guanfacine-treated versus atipamezole-treated. The significance of the presence of I_h currents in PBN-inhibited and PBN-excited cells were determined used a Chi Square test. Chi Square analysis was also used to determine if the frequency of α_{2A}-AR-containing asymmetric axosomatic contacts were greater than those for symmetric axosomatic or asymmetric axodendritic contacts in both the dorsal and the ventral BNST. Results are reported in text and figure legends. Significant differences were defined as having a $P<0.05$.

Reagents used

Guanfacine hydrochloride (Tocris) stock solution was made in water. Picrotoxin (Tocris) stock solution was made in DMSO. Atipamezole hydrochloride (Tocris) stock solution was made in water. Kynurenic acid (Tocris) was added directly to the ACSF. Primary antibodies included mouse monoclonal NeuN (Chemicon MAB377; 1:1K), mouse monoclonal anti-GAD67 (Millipore MAB5406; 1:800) and goat polyclonal anti-CGRP (Abcam ab36001; 1:1K). Secondary antibodies labeled with Dylight 405 (715-475-150; 1:250) (for NeuN images), cy3 for GAD 67 (715-166-150; 1:1K, or cy5 (715-176-150; 1:1K) (for CGRP images) and raised in donkeys were purchased from JacksonImmuno Research. For immoelectron microscopy, the primary antibody mouse monoclonal anti-HA was used (Covance, clone 16B12; 1:500). The secondary antibody used was biotinylated horse anti-mouse IgG (Vector BA2000; 1:200).

Results

PBN input to the dorsal anterior BNST elicits EPSCs that drive two classes of postsynaptic responses

I used an optogenetic strategy to activate PBN or BLA inputs to the BNST through stereotaxic injection of one of these regions with AAV5-CaMKIIα-ChR2:YFP (Figure 3A, D2, Figure 5F (inset, right)). After a minimum of 5 weeks, mice expressed ChR2-YFP at the injection site (Figure 3 D2, Figure 5F (inset, right)), as well as in axons within the BNST (Figure 3 D1 and Figure 5F (inset, left)).

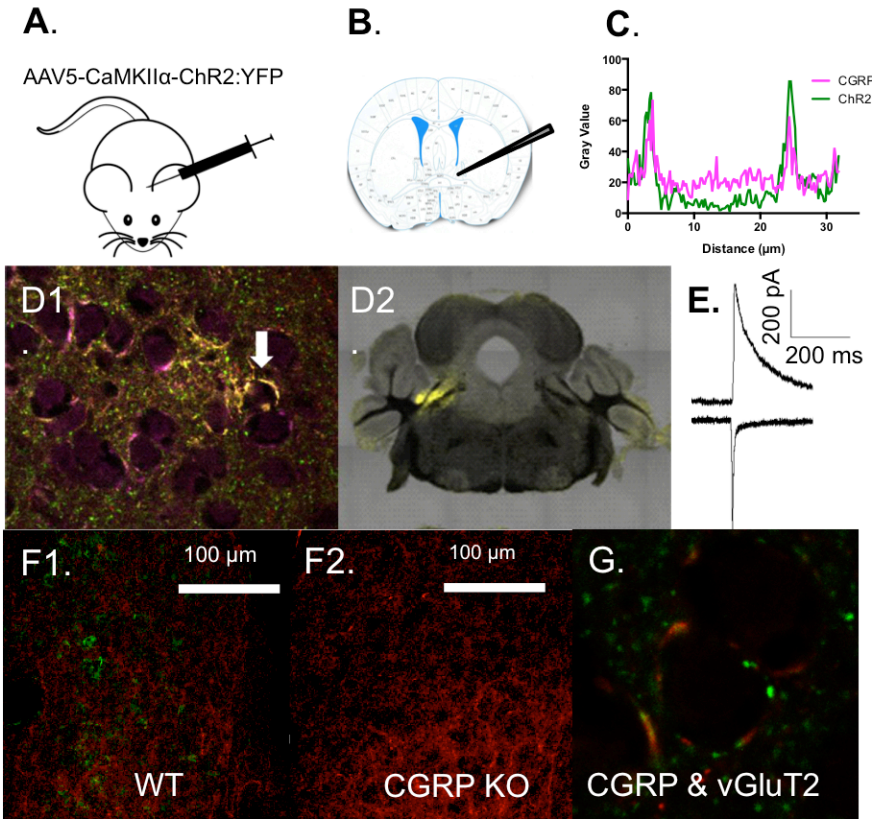

Figure 3. Optogenetic targeting of the parabrachial input to the BNST. A) Illustrated mouse indicating that the experiments done in panels A-E of Figure 1 used a C57Bl/6J mouse that was injected with AAV5-CaMKIIα-ChR2:YFP at least 5 weeks prior. B) Atlas image of BNST slice indicating that we are recording within the dorsal BNST while optically stimulating PBN terminals in the BNST (Slice image adapted from the Franklin and Paxinos Mouse Brain Atlas). C) Representative image of ImageJ (Fiji) image analysis done of a BNST cell and its surrounding neuropil after injection of AAV5-CaMKIIα-ChR2:YFP into the PBN of a C57/Bl6J mouse 5 weeks prior. Colocalization of the gray value of CGRP (purple) with the gray value of ChR2 (green) is observed. D) Image (63x) characterizing expression of ChR2-YFP in the BNST (D1, left) and at the PBN injection site (D2, right) 5 weeks after microinjection into the PBN. Left shows colocalization (yellow, indicated by white arrow) of CGRP (purple) with ChR2-YFP (green) in the dorsal BNST (D1). Right shows ChR2-YFP expression (green) at the PBN injection site (D2). E) Representative traces of the dual component oEPSC generated by stimulation of the PBN input to the BNST. F) CGRP staining (green) can be seen in the dorsal anterolateral BNST of wild-type mice (F1, left) and is absent in CGRP KO mice (F2, right). GAD67 staining is shown in the dorsal BNST (red). G) Colocalization of VGluT2 (green) with CGRP staining (red) in the dorsal anterolateral BNST.

In addition to visual inspection of the injection site, the specificity of the ChR2-YFP viral vector injection into the PBN was confirmed by fluorescent immunohistochemical colocalization of ChR2-YFP with calcitonin gene-related peptide (CGRP), a high-fidelity marker of PBN inputs within the BNST (Shimada et al., 1985; Shimada et al., 1989; Dobolyi et al., 2005). Axosomatic synapses containing CGRP are found in PBN projections to the dorsal BNST (Shimada et al., 1989; Dobolyi et al., 2005). CGRP-expressing neurons that project from the lateral PBN to the extended amygdala have been shown to have functional importance. For example, CGRP-containing neurons that project from the outer external lateral PBN to the central nucleus have been shown to modulate feeding behavior (Carter et al., 2013). Projections from the PBN to the BNST are also believed to be the only source of CGRP within the BNST (Shimada et al., 1985). Therefore, we used CGRP as a marker of PBN terminals in the BNST, though I cannot exclude the possibility that there may be other PBN inputs to the BNST that are not CGRP-containing. Colocalization of ChR2-YFP and anti-CGRP fluorescent label was seen in the dorsal BNST (Figure 3 D1), indicating that the PBN viral injections resulted in expression of ChR2-YFP in PBN axons in the dBNST. I also performed image analysis with ImageJ (Fiji) software to illustrate a colocalization of ChR2-YFP and CGRP in the BNST, further affirming that some CGRP-expressing PBN terminals in the BNST also express ChR2 (Figure 3C). Additionally, as has previously been reported, CGRP immunoreactivity was densest in the dorsal anterolateral portions of the BNST (Figure 3 F1) (Dobolyi et

al., 2005; Gungor and Pare, 2014). CGRP immunoreactivity was not observed in brains taken from CGRPα knockout mouse brains (Figure 3 F2).

The PBN has previously been demonstrated to contain vGluT2-containing projection neurons (Niu et al., 2010; Kaur et al., 2013). We confirmed that CGRP immunoreactivity colocalized with vGluT2 in mouse BNST (Figure 3G). Further, the pattern of ChR2-YFP that we observed in the BNST was overall similar to published CGRP immunoreactivity in the BNST (Dobolyi et al., 2005; Gungor and Pare, 2014). Therefore, I focused our recordings on the anterior dorsal lateral portions of the BNST. Using whole-cell patch clamp recordings from dorsal anterolateral BNST neurons in acutely prepared brain slices, I confirmed that optical recruitment of these fibers in the BNST using full-field blue LED illumination produced excitatory postsynaptic currents (optical EPSCs or oEPSCs). oEPSCs in BNST recorded from PBN-injected mice were observed in the vast majority of cells tested. I could see large oEPSCs ranging up to ~1 nA produced by full field illumination. oEPSC sizes were reduced for study through the use of neutral density filters and manipulation of the aperture to produce amplitudes for analysis between 100-650 pA therefore keeping all baseline oEPSCs within a defined amplitude range. I then stimulated the slice once every 10-20 seconds. One oEPSC was generated from each light stimulation. Evoked oEPSCs were of a very short, relatively invariant latency, consistent with monosynaptic excitation. Representative traces of the dual component oEPSC generated by stimulation of the PBN input to the BNST are shown in Figure 3E. The reversal potential of the synaptic inputs of the PBN onto BNST neurons was

-2.7 mV. The AMPA/NMDA ratio of the PBN inputs to the BNST was 0.849 ± 0.122 (n=5). Application of the AMPA receptor antagonist NBQX (10 μM) reduced the oEPSC at -70 mV (80.6% ± 6.1%, $t(2)=13.1$, $p<0.01$, n=3). Altogether, these data are consistent with full field illumination producing EPSCs from activation of the PBN projection to the BNST.

To establish the impact of the PBN input on BNST neuronal activity, I optically stimulated this input while recording in current clamp mode. When activating PBN inputs to the BNST in *ex vivo* slices prepared from C57Bl/6J mice that had been injected with AAV5-CaMKIIα-ChR2:YFP at least 5 weeks prior (Figure 4A), I observed two overall types of responses to optical stimulation of the PBN input to the BNST. Some PBN afferents within the BNST end in large axosomatic terminal zones that envelop BNST neurons in a manner consistent with “detonator” type synapses such as the climbing fiber input onto Purkinje neurons in cerebellum (Eccles et al., 1966; Shimada et al., 1989; Dobolyi et al., 2005). Thus, I predicted that I would observe PBN-induced firing in BNST neurons. In 18 of 34 neurons (52.7%) recorded from 14 mice, I indeed observed an EPSP followed by burst firing (Figure 4 B1, B3). In the remaining 16 neurons (41.7%), I observed a large inhibitory postsynaptic potential (IPSP) in response to PBN stimulation (Figure 4 B2, B3). I hypothesized that this IPSP was generated by feed-forward recruitment of either GABA interneurons or GABA projection neurons in the BNST, as recent evidence indicates a considerable amount of intra-BNST signaling (Poulin et al., 2009; Gungor and Pare, 2014). This was confirmed by blocking the IPSP through application of the ionotropic

glutamate receptor antagonist kynurenic acid (4 mM, Figure 4 D1, D2, Figure 4E) (89.9% ± 9.0%, $t(4)=10.0$, $p<0.01$, $n=5$).

Since the BNST contains many distinct cell types, and I observed that two types of responses were exhibited by BNST neurons in response to stimulation of the PBN input, I examined the intrinsic excitable properties of these cells to determine if the two types of responses were indicative of two populations of postsynaptic neurons. I injected hyperpolarizing and depolarizing current in a step-wise fashion through the patch clamp electrode into both PBN-inhibited cells and PBN-excited cells in the BNST. I noted several features of the cells' responses to current injection that suggested commonality within these two response groups and distinctions across the groups (Figure 4 C1, C2, C3). First, I saw that 56% (n=9 out of 16) of PBN-excited cells exhibited I_h current activity during hyperpolarizing steps, while only 20% (n=3 out of 15) of PBN-inhibited cells exhibited I_h current (Figure 4 C1 compared to Figure 4 C2). Chi squared analysis of the presence of I_h current in each of the cell types revealed a significant difference between the PBN-inhibited and PBN-excited cells (Chi-square=4.3, df=1, $p<0.05$, $n=31$). Second, PBN-excited cells had significant differences in their input resistances from PBN-inhibited cells, with the PBN-inhibited cells showing lower input resistances (371.0 MΩ ± 27.3 MΩ, $t(23)=3.1$, $p<0.05$, $n=13$) as compared to higher input resistances in PBN-excited cells (494.1 MΩ ± 29.1 MΩ, $n=12$).

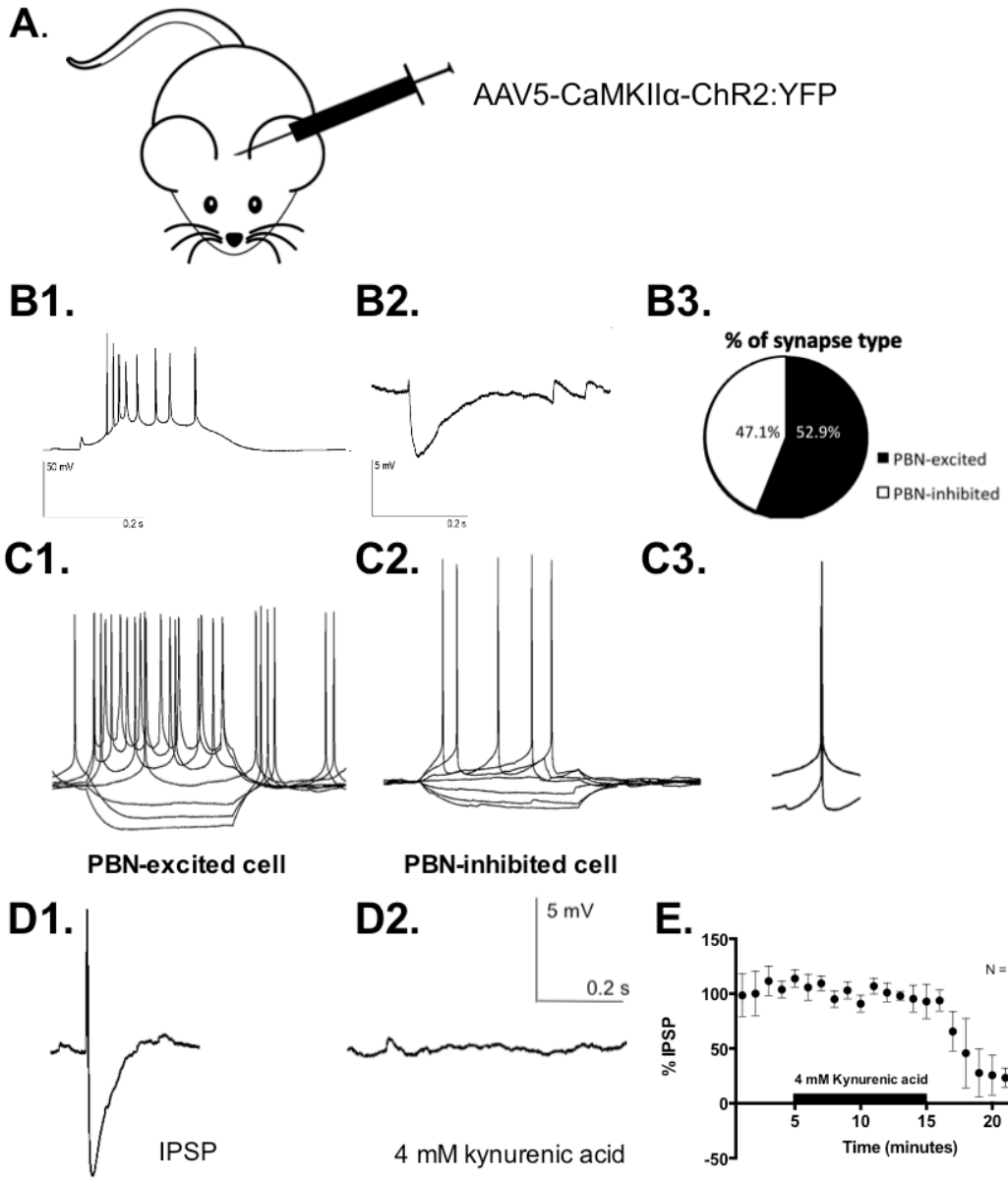

Figure 4. Parabrachial inputs to the BNST innervate at least two types of neurons. A) Illustrated mouse indicating that the experiments done in Figure 2 used C57Bl/6J mice that were injected with AAV5-CaMKIIα-ChR2:YFP at least 5 weeks prior. B) A representative trace of a PBN-activated cell firing action potentials is shown (B1). A representative trace of an IPSP recorded from a PBN-inhibited cell is shown (B2). A pie chart showing the relative prevalence of each cell type is shown. PBN-activated cells comprise 52.9% of the 34 cells recorded from and PBN-inhibited cells comprise 47.1% (B3). C) Step-wise current injection into a PBN-activated cell, I_h current can be seen at

hyperpolarized potentials (C1). Step-wise current injection into a PBN-inhibited cell, no I_h current is seen at hyperpolarized potentials (C2). Overlapping action potentials showing that action potentials generated in PBN-activated cells (top) have a faster rise time than PBN-inhibited cells (bottom) (C3). D) Kynurenic acid (4mM) blocks the feed-forward IPSP generated by PBN-inhibited cells. Representative traces of an IPSP prior to drug application (D1) and after drug application (D2) are shown. E) Time course showing the block of feed-forward IPSPs generated in PBN-inhibited cells by kynurenic acid (4mM), ($p<0.01$, $n=5$).

Third, I observed that PBN-inhibited cells had a slower rising phase on their action potentials (APs) based on visual inspection, with 15 out of 16 PBN-inhibited cells showing slower rising APs, compared to PBN-excited cells where only 1 out of 15 firing-type cells had slower rising APs (Figure 4 C3, slow-rise (bottom trace) compared to fast-rise (top trace)). These differences between PBN-inhibited and PBN-excited cells indicate the possibility of two distinct populations of cells.

Ultrastructural analysis reveals widespread expression of α_{2A}-AR within the BNST and expression in asymmetric axosomatic synapses

α_{2A}-AR stimulation results in depression of excitatory drive in the BNST (Shields et al., 2009). Previous studies in the CeA suggest the possibility that α_2-ARs presynaptically regulate PBN input to that region (Delaney et al., 2007). To assess the localization of α_{2A}-ARs in the BNST we used a genetically modified mouse in which an HA-tag was knocked-in to the N-terminus of the α_{2A}-AR (Figure 5 A1). As antibodies for α_{2A}-ARs have poor specificity, we used this knock-in mouse so that we were able to visualize α_{2A}-ARs using HA antibodies. Our previous light level localization of the α_{2A}-AR using this knock-in HA-tagged-α_{2A}-AR mouse line suggest heavy expression of this receptor postsynaptic to

noradrenergic terminals, in that immunoreactivity far surpassed the pattern of TH staining (Shields et al., 2009). In order to more directly test the idea that α_{2A}-ARs are present on excitatory terminals in the BNST, we used immunoelectron microscopy to confirm a structural substrate for presynaptic action. We used the HA-α_{2A}-AR knock-in mice described above and used previously (Shields et al., 2009) (Figure 5 A1) and labeled BNST sections from these mice with an antibody directed against the HA tag.

Initially we observed strong labeling when sections were examined with the light microscope but when examined with the electron microscope we observed only a few profiles containing DAB in the neuropil of the BNST. Instead, we observed what appeared to be DAB reaction product in the extracellular space outlining neuropil elements that themselves contained no clear label (Figure 5 A2). We reasoned that this was because the HA tag was attached to the N terminus of the receptor, a region predicted to be on the extracellular surface when the receptor is on the plasma membrane. Accordingly, we pretreated animals with the α_2-AR agonist clonidine prior to sacrifice to induce internalization of the receptor (Lu et al., 2009). We found that with clonidine pretreatment, the extracellular label was greatly decreased and neuropil elements containing DAB label were more common. Dendritic shafts and preterminal axons appeared most commonly labeled in this clonidine treated material, but dendritic spines and axon terminals could also be observed, as well as some glial processes (Fig. 5B-E). In some cases the axon terminals could be observed making asymmetric synaptic contacts.

We were particularly interested in the labeled axon terminals. In order to determine the synaptology of α_{2A}-AR containing axon terminals in the dorsal BNST, we examined 235 images taken from the dorsal anterolateral BNST in four animals, representing 3,872.5 μm^2. We identified a total of 106 asymmetric synapses in this sample, 40 terminated onto dendritic shafts and 66 onto dendritic spines. None of the axon terminals giving rise to asymmetric synapses onto dendritic shafts were labeled for α_{2A}-AR; 5% of the terminals synapsing onto dendritic spines were labeled for α_{2A}-AR (Figure 5F).

Another possible target for α_{2A}-AR containing terminals in the BNST are cell bodies. Accordingly, we examined 34 cell bodies in dorsal anterolateral BNST. We identified all axon terminals making synaptic contacts onto these soma in the single ultrathin section. A total of 60 synaptic contacts were identified, 32 of which were asymmetric and 28 of which were symmetric. Of the terminals making symmetric contacts onto cell bodies, 7% contained label for α_{2A}-AR (Figure 5F). On the other hand, 25% of the terminals making asymmetric synaptic contacts onto cell bodies were labeled for α_{2A}-AR (Figure 5F). We hypothesized that these α_{2A}-AR-containing terminals making axosomatic asymmetric synapses arose from parabrachial nucleus. To further evaluate this hypothesis we examined the axon terminals in the ventral BNST. We reasoned that if our hypothesis was correct the percentage of labeled axosomatic syanpses in the ventral BNST should be lower than in the dorsal BNST in keeping with the lighter parabrachial innervation of this region of the BNST.

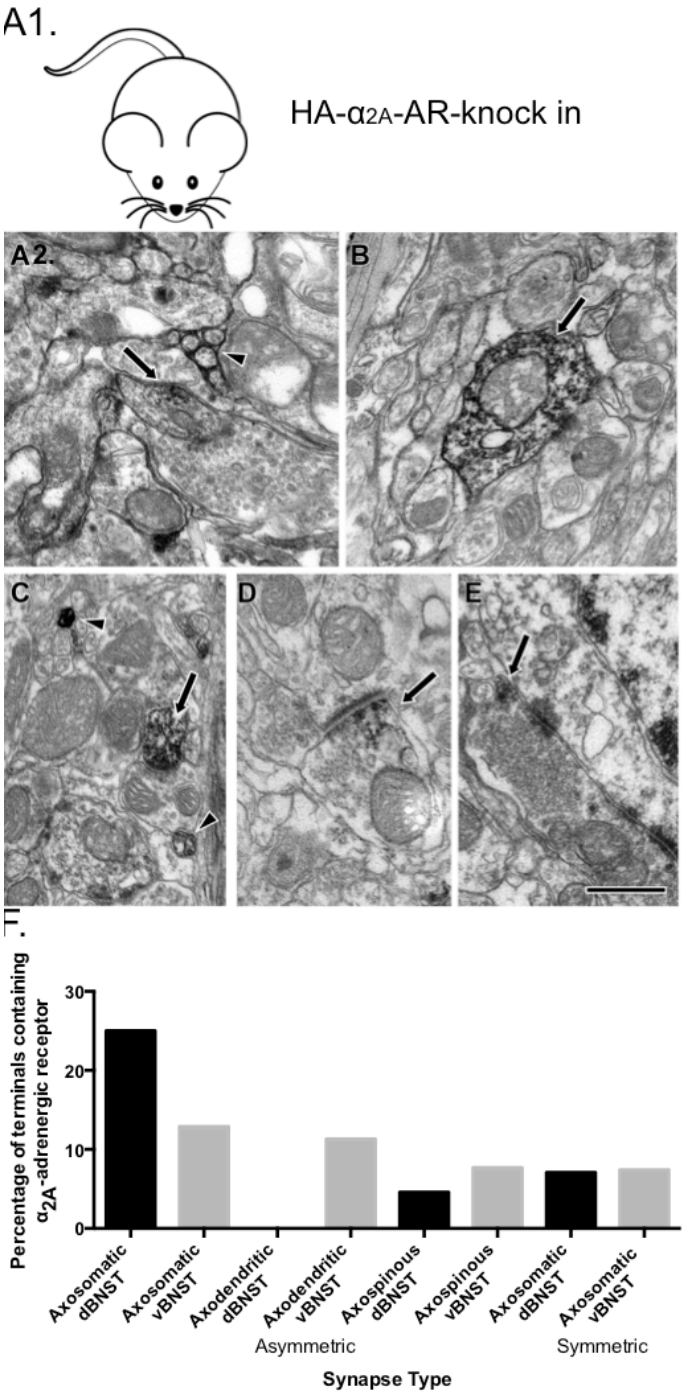

Figure 5. Immunolabeling for HA-tagged α_{2A}-AR in mouse BNST. A) Illustrated mouse indicating that the experiments done in Figure 3 used HA-α_{2A}-AR-knock in mice (A1). Immunolabeling directed against the HA tag produced some patches of intracellular labeling in neuronal elements (arrow); however, the bulk of labeling observed appeared to be extracellular (arrowhead), appearing to

fill spaces between elements of the neuropil, producing the effect of 'outlining' them with reaction product (A2). B-E) When animals were treated with clonidine before sacrifice the 'outlining' was less frequent and instead reaction product was observed inside neuronal elements. Dendrites (B, arrow) and preterminal axons (C, arrowheads) were commonly observed. Labeled dendritic spines (C, arrow) and axon terminals (D and E, arrows) were also seen. The labeled axon terminals sometimes made asymmetric synaptic contacts (E). Scale bar, 500 nm. F) Bar graph showing relative abundance of α_{2A}-ARs in each synapse type in both the dorsal and ventral BNST.

We examined 195 images taken from the ventral BNST in four animals, representing 3,213.4 μm^2. We identified a total of 119 asymmetric synapses in this sample, 80 terminated onto dendritic shafts and 39 onto dendritic spines. Of the axon terminals giving rise to asymmetric synapses onto dendritic shafts, 11.3% were labeled for α_{2A}-AR; 7.7% of the terminals synapsing onto dendritic spines were labeled for α_{2A}-AR. We then examined 43 cell bodies in ventral BNST. We identified all axon terminals making synaptic contacts onto these soma in the single ultrathin section. A total of 58 synaptic contacts were identified, 31 of which were asymmetric and 27 of which were symmetric. Of the terminals making symmetric contacts onto cell bodies, 7.4% contained label for α_{2A}-AR, while 12.9% of the terminals making asymmetric synaptic contacts onto cell bodies were labeled for α_{2A}-AR, roughly half the level seen for dorsal BNST (Figure 5F). This is consistent with our hypothesis that these α_{2A}-AR containing axosomatic asymmetric synapses arise from the parabrachial nucleus.

I performed Chi-square analysis on our EM data for both the dorsal and ventral BNST to determine if the frequency of α_{2A}-AR-containing contacts were greater in asymmetric axosomatic contacts versus symmetric axosomatic

contacts. I also performed a Chi-square analysis to determine if the frequency of α_{2A}-AR-containing contacts were greater in asymmetric axosomatic contacts versus asymmetric axodendritic contacts. In the dorsal BNST, there was no statistical difference in frequency of symmetric axosomatic α_{2A}-AR-containing contacts versus asymmetric axosomatic α_{2A}-AR-containing contacts (Chi-square=3.4, df=1, n.s., n=60). There was, however, a significant difference in the frequency of asymmetric axosomatic α_{2A}-AR-containing contacts as compared to asymmetric axodendritic α_{2A}-AR-containing α_{2A}-ARs contacts (Chi-square=11.3, df=1, $p<0.01$, n=72). In the ventral BNST there was no significant difference between the frequency of asymmetric axosomatic α_{2A}-AR-containing contacts compared to either symmetric axosomatic α_{2A}-AR-containing contacts (Chi-square=0.5, df=1, n.s., n=58) or to axodendritic asymmetric α_{2A}-AR-containing contacts (Chi-square=0.06, df=1, n=111).

In total, these Chi-square analyses reveal that in the dorsal BNST there is a higher frequency of α_{2A}-AR-containing asymmetric axosomatic contacts than α_{2A}-AR-containing asymmetric axodendritic contacts. It also reveals that there is no significant difference between the α_{2A}-AR content of these types of synapses in the ventral BNST. This finding is consistent with what is known of the anatomy of the PBN input to the BNST, in which CGRP-containing axosomatic inputs from the PBN are predominantly observed in the dorsal BNST (Dobolyi et al., 2005). While non-axosomatic PBN inputs are observed in the ventral BNST, the overall density of PBN projections to the BNST are higher in the dorsal BNST than in the ventral BNST (Shimada et al., 1989; Alden et al., 1994). Therefore, the presence

of α_{2A}-ARs on significantly more asymmetric axosomatic synapses selectively in the dorsal BNST is consistent with α_{2A}-AR expression on PBN terminals in this region.

Guanfacine suppresses oEPSCs elicited by PBN fiber recruitment in BNST

Given the likelihood that α_{2A}-ARs are present on PBN terminals in the BNST, I next assessed whether the α_{2A}-AR agonist guanfacine differentially affected individual inputs to the BNST using optogenetic strategies outlined in Figure 3. I tested the sensitivity of two different excitatory inputs to the BNST: the BLA and the PBN. I targeted the PBN input to the BNST as described above (Figure 3, Figure 6A). Voltage-clamped whole-cell recordings were made in the presence of 25 μM picrotoxin to further isolate oEPSCs. Application of guanfacine (1 μM) depressed oEPSCs produced by activation of PBN afferents within the BNST (Figure 6B,C,D) ($t(2,8)=9.4$, $p<0.01$, $n=7$). After application of the selective α_2 antagonist atipamezole (1 μM), the amplitude of oEPSCs returned to a level not significantly different from baseline (Figure 6B,C). I did observe some variability across experiments (Figure 6C). In some instances, such as the individual experiment (Figure 6B), there was a clear depression of excitatory transmission by guanfacine that was reversed by atipamezole. In contrast, in other experiments weaker effects of guanfacine on excitatory transmission were observed (Figure 6C). Additionally, I performed experiments in which I applied guanfacine (1 μM) to oEPSCs recorded from stimulation of the PBN afferents in the BNST and then allowed for a long washout of guanfacine

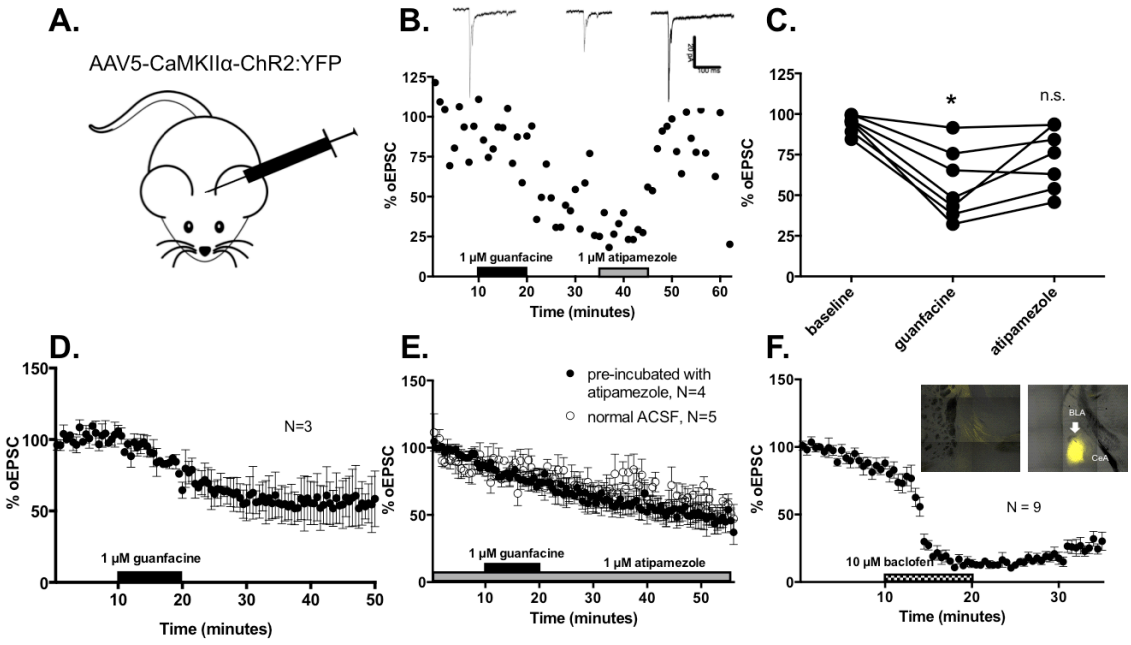

Figure 6. Guanfacine depresses excitatory transmission from the parabrachial nucleus projection to the BNST. A) Illustrated mouse indicating that the experiments done in Figure 4 used C57Bl/6J mice that were injected with AAV5-CaMKIIα-ChR2:YFP at least 5 weeks prior. B) Individual experiment showing decrease in excitatory transmission of the PBN input to the BNST by guanfacine that is reversed by atipamezole (1 μM). Example traces of each phase of drug application are shown (insets). C) Individual experiments showing that excitatory transmission is significantly decreased from baseline by guanfacine (1 μM) ($p<0.01$, n=7). Subsequent application of atipamezole reverses this depression such that amplitudes of oEPSCS are no longer significantly different from baseline (n.s., n=7). D) Guanfacine (1 μM) was applied to oEPSCs recorded from stimulation of the PBN afferents in the BNST. Guanfacine was allowed to washout for 30 minutes. With prolonged washout the depression of the excitatory PBN input to the BNST did not reverse to baseline levels ($p<0.05$, n=3). E) Guanfacine (1 μM) has no apparent effect on excitatory transmission from the BLA to the BNST in normal ACSF (white circles) ($p<0.01$, n=5). Pre-incubation of *ex vivo* BNST slices with atipamezole (1 μM) does not alter the effect of guanfacine on excitatory transmission from the BLA to the BNST (black circles) ($p<0.01$, n=4). F) Baclofen (10 μM) depresses excitatory transmission from the BLA to the BNST ($p<0.01$, n=9). Image of the BLA injection site 5 weeks after injection of the AAV5-CamKIIα-ChR2:YFP into the BLA (inset, right). Expression of ChR2-YFP in the dorsal BNST 5 weeks after injection of the viral vector into the BLA (inset, left).

without subsequent application of atipamezole to the recordings (Figure 6D).In such experiments, after prolonged washout of guanfacine, the size of oEPSC did not return to baseline levels (Figure 6D) as was observed in Figure 6B,C (48.3 ± 11.2%, $t(2)=4.3$, $p<0.05$, $n=3$). Therefore, application of the α_2-AR antagonist atipamezole appears to be necessary for the reversal of the depression of excitatory transmission from the PBN to the BNST by guanfacine.

I also assessed the effect of guanfacine on oEPSCs produced by activation of BLA afferents within the BNST using a similar strategy involving injection of the ChR2-expressing viral vector (AAV5-CaMKIIα-ChR2:YFP) into the BLA 5-12 weeks prior to brain slice preparation. I observed expression of ChR2-YFP fluorescence at both the BLA injection site (Figure 6F (inset, right)) and in axons within the BNST (Figure 6F (inset, left)). Full field illumination produced robust oEPSCs that were brought to a range of 100-650 pA through the use of neutral density filters and manipulations of the light aperture. The BLA input to the BNST, in the presence of picrotoxin, showed very little, if any, sensitivity to guanfacine (Figure 6E, open circles) (32.4% ± 6.3%, $t(4)=5.2$, $p<0.01$, $n=5$). I observed marked rundown in the recordings of the BLA input to the BNST, but the extent of the rundown was the same when *ex vivo* BNST slices were pre-incubated in atipamezole (1 μM) (Figure 6E, closed circles) (42.7% ± 6.2%, $t(3)=6.8$, $p<0.01$, $n=4$) or not (Figure 6E, open circles). Due to the lack of difference between recordings done in normal ACSF and recordings done with atipamezole pre-incubation I believe that any differences in amplitude between oEPSCs recorded at baseline and oEPSCs recorded after guanfacine application

were due to rundown of recordings. In the case of these *ex vivo* optogenetic recordings, I refer to "rundown" as a decrease in the size of the oEPSC over the duration of the recording that appears to be independent of either a drug effect or of cell health. Interestingly, this rundown was observed in the BLA input to the BNST but not the PBN inputs. The 1 μM concentration of atipamezole used was previously sufficient to reverse the effect of α_{2A}-AR agonist actions on electrically-evoked EPSCs (Shields et al., 2009). To ensure that I would be capable of observing $G_{i/o}$-protein coupled receptor modulation of BLA inputs in the BNST even with the rundown of the oEPSC, we examined actions of the $GABA_B$ agonist baclofen. The $GABA_B$ receptor is virtually ubiquitously expressed on glutamatergic terminals in the CNS, where it depresses glutamate release. Despite the rundown observed in our BLA-to-BNST recordings, I was able to observe robust depression of oEPSCs elicited by BLA fiber activation by baclofen (10 μM) (Figure 6F) (69.6% ± 9.7%, $t(8)=7.2$, $p<0.001$, $n=9$). While the level of expression of α_{2A}-ARs on BLA terminals in the BNST is unknown, our electrophysiological data suggest that excitatory transmission from the BLA input to the BNST is insensitive to activation of α_{2A}-ARs (Figure 6E). These data suggest that guanfacine selectively modulates PBN inputs to the BNST.

Guanfacine depresses PBN-induced current clamp responses on BNST neurons

As described above, I observed two types of membrane potential responses of BNST neurons to stimulation of the PBN input: **"**PBN-excited**"** and **"**PBN-inhibited.**"** I sought to determine if there were any differences in the

sensitivity of each type of response to guanfacine. I again targeted the PBN using the optogenetic strategies described above (Figure 3, Figure 7A). For PBN-excited responses, I applied 1 μM guanfacine to the optically-evoked EPSPs recorded from the BNST neuron at the cell's resting membrane potential. I observed that PBN-excited cells show a marked decrease in EPSP size with guanfacine application (Figure 7B) (40.2% ± 6.0%, $t(4)=6.7$, $p<0.01$, $n=5$). Further, this decrease in EPSP size with guanfacine was seen in all PBN-excited cells that I tested (Figure 7D). In contrast, while the PBN-inhibited cells showed a trend for a decrease in size of IPSP with 1 μM guanfacine application (Figure 7C) (15.1% ± 7.4%, $t(10)=2.0$, n.s., $n=11$), the decrease was not significant. Interestingly, I observed that some PBN-inhibited cells show a decrease in IPSP size with guanfacine application, while others did not (Figure 7E). Therefore, the lack of significance of the decrease in the IPSP may be due to heterogeneity in the sensitivity to guanfacine of the PBN input onto each of these PBN-inhibited cells. Further, since these IPSPs are feed-forward, the variability of the IPSPs response to guanfacine likely depends on the sensitivity of both the glutamatergic input and the intervening inhibitory interneuron to α_{2A}-AR activation by guanfacine.

Differential action of guanfacine on optically-evoked excitatory responses in Thy1-COP4 mouse BNST

Analysis of extracellular field potentials can provide a more global analysis of the impact of modulatory receptors on circuit activity by allowing us to record from populations of neurons in the BNST. In examining ChR2-YFP expression

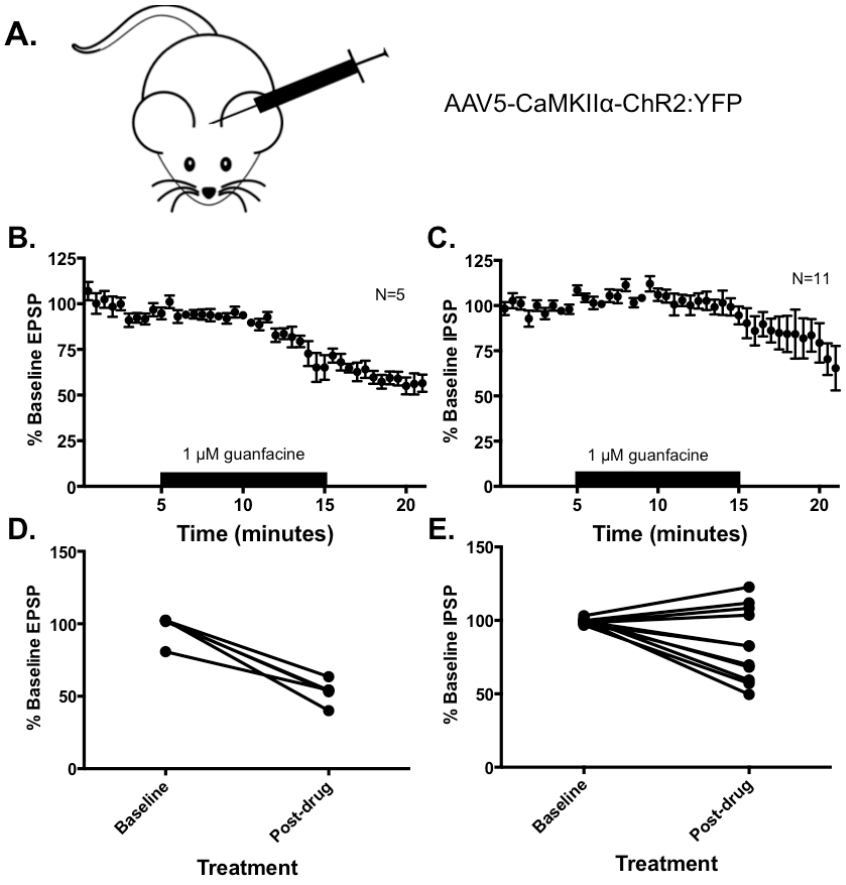

Figure 7. Guanfacine reduces EPSPs of PBN-activated cells in the BNST. A) Illustrated mouse indicating that the experiments done in Figure 5 used C57Bl/6J mice that were injected with AAV5-CaMKIIα-ChR2:YFP at least 5 weeks prior. B) Guanfacine (1 μM) significantly decreases the size of EPSPs recorded from PBN-activated cells in the BNST ($p<0.05$, n=5). C) Guanfacine (1 μM) has variable effects on IPSPs recorded from the PBN-inhibited cells in the BNST (n.s., p=11). D) Individual experiments showing the effect of guanfacine (1 μM) on EPSPs recorded from PBN-activated cells in the BNST. EPSPs are reduced by guanfacine across all experiments. E) Individual experiments showing the effect of guanfacine (1 μM) on IPSPs recorded from PBN-activated cells in the BNST. The effect of guanfacine on IPSPs is more variable with IPSPs being reduced in some experiments and unaltered in others.

in Thy1-COP4 transgenic mice, we determined that while ChR2-YFP was heavily expressed in regions that project to the BNST such as the BLA, cortical regions, and the hippocampus, ChR2-YFP did not colocalize with immunoreactivity from CGRP neuropeptide, a marker of a PBN input to the BNST (Figure 8A, Figure 8 B1). I performed image analysis using ImageJ (Fiji) software to illustrate that the fluorescent signal from CGRP immunohistochemistry staining that surrounds dBNST cell bodies does not overlap with ChR2-YFP fluorescence in Thy1-COP4 mice. A representative image of this analysis is shown in Figure 8 B2.

I prepared *ex vivo* slices from Thy1-COP4 transgenic mice and performed optical field potential recordings in the dBNST (Figure 8A). I found that full-field optical stimulation in BNST slices from Thy1-COP4 mice produced a synchronized field potential response that was substantially reduced by AMPA receptor antagonists (76.2% from baseline, n=1), which is consistent with N2 responses that we have previously published (Egli et al., 2005; Grueter and Winder, 2005). This indicates only a small amount of expression of ChR2 in postsynaptic BNST neurons in this mouse line and that the optical field potential elicited is driven by recruitment of glutamatergic afferents. I found that I was able to elicit optical field potentials (oN) that were similar in size to our previously published N2 responses (inset, Figure 8C) (Egli et al., 2005; Grueter and Winder, 2005). Surprisingly, when I applied guanfacine (1 μM) to the optical extracellular field potential recordings, I observed an increase in the size of the oN (Figure 6C) (18.6% ± 6.5%, $t(6)=2.9$, $p<0.05$, n=7). This increase in field potential size with guanfacine (1 μM) contrasts with our previous work done using electrical

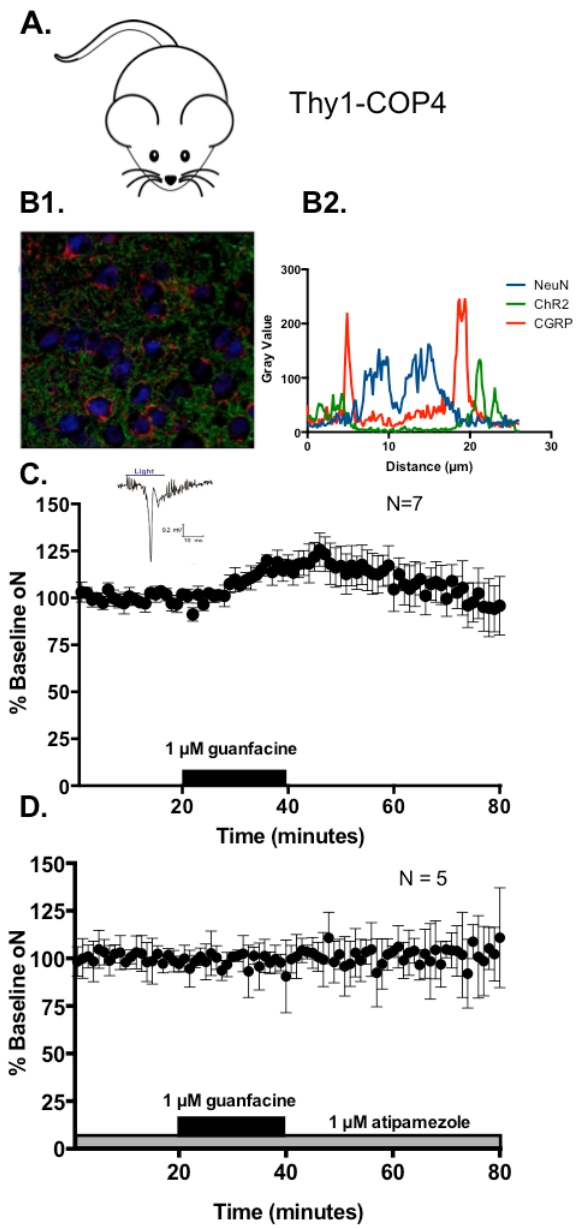

Figure 8. Guanfacine increases field potentials in the dBNST of Thy1-COP4 transgenic mice. A) Illustrated mouse indicating that the experiments done in Figure 6 used Thy1-COP4 transgenic mice. B) Image of dorsal BNST (63x) showing lack of colocalization of CGRP (red) with ChR2 (green) in Thy1-COP4 mice. NeuN staining is shown in blue (B1). Representative image of ImageJ (Fiji) analysis done of a BNST cell and its surrounding neuropil in a Thy1-COP4 transgenic mouse. ImageJ (Fiji) image analysis does not show colocalization of CGRP (red) with the ChR2 (green). There is also no observed colocalization of CGRP or ChR2 with NeuN (blue) (B2). C) Optical field potential (oN) size is increased with guanfacine (1 μM) application in Thy1-COP4 mice ($p<0.05$, n=7). Representative trace of oN is shown (inset). D) Preincubation of *ex vivo* BNST

slices with atipamezole (1 μM) blocks the increase in size of the optical field potentials with subsequent guanfacine (1 μM) application (n.s., n=5).

stimulation that shows a decrease in excitatory transmission with guanfacine application (Shields et al., 2009). This increase in optical field potential size with guanfacine application to *ex vivo* BNST slices of Thy1-COP4 mice was blocked by pre-incubation of slices with atipamezole (1 μM) further confirming this enhancement is mediated through activation of α_2-ARs (Figure 6D) (0.1% ± 5.2%, t(4)=0.02, n.s., n=5).

Discussion

Here I have optogenetically activated PBN inputs to the BNST for electrophysiological analysis. I find that full-field illumination of *ex vivo* BNST slices that have been prepared from mice with AAV5-CaMKIIα-ChR2:YFP injected into the PBN at least 5 weeks prior yields a dual component oEPSC that produces cell-type specific responses. In one cell type, stimulation promotes robust feed-forward inhibition. In another, stimulation produces repetitive firing. I found that the α_{2A}-AR agonist guanfacine filters excitatory drive into the BNST by depressing oEPSCs contributing to the depolarizing effects of the PBN input. Using immunoelectron microscopy and a novel knock-in HA-tagged α_{2A}-AR mouse strain, we show that α_{2A}-ARs are present on asymmetric axosomatic synapses in the dorsal BNST, which are consistent with localization to PBN inputs.

α_{2A}-ARs specifically modulate excitatory PBN inputs to the extended amygdala

In contrast to the PBN input to the BNST, our data suggest that the BLA input to the BNST is largely insensitive to guanfacine. These data are consistent with previous work examining the sensitivity of electrically-evoked PBN and BLA inputs to the CeA (Delaney et al., 2007). Similar to our findings in the BNST, this work suggests that the PBN input to the CeA is depressed by α_2-ARs while the BLA is unaffected (Delaney et al., 2007). While the relative expression of α_{2A}-ARs on the BLA terminals in the BNST is unknown, our study suggests that these terminals are insensitive to α_{2A}-AR activation.

Until the advent of optogenetic approaches, studies in which specific inputs to the BNST are targeted using electrical stimulation were not possible due to the close proximity of afferent fibers to the BNST. Through the use of *ex vivo* slice ChR2 recordings, we are now able to dissect neural circuits in ways that were previously not feasible by targeting individual inputs using optogenetic strategies outlined in this study. Here, I focus on the selective modulation of a PBN input to the dorsal BNST by α_{2A}-ARs because past behavioral work has shown that α_2-AR agonists in the dorsal BNST block stress-induced relapse to drug seeking behavior (Wang et al., 2001). However, recent work has shown that the PBN projects to the CeA and the vlBNST with differing densities (Bienkowski and Rinaman, 2013). In future work, it may be interesting to more closely study the impact of the PBN input to these regions on synaptic transmission. Here I demonstrate that optogenetic strategies can be utilized to explore neuromodulation of excitatory synapses from selective inputs to the BNST *ex*

vivo.

α_2-ARs Regulate Axosomatic Synapses in the Extended Amygdala and in the Cerebellum

This work in the context of other studies suggests similarity in PBN control of extended amygdala neurons and in climbing fiber control of Purkinje cells. First, the PBN input to the BNST shares anatomical features with the climbing fiber input in the cerebellum with heavy axosomatic innervation (Eccles et al., 1966; Shimada et al., 1989). Second, both generate two types of responses upon stimulation: pronounced firing or feed-forward inhibition (Mathews et al., 2012). Third, both inputs are selectively regulated relative to other glutamate afferents in the respective regions by α_2-ARs (Carey and Regehr, 2009).

I observed that the PBN-initiated current-clamp responses in BNST have differential sensitivity to guanfacine. Both the multiple types of post-synaptic responses in the BNST to PBN stimulation and the variable sensitivity of these responses to guanfacine highlight the complex microcircuitry of the BNST. The BNST is composed of many cell types (Hammack et al., 2007), therefore it is not surprising that these post-synaptic responses show variable sensitivity to guanfacine, in particular the feed-forward PBN-inhibited responses where sensitivity of the intermediary interneuron to guanfacine is also a factor. These data suggest that guanfacine administration may preferentially filter inhibition of one cell type over activation of another by the PBN. In future studies, determining the nature of these neurons, in particular whether they are projection neurons or interneurons, will begin to provide a more complete picture of how

this circuit is regulated. Further, I cannot rule out the possibility of infection by the ChR2-expressing viral vector of CGRP-negative projections from the PBN to the BNST that could influence these responses in unforeseen ways.

Evidence for a Possible Excitatory Role of α_{2A}-ARs in the BNST

To my surprise, I observed an increase in the size of an optically-induced field potential by guanfacine in Thy1-COP4 mice. These mice have no observed colocalization of the neuropeptide CGRP, a marker of one PBN input to the BNST, with ChR2-YFP and have very low postsynaptic expression of ChR2 in the BNST, suggesting that α_{2A}-ARs may enhance the actions of another excitatory input to the BNST. As shown in Figure 5, we do observe expression of the α_{2A}-ARs on other presynaptic terminal types. Another possibility is that post-synaptic α_{2A}-ARs in the BNST may increase excitability of BNST cells. For example, post-synaptic α_{2A}-ARs can increase excitability by modulation of I_h, as has been shown in the prefrontal cortex (Wang et al., 2007). Furthermore, i.p. injections of guanfacine increase c-fos expression in the BNST, suggesting a possible excitatory role for α_{2A}-ARs (Savchenko and Boughter, 2011), though other mechanisms could underlie the increase in c-fos expression with i.p. injection of guanfacine. Finally, it is also possible that guanfacine is decreasing $GABA_B$ signaling or increasing glutamatergic signaling from another input. We will further discuss the putative excitatory role for α_{2A}-ARs in the second chapter of this dissertation.

The PBN Input May Influence Downstream BNST Signaling

Because of the behavioral effects of activation of α_{2A}-ARs in the BNST, it seems likely that the depression of the PBN input to the BNST by guanfacine that we observe here may alter downstream signaling of the BNST to brain regions involved in addiction and relapse such as the VTA (Georges and Aston-Jones, 2001, 2002; Dumont and Williams, 2004; Silberman et al., 2013) and the NAc (Dong et al., 2001). Alterations in the BNST's outputs may curb stress-induced drug cravings or stress-induced re-emergence of negative symptoms of withdrawal. In fact, it has been shows that guanfacine treatment reduces withdrawal-induced anxiety in rats treated with guanfacine (Buffalari et al., 2012). Additionally, it has been shown that injection of an α_2-AR agonist into the BNST will block withdrawal-induced place aversion (Delfs et al., 2000). Therefore, a decrease in excitatory transmission from the PBN to the BNST by α_{2A}-ARs may decrease the aversive withdrawal-like symptoms brought on by stress and help to prevent relapse.

In addition to stress-induced relapse to drug-seeking behaviors, the modulation of BNST signaling by the PBN input may influence anxiety-like behaviors and fear-conditioning (Sink et al., 2011; Sink et al., 2013b; Sink et al., 2013a; Gungor and Pare, 2014). The PBN input to other regions of the extended amygdala has been implicated in feeding behavior (Carter et al., 2013) and pain sensitization (Han et al., 2005; Han et al., 2010). The PBN efferents have also been implicated in taste aversion (Mungarndee et al., 2006) and hypercapnic arousal (Kaur et al., 2013). Therefore, the optogenetic strategies outlined in this

study for the targeting of PBN inputs to the extended amygdala and other brain regions could be beneficial in better understanding a wide range of conditions, from anxiety disorders, to disorders of energy homeostasis, to pain disorders, to sleep apnea.

In summary, this work demonstrates divergent actions of the PBN input on cell responses in the BNST. I demonstrate that depolarizing effects of the PBN appear to be preferentially reduced by the α_{2A}-AR agonist guanfacine. Finally, we show that in the relative absence of PBN signaling, guanfacine has very different actions on BNST excitability, suggesting a state-dependent aspect to the actions of guanfacine. In future work, it will be important to examine the consequences of specific regulation of the PBN in vivo by guanfacine.

CHAPTER III

α_{2A}-Adrenergic Receptors Can Increase Postsynaptic Responses to Excitatory Inputs to the Bed Nucleus of the Stria Terminalis

Introduction

The bed nucleus of the stria terminalis (BNST) is a brain region that is shown to play a critical role in stress-induced relapse to drug-seeking behavior (Briand et al., 2010). α_2-AR agonists are capable of blocking stress-induced reinstatement of drug-seeking behavior in rats with both peripheral administration (Erb et al., 2000; Shaham et al., 2000; Highfield et al., 2001; Mantsch et al., 2010) and also with direct administration into the BNST (Wang et al., 2001). Recent clinical studies support therapeutic potential for α_2-AR agonists, as α_2-AR agonists have shown promise in curbing cravings in drug-addicted individuals (Sinha et al., 2007; Jobes et al., 2011; Fox and Sinha, 2014; Fox et al., 2014). However, the efficacy of the α_{2A}-AR agonist guanfacine in preventing stress-induced relapse of drug-seeking in humans has not been as great as predicted by rodent models (Fox and Sinha, 2014; Fox et al., 2014).

This diminished efficacy of guanfacine in preventing relapse may be due to competing actions of guanfacine-mediated α_{2A}-AR activation in the BNST. The multiple effects of α_{2A}-AR in the BNST include: a presynaptic decrease in norepinephrine release, a presynaptic decrease in excitatory transmission from the PBN input to the BNST as discussed in chapter 1, increased postsynaptic response to other glutamatergic inputs which will be discussed in this chapter,

and a postsynaptic population of α_{2A}-ARs on BNST neurons whose actions need further investigation. In particular, the increased postsynaptic response to other glutamatergic inputs by α_{2A}-ARs is a novel finding in the BNST (Flavin et al., 2014). However, it has previously been shown in the PFC that postsynaptic α_{2A}-ARs can enhance excitability of PFC neurons through downstream closing of HCN channels (Wang et al., 2007). Therefore, while an excitatory action of α_{2A}-ARs in the BNST is relatively novel, α_{2A}-ARs have been shown to have excitatory actions in other parts of the brain. It is not known whether this excitatory action of α_{2A}-ARs in the BNST complements the described decrease in excitatory transmission to the BNST (Chapter II) in preventing stress-induced relapse of drug-seeking behavior (Shields et al., 2009; Flavin et al., 2014), or if these actions work at cross purposes. Therefore, it will be important to further investigate the mechanism and timing of the excitatory actions of α_{2A}-ARs in the BNST, as further understanding this mechanism could help in increasing the efficacy of guanfacine in preventing stress-induced relapse of drug-seeking.

In summary, while there are multiple roles of α_{2A}-ARs in the BNST, it is not yet understood whether these actions work together to influence stress-induced relapse behavior or whether these actions contend with each other. I hope that a better understanding each of these roles of α_{2A}-ARs in the BNST will allow for more selective targeting of guanfacine therapy in humans to increase the efficacy of guanfacine in preventing stress-induced relapse of drug-seeking in addicts. In this chapter, I will further investigate a potential excitatory role for α_{2A}-ARs in the BNST.

Evidence for several effects of guanfacine in the BNST

Recent evidence suggests that the less-than-expected efficacy of guanfacine in preventing stress-induced relapse in addicted individuals may be due to multiple, possibly competing, effects of guanfacine in the BNST (Savchenko and Boughter, 2011; Flavin et al., 2014). Previous work has shown that α_2-AR agonists depress excitatory transmission in the BNST (Egli et al., 2005; Shields et al., 2009; Flavin et al., 2014). However, recent work shows an increase in c-fos expression with i.p. injection of the α_{2A}-AR agonist guanfacine (Savchenko and Boughter, 2011). Further, field potential recordings done in Thy1-COP4 mice that do not show colocalization of ChR2 with CGRP in the BNST have an increase in excitatory optical field potentials with guanfacine application (Flavin et al., 2014) (Figure 8). Taken together, these data indicate an increased postsynaptic response of α_{2A}-ARs in the BNST to other glutamatergic inputs. This chapter will seek to further investigate this excitatory role for α_{2A}-ARs in the BNST.

Guanfacine may increase c-fos expression in the BNST through several possible mechanisms

There are several possible mechanisms that could account for this increase in c-fos expression in the BNST. First, an increase in excitatory transmission from one or more inputs to the BNST may be responsible for the increased c-fos expression. This increase in excitatory transmission from a particular input to the BNST may be masked by the large PBN input during field potential recordings (Flavin et al., 2014).

Another possibility is that α_{2A}-ARs increase the intrinsic excitability of a specific population of cells in the BNST. For example, it has been shown in the prefrontal cortex that guanfacine can increase intrinsic excitability of PFC cells through α_{2A}-AR-mediated closing of post-synaptic HCN channels (Wang et al., 2007). A similar mechanism may be occurring in the BNST, as it has been shown that certain types of BNST cells express mRNA from HCN channels (Hammack et al., 2007; Hazra et al., 2011).

Finally, it is possible that guanfacine decreases inhibitory transmission from $GABA_B$ inputs. The $GABA_A$ antagonist picrotoxin was bath applied during the field potential recordings in the Thy1-COP4 mice (Figure 8), so modulation of $GABA_A$ transmission by guanfacine can be ruled out as a mechanism. However, a decrease in $GABA_B$ inhibitory transmission could lead to an increase in c-fos expression by downstream relief of inhibition on this population of cells.

It is important to understand the properties of the population of BNST neurons that are activated by α_{2A}-ARs, as these neurons may influence transmission of projections from the BNST to stress and reward circuitry and modulate stress-induced reinstatement behavior. I will be testing the hypothesis that a population of BNST neurons is activated by α_{2A}-ARs and explore the properties of this neuronal population. In this chapter, I will first investigate whether guanfacine-mediated depression of excitatory transmission in electrical field potential recordings is preserved in slices in which I observe enhancement of optical field potentials. This would suggest that certain inputs that are stimulated in these electrical recordings, but not in the optical recordings, might

mask the excitatory effect of guanfacine. I will next replicate the finding that i.p. guanfacine increases c-fos expression in the BNST and then try to characterize this population of neurons through electrophysiological recordings and immunohistochemistry. Finally, I will address the possible mechanisms for increased c-fos expression and increased field potential size with guanfacine as described above.

Methods

Fluorescent Immunohistochemistry

For colocalization studies of c-fos-eGFP with CGRP and calbindin, 4 transgenic c-fos-eGFP mice (Barth et al., 2004) (B6.Cg-Tg(Fos/EGFP)1-3Brth/J, The Jackson Laboratory) were transcardially perfused with 10 mL of ice-cold phosphate-buffered saline (PBS), followed by 20 mL of ice-cold 4% paraformaldehyde in PBS. Brains were post-fixed in 4% paraformaldehyde overnight at 4°C and were then transferred into 30% sucrose and stored for 2 to 10 days at 4°C. Coronal sections of were cut on a cryostat (Leica, CM3050S) at a thickness of 40 µM. Sections containing the BNST were free-floated in PBS for immuno-labeling. Sections were permeabilized for 30 minutes with 0.5% Triton-X 100 in PBS at room temperature (RT). Next, non-specific binding was blocked with 10% normal donkey serum in PBS containing 0.1% Triton-X-100 for one hour at RT. Sections were then incubated in primary antibody in PBS containing 0.1% Triton-X-100 for 2 days at 4°C, followed by 4 x 10 minute PBS washes.

Sections were then incubated overnight at 4°C with secondary antibodies in PBS containing 0.1% Triton-X-100. Finally, sections were washed with PBS (4 x 10 minutes), mounted on Fisher + slides (Fisher Scientific) and coverslipped with PolyAquamount (Polysciences).

Prior to transcardial perfusion, the c-fos-eGFP mice were handled for 5 days. The three final of the handling days included saline injections in order to habituate mice to injections such that the likelihood of any increase in c-fos-eGFP expression being due to stress from injections rather than guanfacine effects was reduced.

Images of fluorescent marker-labeled brain sections were taken with a Zeiss 710 confocal microscope. Lenses used included a 20X/0.80 N.A. Plan-Apochromat and a 63X/1.4 N.A. Plan Apochromat oil. Excitation/emission wavelengths (nm) for each fluorophor were; Dylight 405, 405/410-505; YFP, 512/519-553; cy3, 561/566-600; cy5, 633/638-759. Mosaic image stitching was done with Zeiss ZEN software.

Diaminobenzidine (DAB) Immunohistochemistry

Eight, 4-month-old male C5BL/6 mice were used, with four mice in each treatment group. Prior to treatment, the mice underwent a progressive handling regimen for 5 days, as previously described by our lab in efforts to reduce stress due to injections on treatment day (Olsen and Winder, 2010). After 5 days of handling, mice were given an i.p. injection of guanfacine (Tocris) at a dose of 1

mg/kg 90 minutes prior to transcardial perfusion. Control mice were given an equivalent amount by volume of saline 90 minutes prior to transcardial perfusion.

Mice were transcardially perfused as described above and 40 μm coronal brain slices were prepared for DAB immunohistochemistry. Sections containing the BNST were free-floated for immunolabeling. Sections were be blocked with 5% normal goat serum containing 0.1% Trition-X-100 in PBS. Sections were then incubated in primary antibody (Fos antibody anti-rabbit, EMDBiosciences) at a concentration of 1:20,000 for 2 days at 4° C, followed by incubation with goat-anti-rabbit-biotinylated secondary antibody (Vector) for 90 minutes at RT. Sections were then incubated in avidin-biotin-complex solution (Vector) for 60 minutes at RT. Finally, DAB staining was developed with the DAB Kit (Vector). Stained sections were mounted on slides and allowed to dry overnight. Stained sections were sealed with mounting media (Permount) the following day. For data analysis, manual cell counts were done while blinded to treatment condition in a 0.25 mm^2 square in the ventrolateral region of the dorsal BNST, using Metamorph software. Statistical analysis with unpaired student's t-test was done with Prism software.

Electrophysiology Recordings in the BNST

Brain slice preparation

Brain slice preparation methods were used as previously described (Grueter and Winder, 2005; Grueter et al., 2006). Mice were removed from colony and allowed to rest for one hour in a Med Associates sound-attenuating

chamber. Following the hour of rest, mice were anesthetized with isofluorane and then decapitated. Brains were removed quickly and transferred to a 1-4°C oxygenated, low sodium sucrose dissecting solution (in mM: 194 sucrose, 20 NaCl, 4.4 KCl, 2 $CaCl_2$, $MgCl_2$, 1.2 NaH_2PO_4, 10 glucose, 26 $NaHCO_3$). A Leica vibratome was used to prepare coronal brain slices (300 μm) containing the dorsal BNST. Slices were then transferred to either an interface chamber for field potential recordings or to a holding chamber for whole cell recordings. Both the interface chamber and the holding chamber contained heated, oxygenated artificial cerebral spinal fluid (ACSF) that was composed of (in mM): 124 NaCl, 4.4 KCl, 2.5 $CaCl_2$, 1.3 $MgSO_4$, 1 NaH_2PO_4, 10 glucose, 26 $NaHCO_3$.

Alternating field potential recordings

For field potential recordings, Thy1-COP4 transgenic mice of at least 5 weeks in age were used. Slice preparation for field potential recordings in the dlBNST was performed as previously reported (McElligott and Winder, 2008). Picrotoxin (25 μM) was added to all recordings to isolate excitatory transmission. For alternating electrical-optical field potential recordings, light stimulation was produced from a Lamba XL light source (Sutter instruments) and shone through a bandpass filter (Semrock, 475 nm wavelength, 20 nm bandwidth). The blue light was guided from the light source through a water-shielded cable that was positioned approximately 5 cm above the surface of the slice, resulting in full-field illumination. The light stimulation produced a shift in potential, the optical field potential (oN) that was shown to be NBQX sensitive (decreased 76% from

mean), similar to the N2 seen in electrical field potential recordings previously described (Weitlauf et al., 2004; Egli et al., 2005). In alternating electrical-optical field potential recordings, the electrical portion of the field potential recording was performed as previously described (McElligott and Winder, 2008). pClamp software (Axon Instruments) controlled light and electrical pulse duration and frequency. Light stimuli were approximately 2 ms in duration and occurred every 40 seconds. Electrical stimulation occurred every 40 seconds and alternated with the optical stimulation such that the slice received either electrical or optical stimulation once every 20 seconds.

Analysis of field potential recordings

All field potential recordings were analyzed via Clampfit 9.2 (Molecular Devices) as previously described (Shields et al., 2009). All field recordings contain a 20 min baseline prior to agonist application and all data points are normalized to the baseline 5 minutes prior to agonist application. Plotted time courses for field experiments are represented as one-minute averages.

Whole cell recordings

Current clamp whole cell Recordings in c-fos-eGFP mice

Transgenic c-fos-eGFP mice (Barth et al., 2004) (B6.Cg-Tg(Fos/EGFP)1-3Brth/J, The Jackson Laboratory) were injected with 1 mg/kg of guanfacine (Tocris) 90 minutes prior to brain slice preparation, as previously described (Egli and Winder, 2003; Grueter and Winder, 2005), to induce c-fos-eGFP expression

in the BNST. The excitable membrane properties of c-fos-eGFP-expressing BNST neurons were characterized in a manner similar to that previously published by our lab (Egli and Winder, 2003). It has been previously shown that populations of cells in the BNST can be characterized using their electrical properties (Egli and Winder, 2003; Dumont and Williams, 2004; Hammack et al., 2007). Recordings were done in current clamp mode at the neurons' resting membrane potential and we tested the response of the neuron's membrane potential to positive and negative current injections in a manner similar to as described above for BNST neurons innervated by the PBN. Neurons were depolarized to characterize action potential firing threshold and frequency. Neurons were also hyperpolarized by tonic current injection to look for the presence of a depolarizing sag with hyperpolarization (Egli and Winder, 2003; Hammack et al., 2007).

Voltage clamp whole cell Recordings in c-fos-eGFP mice

Using electrical stimulation, I assessed the response of c-fos-eGFP positive BNST neurons to subsequent *ex vivo* application of guanfacine. Transgenic c-fos-eGFP mice were injected with guanfacine and prepared for electrophysiological recordings as described above. Electrically-evoked EPSCs were recorded from c-fos-eGFP positive neurons in the dorsal BNST as described previously by our lab (Shields et al., 2009). *Ex vivo* guanfacine (Tocris) was applied at a concentration of 1 μM for 10-20 minutes. Excitatory transmission was isolated by bath application of 25 μM picrotoxin throughout the

duration of the experiment. Student's paired t-test was then used to determine if guanfacine had a significant effect by comparing baseline values to the changes induced by guanfacine.

All whole cell data were recorded with Clampex version 10.2 and analyzed with pClamp version 10.2 (Molecular Devices). Recordings contained a 5 to 10 minute baseline recording prior to drug application. All data points were normalized to the first 5 minutes of baseline. Plotted time courses for whole-cell experiments are represented as 30 second averages.

Statistics

Experiments comparing a difference to baseline were analyzed using a student's T-test. Experiments with multiple drug treatments were analyzed using a One-way repeated measures ANOVA and a Geisser-Greenhouse correction. Experiments comparing baseline levels of c-fos positive neurons to guanfacine-treated c-fos positive neurons in IHC experiments were done using an unpaired T-test. Results are reported in text and figure legends. Significant differences were defined as having a $P<0.05$.

Results

Decrease in stimulation of PBN input to the BNST reveals excitatory actions of α_{2A}-AR activation

As discussed in Chapter 1 of this dissertation, in examining ChR2-YFP expression in Thy1-COP4 transgenic mice, I determined that while ChR2-YFP was heavily expressed in regions that project to the BNST such as the BLA, cortical regions, and the hippocampus, ChR2-YFP did not co-localize with CGRP-immunoreactivity in the BNST (Figure 8). This lack of colocalization between ChR2-YFP and CGRP suggested that PBN axons in the region would not be recruited by blue-light stimulation in the BNST, while cortical, amygdalar, and other afferents would be activated. I prepared *ex vivo* slices from Thy1-COP4 transgenic mice and attempted to perform optical field potential recordings in the dBNST. I found that full-field optical stimulation in BNST slices from Thy1-COP4 mice produced a synchronized field potential response that was substantially reduced by AMPA receptor antagonists (76.2% from baseline), which is consistent with N2 responses that we have previously published and indicates low, if any, postsynaptic expression of ChR2 (Egli et al., 2005). This indicates only a small amount of expression of ChR2 in postsynaptic BNST neurons in this mouse line and that the optical field potential elicited is driven by recruitment of glutamatergic afferents. I found that I was able to elicit optical field potentials ("oN") that were similar in size to our previously published N2 responses (Egli et al., 2005). Given the lack of co-localization between ChR2-YFP with CGRP, as well as and the lack of heavy post-synaptic ChR2

expression, this Thy1-COP4 mouse allowed us to begin to look at guanfacine effects on non-PBN afferents into the BNST.

I applied guanfacine (10 μM) to "alternating" field potential recordings, in which optical stimulation of the *ex vivo* BNST slice was alternated with electrical stimulation of the slice. In these alternating field potential recordings, an enhancement of the oN was seen (Figure 9A) (9.8% ± 2.9%, $t(5)=3.3$, $p<0.05$, $n=6$) in the same slices that we observed a depression of the electrical field potential (Figure 9B) (29.5% ± 7.4%, $t(5)=3.96$, $p<0.02$, $n=6$). Therefore, guanfacine produces an enhancement of field potential size with optical stimulation that of inputs that show no colocalization of CGRP with ChR2-YFP, likely indicating a substantial reduction of PBN afferent stimulation, and a depression of glutamatergic transmission in field responses with electrical stimulation that includes the PBN. These results may indicate that the large, axosomatic PBN input masks a potential excitatory role for α_{2A}-ARs in the BNST.

Intraperitoneal guanfacine increases c-fos expression in the dorsal BNST

Next, I examined the findings of Savchenko et al. (2010) that showed that c-fos expression in the BNST is significantly increased with i.p. injection of guanfacine. In the work done by Savchenko et al. (2010), the mice were not handled or habituated to injection prior to i.p. injection of guanfacine and transcardial

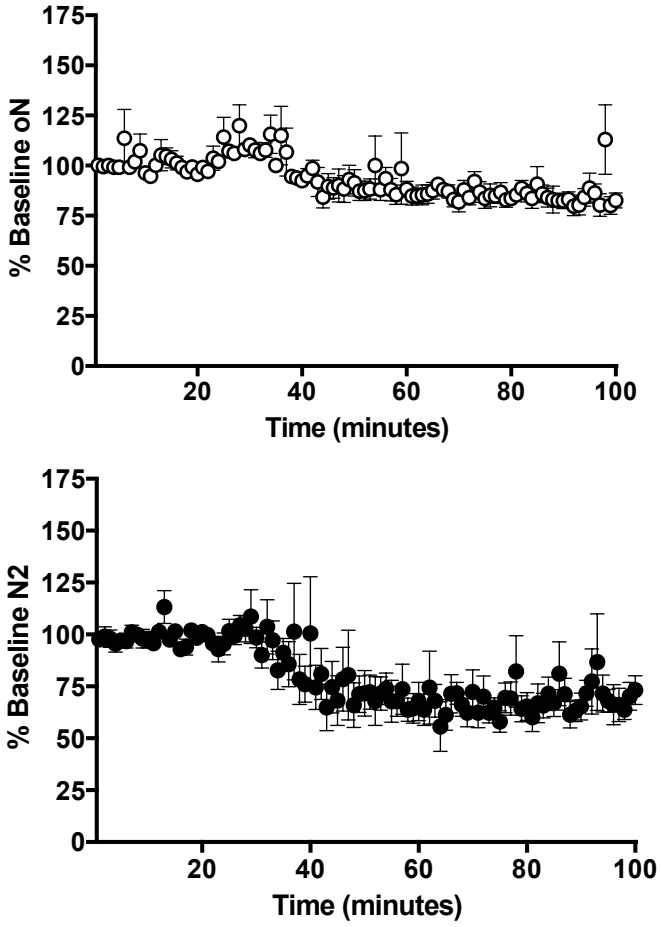

Figure 9. Alternating electrical and optical stimulation of the BNST in Thy1-COP4 mice yields two different responses. A. Guanfacine application to optical field potential recordings in the BNST of Thy1-COP4 mice leads to an increase in field potential size. B. Guanfacine application to electrical field potential recordings in the BNST of Thy1-COP4 mice leads to a decrease in field potential size.

perfusion. Therefore, it is possible that the increase in c-fos expression that was seen was due to stress experienced with injection. I tried to control for injections in our experiment by handling the mice five days prior to i.p. injection of guanfacine and transcardial perfusion. The five-day handling paradigm included

three days of exposure to injection through i.p. saline injections. I performed diaminobenzidine (DAB) IHC staining for c-fos in free-floated slices prepared from transcardially perfused mice that received an i.p. injection of guanfacine two hours prior to killing. I saw a significant increase in c-fos expression in the BNST after i.p. injection of guanfacine as compared to saline-injected animals ($t(6)=2.7$, $n=8$, $p<0.05$), consistent with previous Savchenko et al. (2010) (Figure 10).

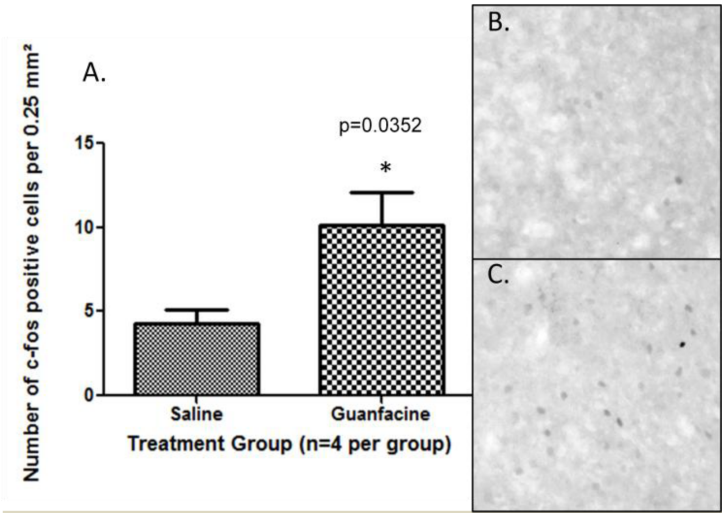

Figure 10. *In vivo* α_{2A}-AR agonists activate dorsal BNST neurons. A. Enhancement of c-fos expression in the dorsal BNST after i.p injection of guanfacine (1 mg/kg) as compared to saline injection (p=0.03). B. c-fos staining in dorsal BNST of saline injected mouse. C. c-fos staining in dorsal BNST of guanfacine injected mouse.

Characterization of c-fos-eGFP cells in the BNST after in vivo guanfacine

Once I established that there is a significant increase in expression of c-fos in the BNST of guanfacine-injected animals as compared to saline-injected animals, I next sought to characterize this population of cells that express c-fos in

response to i.p. guanfacine. We used both fluorescent immunohistochemistry and current clamp whole cell analyses to try to find common characteristics of the population of cells in the BNST that expresses c-fos in response to i.p. guanfacine injection.

Previous work suggests that neurons in the BNST can be divided into sub-groups according to electrophysiological characteristics (Egli and Winder, 2003; Dumont and Williams, 2004; Hammack et al., 2007). In trying to identify the electrophysiological properties of BNST neurons that are activated by *in vivo* administration of guanfacine, I made use of transgenic c-fos-eGFP mice. These c-fos-eGFP mice were made in the Barth lab and express GFP under the control of the activity dependent c-fos gene (Barth et al., 2004). These transgenic mice express a c-fos-eGFP fusion protein when the c-fos gene is turned on with cell activity (Barth et al., 2004). I handled each of these transgenic mice for the five days prior to recordings in the same manner that I handled the mice prior to transcardial perfusion for DAB staining as described above. I then injected the transgenic mice with i.p. guanfacine (1 mg/kg) ninety minutes to two hours prior to *ex vivo* slice preparation. During my electrophysiological recordings, I injected step-wise depolarizing and hyperpolarizing currents into the cell while recording in current clamp configuration (Figure 11). I found that c-fos-eGFP positive cells that I record from displayed I_h currents at hyperpolarizing potentials and fire rapidly at depolarizing potentials (Figure 11). The resting membrane potentials of the c-fos-eGFP cells rested between -60 mV and -80 mV.

I also sought to determine if staining for certain fluorescent immunohistochemical markers would help us to identify the population of c-fos-eGFP neurons. Prior work suggests that subpopulations of BNST neurons can also be classified based on expression of neuropeptides (Day et al., 1997; Day et al., 1999; Day et al., 2001; Day et al., 2005), such as corticotrophin releasing factor (CRF). CRF signaling has previously been demonstrated by our lab

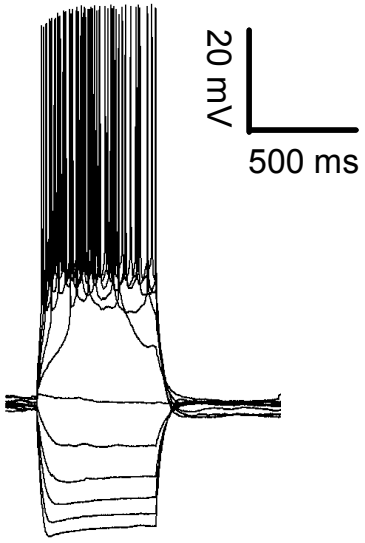

Figure 11. Representative traces of step-wise current injection into c-fos-eGFP positive cell. Two hours after i.p. guanfacine injection (1 mg/kg) c-fos-eGFP positive cells in the BNST were injected with step-wise hyperpolarizing and depolarizing current and cell responses were recorded. The majority of cells displayed Ih current with hyperpolarizing current steps and fired with depolarizing current steps.

to modulate NE signaling in the BNST (Nobis et al., 2011). Calbindin is expressed in inhibitory neurons in the BNST (Fudge and Haber, 2001; Gos et al., 2013). In order to facilitate the fluorescent staining, I perfused transgenic c-fos-

eGFP mice that had been handled for 5 days prior to transcardial perfusion, as has been described above for DAB staining. Ninety minutes to two hours prior to perfusion, the mice received an i.p. injection of guanfacine (1 mg/kg) in order to induce c-fos-eGFP expression in the guanfacine-activated cell population. I also injected another set of handled c-fos-eGFP mice with saline as a control group. After transcardial perfusion, we prepared free-floating slices for immunohistochemistry staining. We then stained one set of BNST slices for calbindin and another set of BNST slices for CGRP. We found that some of the c-fos-eGFP colabeled for calbindin (Figure 12), while others did not. There were very few colabeled cells in the guanfacine-injected group as well as in the saline injected group. We also saw some c-fos-eGFP cells that were surrounded by CGRP staining while others did not (Figure 12). Again, there were comparable levels of CGRP-surrounded c-fos-eGFP cells in guanfacine-injected versus saline-injected mice. Altogether, these data suggest a heterogeneity of the c-fos–eGFP positive cells in the BNST after i.p. guanfacine.

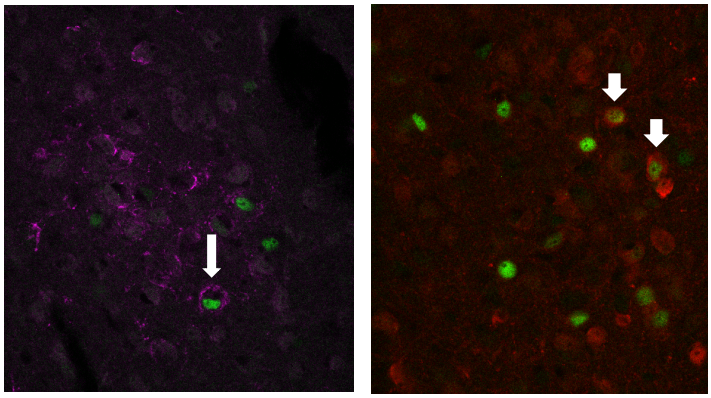

Figure 12. C-fos-eGFP positive cells in the BNST do not colabel with CGRP or calbindin staining. A. Staining of c-fos-eGFP positive BNST cells (green) are sometimes surrounded by CGRP staining (purple) ninety minutes after guanfacine injection (1 mg/kg, i.p.) (white arrow). B. C-fos-eGFP positive cells (green) sometimes colocalize with calbindin staining (red) ninety minutes after guanfacine injection (1 mg/kg, i.p.). Colocalization is shown with white arrow.

Ex vivo guanfacine application decreases excitatory transmission to c-fos-eGFP positive cells after in vivo guanfacine

The increase in c-fos expression with *in vivo* guanfacine suggests an α_{2A}-AR-mediated increase in postsynaptic response to some glutamatergic inputs. I first hypothesized that the c-fos-eGFP positive cells that are activated by *in vivo* guanfacine are activated by an increase in excitatory transmission from a particular input to the BNST. To test this hypothesis, I prepared *ex vivo* brain slices from transgenic c-fos-eGFP mice that had been injected with i.p. guanfacine (1 mg/kg) ninety minutes to two hours prior to slice preparation. These mice were also handled for five days prior to recording, as described above.

I performed whole-cell voltage clamp recordings using electrical stimulation of the stria terminalis, a fiber bundle that carries afferent fibers to the BNST, and recorded in the presence of picrotoxin (25 μM) to isolate excitatory transmission. I then bath-applied guanfacine to voltage-clamped whole cell recordings of EPSCs from c-fos-eGFP cells. I saw that EPSCs decreased in size with guanfacine application to *ex vivo* slices, indicating a decrease in excitatory transmission to c-fos-eGFP positive cells (Figure 13) (54.4% ± 3.0%, $t(6)=18.0$, $p<0.001$, $n=7$). Because there are some cells in the BNST that express c-fos basally without i.p. guanfacine treatment, I made sure to look for variability in guanfacine sensitivity among the c-fos-eGFP cells from which I recorded, since inputs to the c-fos-eGFP cells that are c-fos-eGFP positive basally may be differentially modulated by *ex vivo* guanfacine application compared to cells that express c-fos-eGFP in response to α_{2A}-AR activation, and I do not know whether the c-fos-eGFP cells I record from basally express c-fos-eGFP or are expressing c-fos-eGFP in response to i.p. guanfacine. However, I saw little variability among recordings and noted that excitatory transmission to c-fos-GFP positive cells decreased with ex vivo guanfacine application across all experiments (N=7).

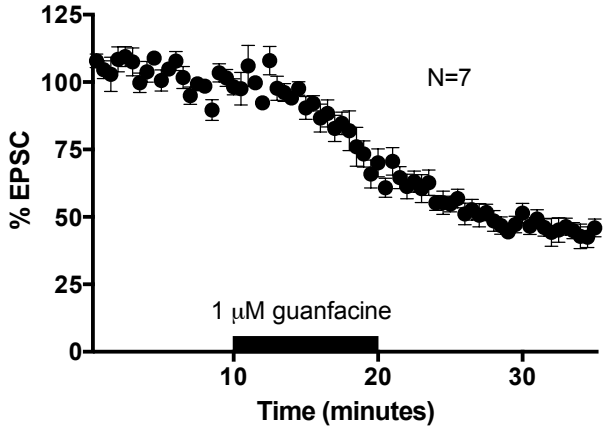

Figure 13. *Ex vivo* guanfacine decreases excitatory transmission to c-fos-eGFP positive cells in the BNST. Voltage clamp whole cell recordings were done from c-fos-eGFP positive cells in the BNST of ex vivo brain slices prepared two hours after guanfacine injection (i.p., 1 mg/kg). Bath application of guanfacine to recordings resulted in decreased excitatory transmission to these c-fos-eGFP positive cells.

We noted that it was possible that we did not see any changes in sensitivity to *ex vivo* guanfacine application because of alterations in α_{2A}-AR sensitivity due to prior i.p. guanfacine treatment. However, I have found that the effects of guanfacine on electrical field potential recordings in the in the BNST are readily reversible with subsequent atipamezole treatment (Figure 14A) ($F(2,5)=1.53$, n.s., n=6). The effects of guanfacine do not reverse without subsequent atipamezole treatment (Figure 14B) (32.8% ± 9.9%, $t(3)=3.3$, $p<0.05$, n=4). Additionally, i.p. injection with an alternate α_2-AR agonist clonidine prior to ex vivo brain slice preparation does not occlude subsequent depression of excitatory transmission by ex vivo guanfacine (Figure 15) (30.1% ± 6.6%, $t(5)=4.6$, $p<0.01$, n=6), as compared to depression of excitatory transmission

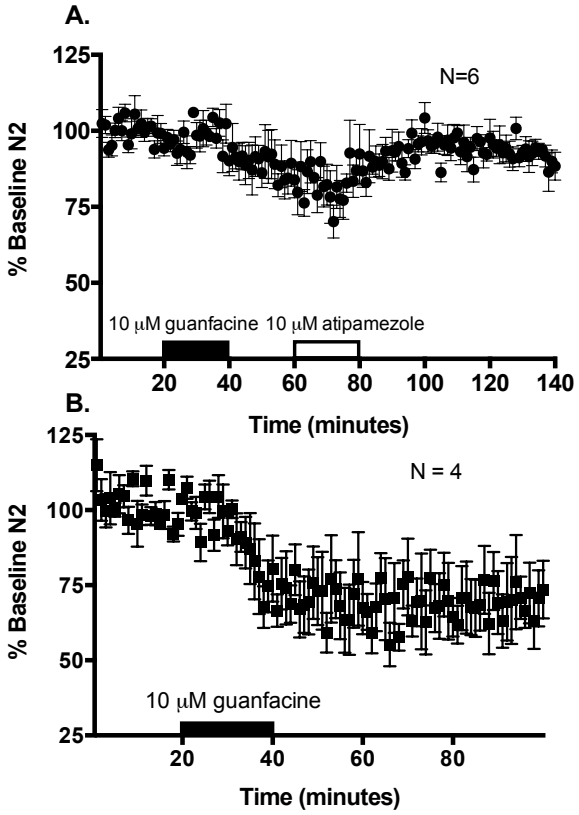

Figure 14. Guanfacine depression is reversible with α_2-AR antagonist atipamezole. A) Field potential recordings done with electrical stimulation reveal that guanfacine will decrease excitatory transmission in the BNST and that this depression is reversed by subsequent atipamezole. B). The decrease in excitatory transmission caused by guanfacine will not reverse with prolonged washout with normal ACSF.

seen in naïve ex vivo brain slices that are treated with guanfacine (32.8% ± 9.9%, $t(3)=3.3$, $p<0.05$, $n=4$). These data together suggest that it less likely that in vivo guanfacine permanently altered excitatory transmission prior to *ex vivo* recordings since α_{2A}-AR-mediated depression of excitatory transmission is readily reversible (Figure 14) and i.p. clonidine also does not alter sensitivity to subsequent guanfacine (Figure 15). Therefore, it seems unlikely that the increase

in c-fos-eGFP expression with i.p. guanfacine is due to α_{2A}-AR-mediated increases in excitatory transmission from particular inputs to this population of cells.

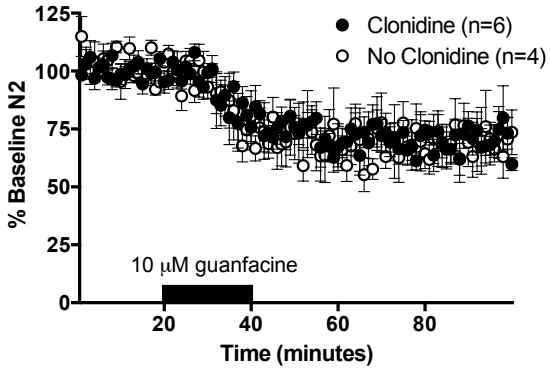

Figure 15. Prior intraperitoneal injection with clonidine does not occlude depression of excitatory transmission by subsequent guanfacine. There is no observed difference in the depression of excitatory transmission in electrical field potential recordings in wild-type mice that had been injected with clonidine thirty minutes prior to *ex vivo* brain slice preparation versus naïve mice.

Discussion

In our exploration of Aim 2 of this dissertation, I found two pieces of evidence that further support a potential excitatory role for α_{2A}-ARs in the BNST that I first observed in Figure 7 of Chapter 1 of this dissertation. First, I found that I was able to observe guanfacine-mediated enhancement of optical field potentials within the same Thy1-COP4 slices that I observe depression of electrical field potentials. Since Thy1-COP4 mice have no observed colocalization of CGRP and ChR2-YFP, these data seem to indicate that

excitatory effects of α_{2A}-ARs can be discerned when there is a relative lack of stimulation of the PBN afferents to the BNST. I also saw that, even with the addition of five days of handling and acclimation to injections, there is an increase in c-fos expression in the BNST with i.p. injection of guanfacine (1 mg/kg), consistent with previous findings (Savchenko and Boughter, 2011). Both the increased c-fos expression as well as the increased field potential size in Thy1-COP4 mice suggest a potential excitatory role for α_{2A}-ARs in the BNST, which is unexpected considering that the presynaptic $G_{i/o}$-coupled α_{2A}-ARs result in a decrease in excitatory transmission in electrically-stimulated field potential and whole cell recordings in the extended amygdala (Dumont and Williams, 2004; Delaney et al., 2007; Shields et al., 2009) through a reduction in presynaptic glutamate release (Delaney et al., 2007; Shields et al., 2009).

I made several attempts to determine the mechanism by which c-fos expression is increased in hopes of better understanding the excitatory role of α_{2A}-ARs. I performed fluorescent immunohistochemical staining and whole cell current clamp electrophysiological recordings in BNST slices prepared from c-fos-eGFP transgenic mice in an effort to see if the population of c-fos-eGFP positive cells had any unifying characteristics. I did not find any common markers among the c-fos-eGFP positive cells for either the calbindin staining or the CGRP staining that I performed on slices prepared from c-fos-eGFP mice that had received i.p. injection of guanfacine (Figure 12).

I did observe some common electrophysiological characteristics of the c-fos-eGFP positive cells, including the presence of an I_h current. The presence of

the I_h current in the c-fos-eGFP positive cells was consistent with previous work that found the presence of HCN1 mRNA in some BNST cell types. The presence of the I_h current is also consistent with previous work done in the mPFC that has found that signaling through activated α_{2A}-ARs leads to closing of HCN channels, which results in an increase in excitability of post-synaptic mPFC pyramidal neurons (Wang et al., 2007). Thus, I hypothesized that the increase in c-fos expression in the BNST was due to a closing of postsynaptic HCN1 channels through α_{2A}-ARs and that this closing of HCN1 channels results in an increase in excitability of postsynaptic BNST cells that I was able to detect in optical field potential recordings in the absence of PBN input (Figure 8C, 9A). However, I found no difference in c-fos expression after i.p. guanfacine injected in HCN KO mice versus WT mice (data not shown). There are four forms of HCN channels in the BNST, so it is a possibility that another HCN channel besides HCN1 is involved in c-fos expression (Barth et al., 2004). This possibility will be discussed further in Chapter V.

I next tested the hypothesis that the increase in c-fos expression was due to increased excitatory transmission from a particular glutamatergic input onto the c-fos positive cells. I tested this by recording from c-fos-eGFP positive cells in BNST *ex vivo* slices prepared from c-fos-eGFP transgenic mice that had been injected with guanfacine (1 mg/kg) and handled for five days prior to slicing. I predicted that if excitatory transmission from a particular input to the c-fos-eGFP positive cells were increased by α_{2A}-AR activation, I would see an increase in excitatory transmission with guanfacine application to electrically-stimulated

whole cell voltage clamp recordings. Instead, I saw a decrease in excitatory transmission with subsequent *ex vivo* guanfacine application. Therefore, it seems unlikely that the increase in c-fos expression is due to increased excitatory transmission from a particular input directly onto the c-fos-eGFP positive cells. It is possible that the *in vivo* guanfacine given ninety minutes prior to slicing altered α_{2A}-AR regulation of excitatory transmission, however, this seems unlikely given the reversibility of guanfacine actions (Figure 14) and given that i.p. clonidine treatment does not alter subsequent *ex vivo* guanfacine application (Figure 15). While initial attempts to determine the mechanism of a potential excitatory role for α_{2A}-ARs in the BNST have been unsuccessful, the future work proposed in the Future Directions section of this dissertation may lead insights into the excitatory role of α_{2A}-ARs.

CHAPTER IV

Discussion and Future Directions

Adrenergic receptors in the BNST influence stress-induced relapse of drug-seeking behavior

Evidence implicates ARs in the extended amygdala in stress-induced reinstatement of drug-seeking behavior, with behavioral data showing that β- and α_1-AR antagonists can block stress-induced reinstatement of drug-seeking (Leri et al., 2002; Mantsch et al., 2010; Le et al., 2011; Vranjkovic et al., 2012), while α_2-AR agonists block reinstatement (Wang et al., 2001). α_2-ARs mediate transient depression of excitatory transmission and appear to differentially modulate excitatory inputs to the extended amygdala (Delaney et al., 2007; Flavin et al., 2014). Differential modulation would allow for certain inputs to dominate regulation of synaptic transmission in the extended amygdala depending on the neural context of information reaching the BNST. Integration of inputs to the extended amygdala and modulation of neural activity within the region allow ARs to regulate stress-induced reinstatement of drug-seeking. α_{2A}-ARs also appear to have multiple other functions in the BNST including an excitatory role, modulation of norepinephrine release, and postsynaptic expression whose function has not yet been explored. Therefore, α_{2A}-ARs appear to have complex actions in the BNST that require further study in order to understand the role of each of these functions in stress-induced relapse of drug-seeking behavior.

While some of the key ARs underlying stress-induced relapse to drug-seeking behavior have been identified, there is still work to be done in understanding the specific mechanisms of stress-induced relapse. In particular, there is a need for an understanding of the particular afferent and efferent connections of the BNST that may be modulated by specific ARs. Delaney et al., 2007 have shown that the PBN and BLA inputs to the CeA appear to be differentially modulated by α_2-ARs, and I have shown that the PBN and BLA inputs to the BNST are differentially regulated by α_{2A}-ARs (Flavin et al., 2014). It is quite possible that many of the extended amygdala's inputs and outputs are differentially modulated by ARs. An understanding of such differential modulation would further elucidate the specific neural circuitry underlying stress-induced relapse.

Additionally, the BNST is composed of a heterogenous population of cells, including interneurons and projection neurons. Various types of ARs may differentially regulate excitability of these numerous cell types within the BNST. Both differential modulation of afferents to the BNST and differential excitability of various cell types within the BNST may influence regulation of the BNST's projections neurons. A deeper understanding of how ARs affect the strength of the BNST's downstream projections may elucidate some of the key components of the neural circuitry that are engaged during stress-induced reinstatement of drug-seeking. Thus, investigation of how ARs regulate synaptic transmission in the extended amygdala may also shed light on the therapeutic potential for α_1-

and β-antagonists and α_2-agonists in preventing stress-induced relapse to drug-seeking.

Excitatory transmission from PBN afferents to the BNST is regulated by α_{2A}-ARs

In my work done on Aim 1, I used optogenetic strategies to target the PBN input to the BNST for electrophysiological analysis. I found that optical stimulation of ChR2-expressing PBN afferents in *ex vivo* BNST slices yielded a dual component oEPSC that produced two types of cell-type specific responses. I found that the PBN input to the BNST innervated two potential cell types. In one cell type, stimulation produced robust feed-forward inhibition. In the other, stimulation produced repetitive firing. I found that the α_{2A}-AR agonist guanfacine filtered excitatory drive into the BNST by depressing oEPSCs contributing to the depolarizing effects of the PBN input. Using immunoelectron microscopy of the knock-in HA-tagged α_{2A}-AR mouse strain, we demonstrated that α_{2A}-ARs are present on asymmetric perisomatic synapses, which is consistent with localization to PBN inputs. I also found that removal of the PBN input to the BNST, as indicated by a lack of colocalization of CGRP and ChR2-YFP in the BNST of the Thy1-COP4 mice, reveals a secondary, possibly excitatory, role for guanfacine in the BNST.

The release of CGRP neuropeptide from the PBN may influence synaptic transmission in the BNST

An important future direction for Aim 1 will be to further understand the

effects of the PBN input to the BNST on the microcircuitry of the BNST and to study the impact of the PBN input to BNST on downstream BNST signaling. In order to examine the impact of the parabrachial nucleus input on BNST circuitry, one of the possible next steps will be to investigate whether release of the CGRP neuropeptide from PBN terminals influences the post-synaptic BNST cell firing. We will also need to further elucidate which types of BNST cells are being innervated by the PBN.

The PBN input to the BNST is largely glutamatergic, but the PBN can release CGRP from many of its terminals with appropriate stimulation (Gungor and Pare, 2014). It is possible that the different responses of postsynaptic BNST cells that we see in current clamp (i.e. PBN-excited versus PBN-inhibited) may be partially due to by CGRP release. A differential regulation of these two types of responses by CGRP could have downstream effects on BNST inputs to other regions of the brain involved in stress and reward.

For example, it is possible that the strong firing observed in PBN-activated responses is due to a release of the CGRP neuropeptide. The PBN-activated cells may receive CGRP signaling while the PBN-inhibited do not. In fact, it may be the case that if we block the synaptic transmission of the CGRP neuropeptide in the BNST that we will shift the previously observed ratio of PBN-inhibited to PBN-activated responses (Figure 4). Intense postsynaptic firing produced by CGRP neuropeptide signaling may be mask a PBN-inhibited type response in some cases, making it look like a PBN-activated type response.

In order to further investigate the role of CGRP signaling in the BNST we

will be able to make use of the Calca-Cre mouse line (McCoy et al., 2013). The Calca-cre mouse line expresses Cre recombinase under the CGRP promoter, Calca. Therefore, by injecting a DIO-ChR2 virus into the PBN we will be able to selectively target ChR2 expression to CGRP-expressing neurons in the PBN. We will then be able to record in *ex vivo* slices of dorsal BNST using light stimulation of the ChR2 that will be targeted to the CGRP-expressing PBN input to the BNST and look at changes in PBN-inhibited versus PBN-activated cell populations.

Further classification of types of BNST neurons that receive PBN input

Further classifying the types of neurons in the BNST that are innervated by the PBN and determining how each of these types is influenced by PBN stimulation may help us to understand how the PBN input to the BNST influences downstream signaling of the BNST. We have already attempted to classify the BNST cells that are innervated by the PBN by their electrophysiological characteristics (Figure 4) and their sensitivity to guanfacine (Figure 7). We could further classify these neurons based upon their morphology, which we would be able to examine through cell filling experiments. We could also investigated whether each of the classes of neurons are projection neurons or interneurons.

To determine which of the cells innervated by the PBN are projection neurons we could inject retrograde tracer beads into some of the known downstream targets of BNST projection neurons, such as the NAc (Dong et al., 2001) and the VTA (Georges and Aston-Jones, 2001, 2002; Dumont and Williams, 2004). In these same animals we could then inject AAV-CaMKIIα -

ChR2-YFP into the PBN. We would then transcardially perfuse some of these animals to look for ChR2-YFP-labelled axosomatic innervation of BNST projection neurons that are labeled by retrograde tracer beads that have been injected into either the VTA or the NAc. This would give us some initial evidence that projection neurons receive inputs from the PBN.

We could also record from BNST projection neurons that have been labeled by the retrograde tracer beads from one of the downstream BNST targets. We could optically stimulate the PBN input to these projection neurons to determine their response to PBN stimulation. It is possible that projection neurons in the BNST comprise one of the two types of neurons that we found to be innervated by the PBN, such as the PBN-inhibited or the PBN-activated populations. Recording from retrogradely-labeled BNST projection neurons while stimulating the PBN input onto these neurons will help us to determine whether projection neurons show both PBN-inhibited and PBN-activated responses to PBN stimulation or only one type of response. If projection neurons from a particular downstream target only show one type of response, it may then be the case that another type of cell, such as interneurons or projection neurons to another brain region, comprises the other population. Further studying the effects of the PBN input on different classes of BNST neurons, such as projection neurons, and the α_{2A}-AR regulation of the PBN input onto these classes of neurons, will help us to better understand the influences of α_{2A}-AR-regulation of the PBN input on the downstream signaling of the BNST. Such studies may help us to elucidate the neural circuitry that underlies the ability of α_2-ARs in the BNST

to block stress-induced reinstatement of drug-seeking in rodent models.

α_2-AR regulation of the PBN input to the BNST may regulate induction of depolarization-induced suppression of excitation

Prior work has shown that in the cerebellum α_2-ARs on axosomatic terminals can influence depolarization-induced suppression of excitation (DSE) (Carey and Regehr, 2009). In the cerebellum, the axosomatic climbing fiber input has been shown to innervate purkinje cells (Mathews et al., 2012). α_2-ARs have been shown to decrease synaptic transmission from the axosomatic climbing fiber input to purkinje cells (Carey and Regehr, 2009) analogous to the α_{2A}-AR-induced depression of transmission from the PBN to the BNST (Flavin et al 2014). It has further been shown that α_2-ARs regulate the induction of DSE in the climbing fiber input to the cerebellum with activation of α_2-ARs blocking the induction of DSE (Carey and Regehr, 2009). It would be interesting to examine whether the α_{2A}-ARs regulate induction of DSE for the axosomatic PBN input to the BNST, as it would demonstrate a possible physiological action of α_{2A}-AR regulation of the PBN input to the BNST that would have important consequences of downstream signaling of the BNST to other stress and reward centers in the brain, such as the VTA (Georges and Aston-Jones, 2001, 2002; Dumont and Williams, 2004) and NAc (Dong et al., 2001). *In vivo*, it has been shown that endocannabinoid signaling and noradrenergic signaling interact with one another to influence stress-induced reinstatement of drug-seeking behavior in rodent models (Vaughn et al., 2012). Evidence suggests that cannabinergic and noradregergic signaling may work synergistically to mediate stress-induced

reinstatement of drug-seeking, as i.p. injection of a cannabinoid agonist together with an α_2-AR antagonist will induce reinstatement of drug-seeking, even at doses that would not induce reinstatement if the drugs were given individually (Vaughn et al., 2012). Taken together, both the evidence of α_2-ARs regulation of DSE induction in the cerebellum, a region of the brain where α_{2A}-ARs may regulate climbing fiber inputs analogously to the regulation of the PBN inputs to the BNST, and the evidence of *in vivo* synergistic influences of cannabinergic and noradrenergic signaling on stress-induced reinstatement of drug-seeking indicate the need for further studying α_{2A}-AR control of DSE in the BNST. If α_{2A}-AR activation in the BNST can regulate DSE, this finding may be important in mechanistically understanding the ability of α_2-AR activation in the BNST to block stress-induced reinstatement of drug-seeking. If interactions of α_{2A}-ARs and endocannabindoids are found in the BNST, this mechanism may help us in more effectively targeting guanfacine treatments to prevent stress-induced relapse in human populations.

Guanfacine may influence stress-induced reinstatement of conditioned place preference in mice

It will also be important to study the influences of the PBN input to the BNST and its regulation by α_{2A}-ARs on stress-induced reinstatement of drug-seeking in rodent models. Thus far, α_2-AR agonists have only been shown in rat behavioral models to block stress-induced reinstatement of drug-seeking (Erb et al., 2000; Highfield et al., 2001; Wang et al., 2001; Mantsch et al., 2010), however, since I have been using mouse models for our electrophysiological

recordings, it is important that we be able to replicate the ability of α_2-AR agonists to block stress-induced reinstatement of drug-seeking in mice. I have attempted to block stress-induced reinstatement of conditioned place preference (CPP) for cocaine with i.p. guanfacine injections, but the results were inconclusive (see Appendix Figure 16). Therefore, we should first repeat our efforts to show a block of stress-induced reinstatement of drug-seeking with guanfacine treatment in mice.

The effect of selective ablation of CGRP neurons in the PBN on stress-induced reinstatement of conditioned place preference in mice

Once we establish a block of stress-induced reinstatement of place preference with guanfacine in mice, we can then look more specifically at the PBN's role in stress-induced reinstatement. We can do this through the use of a Calca-DTR mouse line, which expresses the human diphtheria toxin receptor under the promoter for the CGRP gene. We can inject this Calca-DTR virus into the PBN of WT mice so that CGRP-positive neurons in the PBN then express the human diphtheria toxin receptor, thus making those cells susceptible to subsequent i.p. diphtheria toxin injections, which will kill any cells that express the human diphtheria toxin receptor. Therefore, we will be able to selectively lesion CGRP-expressing neurons in the PBN of WT mice. Once we have reinstatement working again in our CPP assay in WT mice, we can then compare stress-induced reinstatement of place preference in WT mice as compared to mice that have had CGRP-expressing neurons in the PBN selectively lesioned. While lesioning of CGRP-expressing neurons in the PBN would lesion all of the

efferent CGRP-releasing projections from the PBN, not just the PBN projection to the BNST, it may provide initial insight into whether the CGRP-expressing PBN neurons are essential for stress-induced relapse to drug seeking behavior.

In vivo studies may allow for better understanding of the role of the PBN on stress-induced reinstatement of drug-seeking behavior

To more specifically look at the PBN input to the BNST and its role in stress-induced reinstatement of drug-seeking, we could use *in vivo* optogenetic approaches. In order to mimic the depression of the glutamatergic PBN input to the BNST by guanfacine, we could inject a halorhodopsin virus under the control of the CaMKIIα promoter into the PBN. We could then implant a yellow light source into the BNST so that light stimulation is selectively targeting the PBN afferents to the BNST. We could then run conditioned place preference for cocaine and determine if inhibiting the PBN input to the BNST with activation of halorhodopsin blocks stress-induced reinstatement of conditioned place preference after extinction.

We could also study the effect of globally decreasing transmission from the PBN to its downstream projections in the brain through the use of DREADDs (Designer Receptor Exclusively Activated by Designer Drug). In this dissertation, I demonstrate that excitatory transmission from the PBN input to the BNST can be decreased by activation of the α_{2A}-AR, which belongs to the $G_{i/o}$ GCPR family. If we inject a transgene that expresses a $G_{i/o}$ DREADD into the PBN of wild type mice, we could then use an i.p. injection of the designer drug that activates the DREADD to study the effect that the decrease in transmission from the PBN to

its downstream target has on stress-induced reinstatement. This use of the $G_{i/o}$ DREADD would allow us an analogous way to study the effect of guanfacine on synaptic transmission from the PBN to its downstream targets. Such an approach could allow us to determine if guanfacine effects on transmission from the PBN is plays a critical role stress-induced reinstatement of drug-seeking behavior.

Effects of heterosynaptic α_{2A}-ARs on anxiety behaviors

Our lab has recently acquired a transgenic line of mice that is a KO of α_{2A}-ARs and α_{2C}-ARs and also overexpresses α_{2A}-ARs under the dopamine beta hydroxylase (DBH) promoter. Since DBH is only expressed on norepinephrine synaptic terminals and the other α_{2A}-ARs and α_{2C}-ARs are eliminated, only the α_{2A}-ARs autoreceptors are expressed in this mouse under the control of the DBH promoter. However, initial electrophysiological analyses suggest that the expression of the α_{2A}-ARs on the NE terminals may not completely restore NE signaling through other adrenergic receptor types in the BNST (Appendix Figure 20). After further characterization of NE signaling in these transgenic mice, we could run general anxiety tests on these mice and compare them to WT mice to see if there are any difference in anxiety levels between mice that have heterosynaptic α_{2A}-ARs versus those that only have autoreceptor α_{2A}-ARs. Some of the initial anxiety tests that we could run include elevated plus maze (EPM) as well as open field testing to look at differences in center time.

The PBN input to the extended amygdala may influence a range of behaviors

In addition to stress-induced relapse to drug-seeking behaviors, the modulation of BNST signaling by the PBN input may influence anxiety-like behaviors and fear-conditioning (Sink et al., 2011; Sink et al., 2013b; Sink et al., 2013a; Gungor and Pare, 2014). The PBN input to other regions of the extended amygdala has been implicated in feeding behavior (Carter et al., 2013) and pain sensitization (Han et al., 2005; Han et al., 2010). The PBN input to other regions of the brain has been implicated in taste aversion (Mungarndee et al., 2006) and hypernapnic arousal (Kaur et al., 2013). Therefore, the optogenetic strategies outlined in this study for the targeting of PBN inputs to the extended amygdala and to other brain regions could be beneficial in better understanding a wide range of conditions, from anxiety disorders, to disorders of energy homeostasis, to pain disorders, to sleep apnea.

The PBN input to the BNST may be relevant to anxiety behaviors

The actions of CGRP in the BNST have been shown to influence anxiety-like behaviors in rodent models (Sink et al., 2011; Sink et al., 2013b; Sink et al., 2013a). The effects of CGRP on anxiety appear to be at least partially dependent on signaling through CRFR1 receptors in the BNST (Sink et al., 2013b). Further, recent work has shown that CGRP effects inhibitory signaling within the BNST by increasing the amplitude of evoked IPSPs (Gungor and Pare, 2014). In future work, it may be interesting to study the effects of guanfacine on BNST neurons that specifically receive innervation from CGRP-expressing PBN terminals in the

BNST. One could investigate if CGRP-expressing PBN terminals in the BNST are preferentially regulated by α_{2A}-ARs. One could also investigate if CGRP-expressing PBN terminals selectively innervate the PBN-inhibited BNST cell population described in Chapter 1 (Figure 4), as it has been recently shown that CGRP in the BNST modulates inhibitory signaling (Gungor and Pare, 2014). Such studies may reveal insights into neurocircuitry involved in anxiety. Therefore, the implications of this study may extend beyond stress-induced relapse to drug-seeking behavior and may open new directions for studying mechanisms underlying anxiety-like behaviors.

Optogenetic approaches may increase understanding of how PBN input to the central nucleus of the amygdala influences pain sensitization

CGRPR1 receptors in the central nucleus of the amygdala have been previously shown to play an important role in pain sensitization in rodent models (Han et al., 2005). Further, CGRPR1 antagonists were found to reverse arthritis pain-related plasticity in the lateral capsular CeA (Han et al., 2005). CGRP has been shown to enhance excitatory synaptic transmission in the lateral capsular CeA (Han et al., 2010), while stereotaxic injection of CGRP in the CeA has been shown to increase pain sensitization in rodent models (Han et al., 2010). Therefore, since CGRP is a neuropeptide released by the PBN input to the extended amygdala (Dobolyi et al., 2005) and CGRP in the CeA has been shown to affect both synaptic transmission and pain sensitization behaviors, the use of optogenetic strategies to specifically stimulate the PBN input to the CeA could further increase our understanding of the neural circuitry underlying pain

sensitization. Both *ex vivo* and *in vivo* optogenetic strategies could be used to further dissect the role of the PBN and its projections to the extended amygdala in mediating pain sensitization.

The PBN input to the BNST may influence feeding behavior

Recent work has shown that the PBN input to the CeA influences feeding behavior (Carter et al., 2013). In particular, optogenetically-targeted activation of CGRP-containing neurons from the lateral PBN that project to the CeA suppresses appetite (Carter et al., 2013). While the PBN input to the BNST was not implicated in feeding behavior in this particular study (Carter et al., 2013), circuitry involving the BNST may play a role in diet failure, analogous to the role that it plays in addiction relapse (Wang et al., 2001; Briand et al., 2010). In this study, the CGRP-containing PBN input to the BNST was stimulated and this stimulation was not shown to alter feeding behavior (Carter et al., 2013). However, depression of this CGRP-containing input to the BNST was not tested and may influence feeding behavior. Further, there are PBN inputs to the BNST that do not contain CGRP (Niu et al., 2010; Kaur et al., 2013; Flavin et al., 2014), and modulation of these inputs may influence feeding behavior. The BNST has been implicated in mediating some of the negative symptoms of withdrawal (Delfs et al., 2000), and similar symptoms may contribute to diet failure. Therefore, the *ex vivo* optogenetic strategies outlined in this paper may increase our understanding of the neural circuitry underling some aspects of feeding behavior.

Ex vivo optogenetic strategies may increase understanding of the PBN regulation of hypercapnic arousal

Glutamatergic neurons in the lateral PBN have been shown to mediate arousal during hypercapnia (Kaur et al., 2013). For example, it was shown that genetic deletion of Vglut2 from lateral PBN neurons increases latency to arousal with hypercapnia in rodent models (Kaur et al., 2013). However, the lateral PBN projects to many brain regions (Saper and Loewy, 1980; Fulwiler and Saper, 1984; Delaney et al., 2007; Flavin et al., 2014) and it is not yet known which of these PBN projections are involved in hypercapnic arousal. Optogenetic strategies that study the PBN efferents to different brain regions in isolation could help to identify which elements of the PBN circuitry contribute to hypercapnic arousal, which could be in treating disorders such as sleep apnea.

The PBN influences taste aversion behavior

Previous work has shown that the lateral PBN is involved in taste aversion behaviors (Mungarndee et al., 2006). More specifically, lesioning of the lateral PBN ablates the viscerosensory neurons in the PBN, which subsequently prevents the viscerosensory malaise caused by food poisoning from reaching the forebrain (Mungarndee et al., 2006). Additionally, lesioning of the medial PBN prevents the association of taste with the malaise caused by food poisoning (Mungarndee et al., 2006).

Since the lateral PBN provides information regarding viscerosensory malaise to the forebrain, it is possible that one of roles of the PBN input to the extended amygdala is to relay information regarding the negative symptoms of

withdrawal, such as malaise, to the extended amygdala. Therefore, it will be interesting in the future to test if lesioning of the lateral PBN can block withdrawal-induced place aversion, which would further indicate that the lateral PBN plays a role in processing negative symptoms of withdrawal. To more specifically test the PBN afferents to the BNST, future work could include halorhodopsin injection into the lateral PBN accompanied by a yellow light source implantation into the BNST. Then, PBN afferent expressing halorhodopsin could be specifically inhibited using the yellow light source and one could test if inhibiting this input to the BNST prevents withdrawal-induced place aversion in rodent models.

Future work is needed to understand the possible excitatory role of α_{2A}-ARs in the BNST

In my work on Aim 2, I was able to confirm previous findings that i.p. injection of guanfacine (1 mg/kg) increases c-fos expression in the BNST (Savchenko and Boughter, 2011). However, the i.p. route of guanfacine administration produces systemic effects that make it difficult to determine a specific mechanism of increased c-fos expression. Therefore, my first goal was to try to find common characteristics of the population of BNST neurons that increase c-fos expression with in vivo guanfacine. I hoped that determining common characteristics of this population of c-fos neurons would help guide us to the mechanism by which c-fos expression was induced. Ultimately, identifying this population of neurons may allow us to better understand the possible excitatory role of α_{2A}-ARs and the BNST and elucidate how these neurons might

influence the BNST's downstream projections to stress and reward circuitry. I hope that by understanding both the input-specific decrease in excitatory transmission of the PBN input to the BNST by α_{2A}-AR activation and the excitatory role of α_{2A}-ARs in the BNST that we will better understand how α_{2A}-AR agonists, such as guanfacine, could be used to prevent stress-induced relapse in human populations.

The increase in c-fos expression in the BNST with i.p. injection of guanfacine (1 mg/kg) is consistent with previous findings (Savchenko and Boughter, 2011) and considered together with Figure 8 from Chapter 1, and Figure 9 from chapter it, it seems that there is a possible excitatory role for α_{2A}-ARs in the BNST, which contrasts with previous findings showing that α_{2A}-ARs decrease excitatory transmission in the BNST through a presynaptic mechanism (Shields et al., 2009).

I attempted to define the mechanism by which c-fos expression is increased in the BNST by α_{2A}-ARs in Chapter 2. I performed fluorescent immunohistochemistry and whole cell current clamp recordings in an attempt to identify to any unifying characteristics of the c-fos positive cell population. We did not find any common markers in either the calbindin or the CGRP staining that we performed (Figure 12). I did observe the presence of an I_h current in the c-fos-eGFP positive cells, which was consistent with previous work showing the presence of HCN1 mRNA in some BNST cell types. The I_h current I observed was also consistent with previous work done in the mPFC that has found that signaling through activated α_{2A}-ARs leads to closing of HCN1 channels, which

results in an increase in excitability of post-synaptic mPFC pyramidal neurons (Wang et al., 2001). Thus, I hypothesized that in the increase in c-fos expression in the BNST was due to a closing of postsynaptic HCN1 channels through α_{2A}-AR signaling. However, I found no difference in c-fos expression after i.p. guanfacine injected in HCN KO mice versus WT mice (data not shown).

I next tested the hypothesis that the increase in c-fos expression was due to increased excitatory transmission from a particular glutamatergic input onto the c-fos positive cells. I recorded from c-fos-eGFP positive cells in BNST slices prepared from transgenic mice that had been injected with guanfacine (1 mg/kg) prior to slicing. I observed a decrease in excitatory transmission with subsequent ex vivo guanfacine application, making it unlikely that the increase in c-fos expression was due to increased excitatory transmission from a particular input directly onto the c-fos-eGFP positive cells. While initial attempts to determine the mechanism of a potential excitatory role for α_{2A}-ARs in the BNST have been unsuccessful, some of the future work outlined in this chapter may lead to new mechanistic insights.

C-fos positive cells may be characterized by expression of CRF or ENK neuropeptides

Calbindin is a marker that has been used in the BNST as a marker of GABAergic interneurons (Gos et al., 2013). We also know from the work described in Chapter 1 of this dissertation that the PBN afferent to the BNST forms axosomatic synapses (Shimada et al., 1985; Shimada et al., 1989; Dobolyi et al., 2005). Therefore, I investigated whether the c-fos positive cells

demonstrated either significant levels of colocalization with calbindin, indicating that it was likely an interneurons population, or if a significant amount of outlining with CGRP staining, indicating that they were highly innervated by the PBN. However, when I compared guanfacine-injected animals with saline-injected animals I saw no noticeable difference in either the amount of colocalization with calbindin or in the outlining with CGRP terminals.

Since my initial studies immunohistochemistry studies did not reveal any specific markers for the c-fos positive cell population in the BNST, the next step will be to pursue methods to characterize this population of neurons by neuropeptide expression of the c-fos positive cell. However, this initial indication of heterogeneity of c-fos expressing neurons may suggest complex downstream modulations of BNST projections to stress and reward circuitry with α_{2A}-AR activation.

Prior work suggests that subpopulations of BNST neurons can be classified based on expression of neuropeptides (Day et al., 1999; Day et al., 2001; Day et al., 2005), such as corticotrophin releasing factor (CRF) and enkephalin (ENK). CRF signaling has previously been demonstrated by our lab to modulate NE signaling in the BNST (Nobis et al., 2011). ENK-expressing neurons in the BNST increase c-fos mRNA expression after exposure to drugs of abuse (Day et al., 2001) and this increased c-fos expression is prevented by prior exposure to stress (Day et al., 2005). Therefore, it is possible that the cell population in the BNST that expresses c-fos in response to guanfacine will show high levels of colocalization with either CRF or ENK. Our lab currently breeds a

CRF-Rosa transgenic mouse line. In the future, it may be possible to cross a c-fos-eGFP transgenic mouse with a CRF-Rosa mouse to generate c-fos-eGFP(+)/CRF-Rosa(+) mouse line. We would then look for a significant increase in colocalization of CRF-Rosa and c-fos-eGFP in mice that are injected with guanfacine (1 mg/kg) as compared to those that are injected with saline.

If we do not see any significant colocalization between CRF-Rosa and c-fos-eGFP, we could then pursue staining with ENK antibodies. Again, we would look for a significant increase in colocalization of c-fos with ENK in mice that had been injected with guanfacine versus those that had been injected with saline. By doing our initial fluorescent IHC with calbindin and CGRP, we attempted a broader classification of the c-fos positive neurons. Staining for neuropeptides in the future may help us to more specifically classify these c-fos cells.

Modulation of the HCN1 channel may not account for increased c-fos expression

As discussed in Chapter 2 of this dissertation, in addition to looking for immunohistochemical marker for guanfacine-sensitive c-fos positive cells within the BNST, I also looked at the electrophysiological characteristics of these c-fos positive cells. Since c-fos is expressed in the dorsal BNST of saline-treated mice, we were sure to record from a large sample size of neurons since some c-fos-eGFP neurons are not guanfacine-dependent. I recorded from a large sample size of recorded neurons to ensure that we record from enough guanfacine-dependent c-fos-eGFP neurons to discern potential differences between these neurons and guanfacine-independent c-fos-eGFP neurons. One of the more

interesting electrophysiological characteristics that we observed across all c-fos-eGFP positive neurons was the presence of an I_h current.

The presence of the I_h current in the c-fos-eGFP cells fits with work that has been done previously demonstrating that BNST cells express mRNA that encodes for HCN channels (Hammack et al., 2007). Additionally, work previously done in the PFC has shown that the activation of postsynaptic α_{2A}-ARs can lead to the closing of HCN channels that increases the excitability of the postsynaptic cell (Wang et al., 2007). We hypothesized that a similar scenario could be happening in the BNST. For example, guanfacine could be closing postsynaptic HCN channels through downstream α_{2A}-AR signaling, leading to increase in excitability of the postsynaptic cell. This increase in excitability of the postsynaptic cells would account for both the c-fos expression in the cell as well as the increase size of the optical field potential that we observe (Figures 8, 9), since field potential recordings can detect both changes in synaptic transmission as well as effects on general cell population excitability.

In order to test the hypothesis that closing of HCN channels was responsible for the increase in c-fos expression in the BNST with i.p. guanfacine, I took advantage of an HCN1 KO mouse line. I expected that if closing of HCN1 channels was responsible for the increase in c-fos expression that I would see a dramatic decrease in c-fos expression with guanfacine treatment in HCN1 KO mice as compared to WT mice. I would also expect to see that c-fos levels were very similar between HCN1 KO mice that had been treated with guanfacine as compared to HCN1 KO mice that had been treated with saline, and that c-fos

expression in both of these conditions would be very low. Yet, I did not detect a noticeable difference in levels of c-fos expression when comparing guanfacine-treated HCN1 KO mice to guanfacine-treated WT mice (data not shown). Further, I observed that guanfacine-treated HCN1 KO displayed noticeably higher levels of c-fos expression in the dorsal BNST when compared to saline-treated HCN1 KO mice. These findings together indicate that α_{2A}-AR-mediated closing of HCN1 channels is not responsible for the increase in c-fos expression seen with guanfacine treatment. However, previous work has shown that mRNA encoding other types of HCN channels is also expressed in the BNST, including HCN2, HCN3 and HCN4 channels (Hammack et al., 2007). I only explored the possibility of HCN1 channels being responsible for the increase in c-fos expression, but it is possible that closing of one of the other types of HCN channels is responsible for the increase in c-fos expression that we see in this population of BNST cells.

We could further test the hypothesis that guanfacine increases c-fos expression in the BNST by blocking HCN channels through sharp electrode recordings of c-fos-eGFP positive cells in the BNST after *in vivo* guanfacine treatment. Whole cell recording of c-fos-eGFP cells in ex vivo BNST slices could be done in which hyperpolarizing steps are given to the cell such that I_h currents can be recorded from the cell. We could then bath apply guanfacine to the BNST slice and see if the I_h current is reduced by guanfacine treatment. As a positive control, the compound ZD7288, a HCN channel blocker, could also be used to ensure that these types of recordings allow us to measure reduction in I_h currents when HCN channels are pharmacologically blocked.

I attempted these recordings during our work done on Aim 2 using regular patch pipettes, but I observed that with 30 minute recordings in normal ACSF, I_h currents decreased in size even without guanfacine treatment, suggesting that this observed reduction of I_h current is independent of guanfacine. I suspect that this reduction in I_h current was due to the dialyzing of components of the $G_{i/o}$ signaling cascade into the pipette tip. However, if similar recordings were done in the future using sharp electrodes this dialyzing of intracellular signaling components may be prevented. Therefore, with sharp electrode recording experiments, I may be able to observe if bath application to *ex vivo* BNST slices reduces I_h current in c-fos-eGFP positive cells after in vivo guanfacine treatment. A reduction of I_h current that was similar to a reduction in I_h current following bath application of ZD7288 would support the hypothesis that the increase in c-fos expression with in vivo guanfacine is due to postsynaptic α_{2A}-ARs blocking HCN channels in the c-fos-eGFP positive cells.

Increased excitatory transmission from glutamatergic inputs likely does not account for increase in c-fos expression

Since identification of the common electrophysiological characteristic of the presence of I_h current in c-fos-eGFP neurons did not lead to a clear mechanism by which c-fos expression may have been increased, I hypothesized that it may be properties of afferent fibers that regulate c-fos expression with α_{2A}-AR activation. An increase in excitatory transmission from a particular glutamatergic input to a population of c-fos-expressing cells would explain the increase in c-fos expression with *in vivo* guanfacine. The increase in excitatory

transmission from a specific input would also account for the increase in size of the optical field potentials with guanfacine application to BNST slices prepared from Thy1-COP4 mice (Figure 9), since the absence of the stimulation of the large PBN input to the BNST in these mice could allow for the effects of guanfacine on other smaller inputs to be revealed.

I did not observe an increase in excitatory transmission to the c-fos-eGFP positive neurons with subsequent *ex vivo* guanfacine application. Instead, I observed a decrease in excitatory transmission to the c-fos-eGFP neurons (Figure 13). I also monitored holding current and input resistance to determine if α_{2A}-ARs grossly change intrinsic excitability properties of the neurons, but did not observe any changes. It is a possible that *in vivo* treatment with the α_{2A}-AR agonists changed the electrophysiological properties of the afferent to the neurons that are activated by α_{2A}-AR agonists. For example, possibly the α_{2A}-ARs expressed on the presynaptic terminal did not re-sensitize by the time of bath application of guanfacine, thus occluding any further enhancement. However, preliminary work from our lab suggests that the effects of α_{2A}-AR agonists in the BNST are readily reversible (Figure 14) and that prior i.p. injections of a non-selective α_2-AR agonist clonidine also does not effect subsequent ex vivo guanfacine application (Figure 15). Therefore, I predict that α_{2A}-ARs expressed on afferents to these c-fos-GFP positive neurons will be re-sensitized prior to ex vivo guanfacine application. Therefore, it is unlikely that an increase in excitatory transmission from a particular glutamatergic input onto the

c-fos-eGFP positive cells is the mechanism underlying the increase in c-fos expression after *in vivo* guanfacine.

Other possible mechanisms for increased c-fos expression

While the list of possible mechanisms underlying the increase in c-fos expression in the BNST that we tested was not exhaustive, I saw no apparent indication that I identified the mechanism underlying both the increase in c-fos expression with *in vivo* guanfacine and the increase in optical field potential size with ex vivo guanfacine application to BNST slices prepared from Thy1-COP4 mice. The underlying mechanism does not appear to be a closing of HCN1 channels or an increase in excitatory transmission from a particular glutamatergic input the specifically innervates the c-fos positive neurons. However, there are other possible mechanisms in addition to the ones already mentioned in this discussion that could be tested in future work.

Alterations in $GABA_B$ signaling may account for increase in c-fos expression

There are several other mechanisms that we could test in future work to see if we can determine the way in which c-fos expression is enhanced by guanfacine. The absence of enhancement of EPSCs that I observed (Figure 13) may indicate that the enhanced c-fos expression is due to a decrease in inhibitory transmission *in vivo*. One possibility is that the increase in c-fos expression is due to a decrease in $GABA_A$ signaling *in vivo* that is not detected in *ex vivo* whole cell recordings due to the presence of picrotoxin, a $GABA_A$

antagonist. However, decreases in $GABA_A$ signaling would not explain the increase in optical field potentials that I see with guanfacine application to *ex vivo* Thy1-COP4 slices (Figure 8), since these recordings were done in the presence of picrotoxin (25 μM). However, guanfacine has been shown by our lab to decrease inhibitory transmission, which may include $GABA_A$ transmission (Shields et al., 2009). Therefore, while changes in $GABA_A$ transmission likely do not contribute to the increase in field potentials seen in Figure 8 due to the presence of picrotoxin, it may contribute to c-fos expression *in vivo*. It is possible that a decrease in $GABA_B$ signaling is responsible for the increase in c-fos expression in a population of cells in the BNST through reduced inhibition of these cells. We have not yet explored modulations of $GABA_B$ signaling by guanfacine, but that may be an important future direction to pursue in understanding both increases in c-fos expression with *in vivo* guanfacine as well as increases in optical field potential recordings with *ex vivo* guanfacine application to BNST slices from Thy1-COP4 mice.

Increased c-fos expression in the BNST in vivo may be due to multisynaptic signaling

Another possibility is that the increase in c-fos expression is due to multisynaptic signaling. For example, an increase in activity in another area of the brain in vivo could indirectly increase c-fos expression in the BNST by multisynaptic signaling that modulates activity in an intervening brain region that projects to the BNST. If this were the case, there would be increased c-fos expression in a population of BNST cells *in vivo*, but that I would not be able to

detect the increased activity of the upstream brain regions *ex vivo*, as the multisynaptic connections would be lost with brain slice preparation.

For example, as described previously, guanfacine acting through postsynaptic α_{2A}-ARs can close HCN channels and lead to increased excitability of postsynaptic pyramidal PFC neurons (Wang et al., 2007). Increased c-fos expression in the BNST may be due to increased excitability of pyramidal neurons in the PFC after guanfacine treatment, which in turns signals through one or more intermediary brain regions to ultimately activate a BNST cell population *in vivo*.

If this were the case, the increase in c-fos expression would require an intact connection between the PFC and all of the intermediary brain regions and the BNST, and would therefore only be found on the *in vivo* level of the mouse. In brain slice preparation, the multisynaptic signaling would be lost and the increased excitability would therefore by undetectable in *ex vivo* brain slice recordings.

In future work, it will be interesting to determine if multisynaptic signaling is a likely mechanism for increased c-fos expression. In order to do so, we will need to determine if increased c-fos expression is able to occur at the *ex vivo* slice level, thus allowing us to determine if α_{2A}-ARs effects on local circuits within BNST slices are sufficient to increase in c-fos expression. If increased c-fos expression is not seen in *ex vivo* brain slices with guanfacine application, it would further support the idea that global brain circuits may need to be intact for increased c-fos expression, such as the PFC connection through intermediary

brain regions to the BNST. However, if increased c-fos expression was seen in *ex vivo* brain slices, it would support the idea that modulation of local circuits in the BNST by guanfacine is sufficient to increase c-fos expression in a particular cell population.

Ex vivo BNST brain slices could be prepared from c-fos-eGFP transgenic mice, then time-lapsed imaging could be performed on the BNST slice to record images of c-fos-eGFP expression in the BNST with *ex vivo* guanfacine application. If we find that c-fos-eGFP expression increases on the slice level, this may indicate that intrinsic BNST circuit effects are sufficient for the increase in c-fos expression seen after *in vivo* guanfacine treatment. However, if we do not observe an increase in c-fos-eGFP in an *ex vivo* slice with guanfacine application, it may indicate that intact brain circuits are needed for the increase in c-fos expression to be seen in the BNST and thus we would only observe increased c-fos expression after *in vivo* guanfacine treatment.

There is a population of PFC neurons that project to the BNST and it is a possibility that these excited PFC neurons that project directly to the BNST may be responsible for the increase in c-fos expression (McDonald et al., 1999). However, our whole cell experiments that show a decrease in excitatory transmission with guanfacine application to electrical stimulation of inputs to c-fos-eGFP positive cells (Figure 13), as well as a decrease in excitatory transmission with guanfacine application to optical stimulation of Thy1-COP4 brain slices (Figure 19), indicate that increased excitability of a direct input to these c-fos positive cells is unlikely.

MAP kinase modulation of Kv4.2 may cause increase in c-fos expression

Finally, downstream signaling from MAP kinase (MAPK)/extracellular signal-regulated kinase (ERK) modulation of the potassium channel Kv4.2 may lead to an increase in c-fos expression in the BNST with guanfacine treatment. It has been previously shown that Kv4.2 channels are expressed in the BNST (Rainnie et al., 2014) and that GPCR signaling can modulate downstream MAPK/ERK signaling which regulates Kv4.2 potassium channels (Yuan et al., 2002; Sweatt, 2004; Hu et al., 2006). It has also been shown that i.p. guanfacine increases ERK phosphorylation in BNST neurons (Savchenko and Boughter, 2011). Therefore, this increased ERK activity could be leading to downstream downregulation of Kv4.2 potassium channels, which could increase excitability of the cell. Therefore, since α_{2A}-ARs signal through $G_{i/o}$ GPCRs, it is possible that α_{2A}-AR activation lead to downstream modulation of ERK that alters regulation of Kv4.2 potassium channels, leading to increased excitability on of a population of cells in the BNST.

Overall Conclusions

The PBN Input May Influence Downstream BNST Signaling

Due to the behavioral effects of activation of α_{2A}-ARs in the BNST, it seems likely that the depression of the PBN input to the BNST by guanfacine may alter outputs of the BNST to brain regions involved in addiction and relapse such as the VTA (Georges and Aston-Jones, 2001, 2002; Dumont and Williams,

2004; Silberman et al., 2013) and the NAc (Dong et al., 2001). Alterations in the BNST's outputs may curb stress-induced drug cravings or stress-induced re-emergence of negative symptoms of withdrawal. In fact, it has been shows that guanfacine treatment reduces withdrawal-induced anxiety in rats treated with guanfacine (Buffalari et al., 2012). Additionally, it has been shown that injection of an α_2-AR agonist into the BNST will block withdrawal-induced place aversion (Delfs et al., 2000). Therefore, a decrease in excitatory transmission from the PBN to the BNST by α_{2A}-ARs may decrease the aversive withdrawal-like symptoms brought on by stress and help to prevent relapse.

I have also observed an excitatory role for α_{2A}-ARs in the BNST. At this time, it is not known whether this excitatory role of α_{2A}-ARs would work to complement the depression of excitatory transmission from the PBN input in preventing stress-induced relapse or if the excitatory role would oppose the effects on PBN transmission. Thus far, the use of guanfacine treatment in human populations has decreased cravings in dug-addicted individuals. However, overall relapse outcomes have not been improved by guanfacine treatment (Fox et al., 2012; Fox and Sinha, 2014; Fox et al., 2014). In the future, it will be important to determine the mechanism of this excitatory role of α_{2A}-ARs in the BNST and explore the timing of this effect and its relation to the depression of excitatory transmission from other afferents such as the PBN. It may be the case that more specific targeting of guanfacine therapy to either the excitatory role of α_{2A}-ARs or the depression of certain excitatory inputs to the extended amygdala will increase the efficacy of guanfacine in preventing stress-induced relapse to

drug-seeking behavior.

In summary, my work demonstrates divergent actions of the PBN input on cell responses in the BNST. I demonstrate that depolarizing effects of the PBN appear to be preferentially reduced by the α_{2A}-AR agonist guanfacine. Finally, I show that in the absence of PBN signaling, guanfacine has very different actions on BNST excitability, suggesting a state-dependent aspect to the actions of guanfacine. In future work, it will be important to examine the consequences of specific regulation of the PBN *in vivo* by guanfacine.

The results of our studies may further elucidate how α_{2A}-ARs in the BNST modulate stress-induced reinstatement behavior. Using optogenetic approaches, we will study individual inputs to the BNST in a manner that has not previously possible. I hope the proposed work will increase our understanding of the therapeutic potential for α_{2A}-AR agonists for the prevention and treatment of stress-induced relapse to drug-seeking.

Directed targeting of guanfacine may be needed to increase clinical efficacy in preventing stress-induced relapse of drug-seeking behavior

It has been shown that both peripheral and intra-BNST administration of α_2-AR agonists can block stress-induced relapse of drug-seeking behavior in rodent behavioral models (Erb et al., 2000; Shaham et al., 2000; Highfield et al., 2001; Wang et al., 2001; Mantsch et al., 2010). However, human clinical trials testing the ability of guanfacine to prevent stress-induced relapse of drug-seeking have not shown as much success; self-reported drug-cravings are decreased in these studies, but overall relapse outcomes are not improved (Fox et al., 2012;

Fox and Sinha, 2014; Fox et al., 2014). The multiple actions of guanfacine-mediated α_{2A}-AR activation described in this dissertation may account for the relative lack of success for guanfacine in clinically treating addiction.

Previous work and work done in this this dissertation has demonstrated that there are multiple effects of the α_{2A}-AR agonist guanfacine in the BNST. First, guanfacine can work on α_{2A}-AR autoreceptors to decrease release of presynaptic norepinephrine release. Second, guanfacine decreases excitatory transmission from selective inputs to the BNST, such as the PBN, while having no apparent effect on transmission from other inputs to the BNST, such as the BLA (Flavin et al., 2014). Guanfacine has also been shown to decrease inhibitory transmission in the BNST (Shields et al., 2009). Further, α_{2A}-AR activation can increase postsynaptic response to other glutamate afferents (Savchenko and Boughter, 2011; Flavin et al., 2014). Finally, our EM work revealed a population of postsynaptic α_{2A}-ARs whose role in BNST synaptic transmission still needs to be evaluated (Flavin et al., 2014).

While multiple functions of α_{2A}-ARs in the BNST have been uncovered, it is still unknown which of these functions contribute to signaling involved in stress-induced relapse of drug-seeking behavior. For example, it is unknown whether these multiple actions of guanfacine work together to prevent stress-induced relapse of drug-seeking behavior in rodents, or if these actions are at cross purposes, with some actions with some actions working to prevent stress-induced relapse while others actions may mitigate such effects. If the multiple actions of guanfacine work at cross purposes it may help to explain the

decreased efficacy of guanfacine in preventing relapse in clinical trials since the beneficial effects of guanfacine may be partially negated by its other effects. Therefore, if it can be determined in future work which of these actions of guanfacine contribute to the ability of α_2-ARs to block stress-induced relapse and which actions are not beneficial, we may be able to more selectively target treatments to relapse-protective α_{2A}-ARs and increase efficacy of clinical prevention of stress-induced relapse.

APPENDIX

Attempt to block stress-induced reinstatement of conditioned place preference with i.p. guanfacine is inconclusive

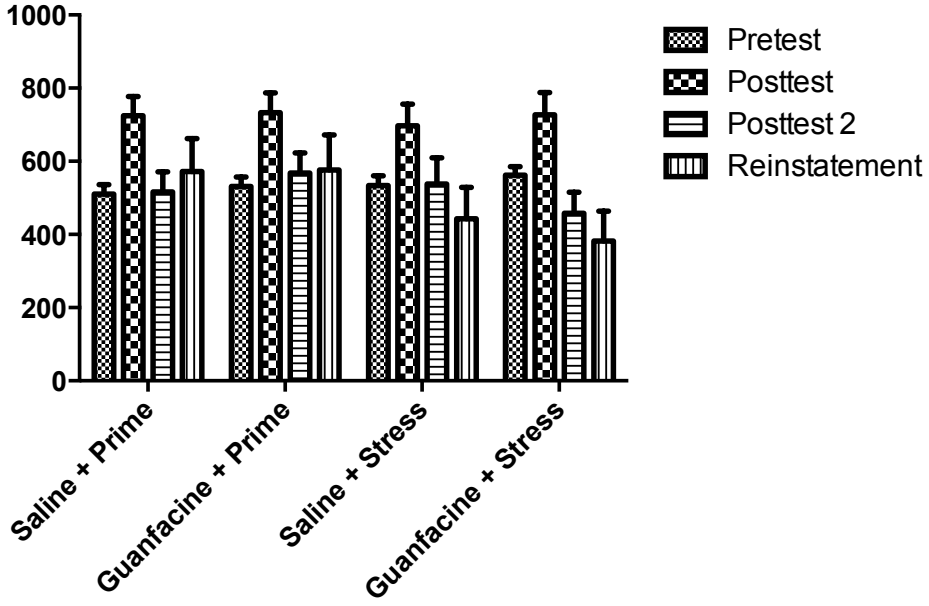

Figure 16. Initial attempt to block stress-induced reinstatement of drug-seeking with guanfacine is inconclusive. We tested four conditions: i.p. saline injection 30 minutes before a priming dose of cocaine, i.p. guanfacine before priming dose of cocaine, i.p. saline before forced-swim stress, i.p. guanfacine before forced-swim stress. We looked at time spent on the preferred side of the two-sided chamber before conditioning (pretest, black dotted bars), after conditioned (posttest, black checkered bars), after extinction (posttest 2, horizontal striped bars), and immediately after priming cocaine or stress (reinstatement, vertical striped bars). However, we did not observe reinstatement in either of the control conditions (saline + prime, saline + stress) and therefore could not interpret if guanfacine blocked either reinstatement condition.

The previous behavioral work done in rodent models showing that α_2-AR agonists can block stress-induced reinstatement of drug-seeking have been done in rats and have been done using non-specific α_2-AR agonists (Highfield et al.,

2001; Wang et al., 2001; Leri et al., 2002). My project, however, focused on the α_{2A}-AR-specific agonist guanfacine and exclusively involved studies done in mice. Therefore, I wanted to confirm that guanfacine could block stress-induced reinstatement of conditioned place preference in mice. For four days mice were conditioned to contextually pair one side of a two-sided chamber with cocaine. To do this, mice were daily given i.p. injections of cocaine and then allowed 30 minutes on the cocaine-paired side of a double sided chamber. Alternately, mice underwent daily sessions in which they received i.p. injections of saline and were only allowed access to the opposite side of the chamber. After four days of conditioning, mice were then tested for place preference through a free exploration session in which we ensured that, given free access to both sides of the chamber, the mice spent significantly more time on the cocaine-paired side than the saline-paired side. After four days of free-exploration sessions, the preference for the cocaine-paired side of the chamber was extinguished. After extinction, we attempted to reinstate preference for the cocaine-paired side of the CPP chamber by two different conditions. Since we think that guanfacine should preferentially block stress-induced reinstatement, but not drug-priming induced reinstatement, we attempted to compare the effects of i.p. guanfacine on these two different methods of reinstatement of drug-seeking. In the stress-induced reinstatement we exposed the mice to forced-swim immediately before giving the mice free access to both sides of the CPP chamber. For drug-priming reinstatement we injected the mice with i.p. cocaine immediately before giving the mice free access to both sides of the chamber. In both the forced-swim and

drug-priming conditions, half the mice were injected with i.p. guanfacine and the other half were injected with i.p. saline 30 minutes before either of the reinstatement conditions. However, reinstatement was not successful in either the drug-priming or the stress conditions, so we could not tell if guanfacine was able to block specifically stress-induced reinstatement of drug-seeking in mice.

The insular cortex input to the BNST and oEPSCs in Thy1-COP4 mice show possible off-target sensitivity to guanfacine

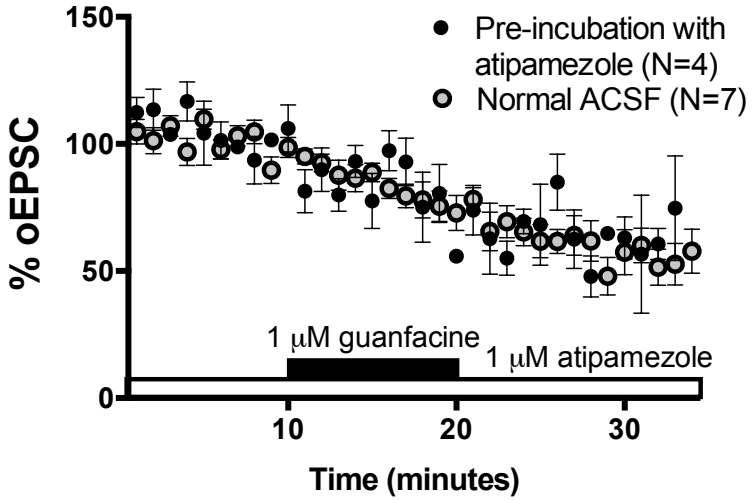

Figure 17. Decrease of excitatory transmission from the insular cortex input to the BNST is not blocked by pre-incubation with atipamezole. Experiments showing the decrease in excitatory transmission from the insular input to the BNST with guanfacine application done in normal ACSF are shown in gray circles. Experiments showing the decrease in excitatory transmission from the insular input to the BNST with guanfacine application after pre-incubation with atipamezole are shown in gray circles (37.9% ± 7.6%, $t(3)=4.98$, $p<0.05$, $n=4$).

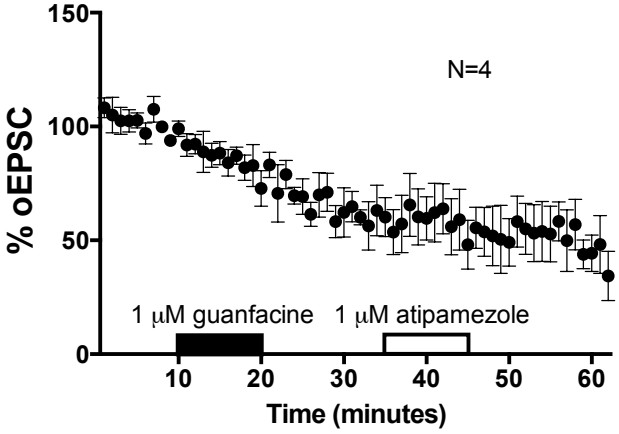

Figure 18. Depression of excitatory transmission from the insular input to the BNST is not reversed by subsequent application of atipamezole. Guanfacine decreased the size of oEPSCs recorded from the insular cortex input to the BNST, but this depression was not reversed by subsequent atipamezole application **(**43.7% ± 7.5%, t(6)=5.82, p<0.01, n=7).

In addition to the PBN and the BLA, another input to the BNST whose sensitivity to guanfacine that I examined was the insular cortex. Application of guanfacine to oEPSCs recorded from the insular cortex input to the BNST showed a decrease in excitatory transmission, similar to the PBN input. However, unlike the PBN input, this depression was not reversed by subsequent application of atipamezole (37.9% ± 7.6%, t(3)=4.98, p<0.05, n=4) (Figure 17). Similarly, this decrease in excitatory transmission in the insular cortex input was not blocked by pre-incubation of slices with atipamezole **(**43.7% ± 7.5%, t(6)=5.82, p<0.01, n=7) (Figure 18). Therefore, it is possible that this decrease in excitatory transmission of the insular cortex input to the BNST may be due to off-target, non-α_{2A}-AR-dependent effects of guanfacine.

Further evidence of a possible off-target action of guanfacine was observed in oEPSC recordings done in Thy1-COP4 mice. In oEPSC recordings done in Thy1-COP4 mice, oEPSCs were decreased by guanfacine, but this decrease was not reversed by subsequent application of atipamezole (Figure 19) ($t(2,7)=15.7$, $p<0.01.$, $n=8$). Taken together, the inability of atipamezole to either reverse or block depression of oEPSCs from the insular cortex or in Thy1-COP4 mice suggest that guanfacine may have off-target, non-specific effects that are able to decrease excitatory transmission in certain studies. Therefore, it will be important in future studies to either block or reverse observed effects of guanfacine with atipamezole to make sure that the effect that we are studying is α_{2A}-AR-mediated and not this off-target effect. In future work it will also be important to figure out the receptor types that guanfacine is acting on to cause these off-target effects as these off-target effects may contribute to the decreased efficacy of guanfacine in preventing stress-induced relapse of drug-seeking behavior in humans.

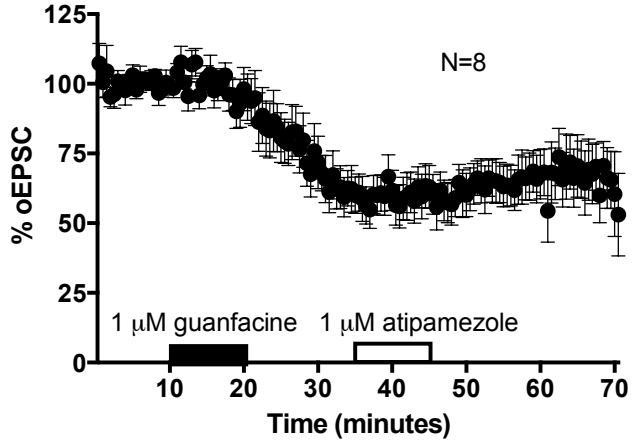

Figure 19. Decrease of excitatory transmission observed in voltage-clamp oEPSC recordings done in Thy1-COP4 mice with guanfacine application is not reversed by atipamezole. Guanfacine decreases the size of oEPSCs recorded from Thy1-COP4 mice and this decrease was not reversed by subsequent application of atipamezole ($t(2,7)=15.7$, $p<0.01$., $n=8$).

Initial pharmacological characterization of α_{2A}-AR heteroreceptor knockout

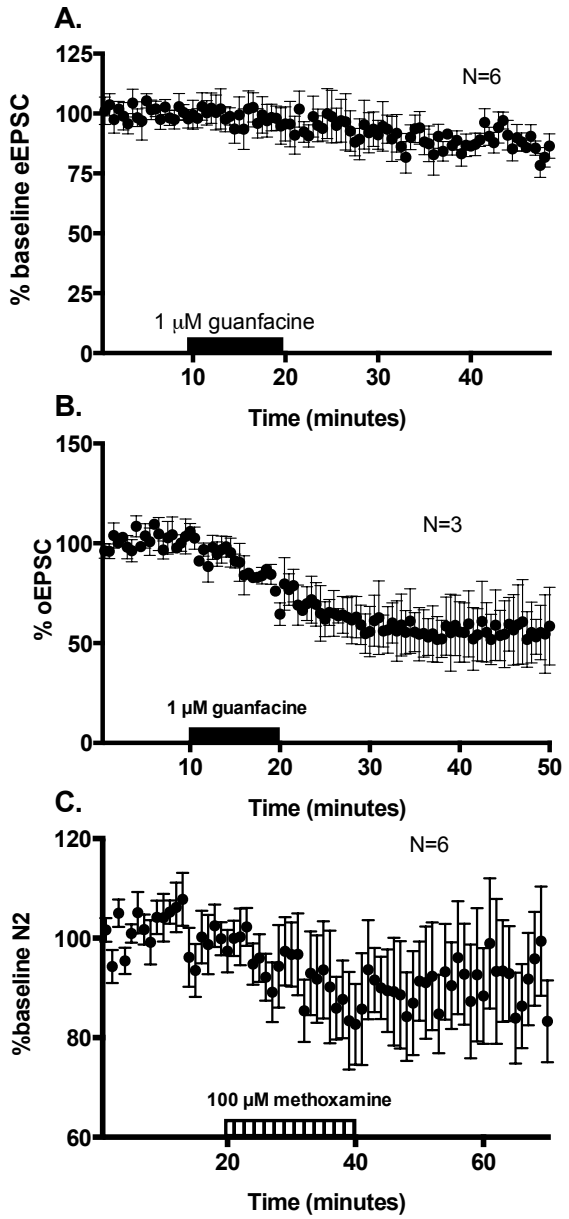

Figure 20. Partial pharmacological characterization of the post-synaptic knock-out mouse. A) Guanfacine does not significantly decrease excitatory transmission in BNST whole cell recordings in α_{2A}-AR postsynaptic KO mice. B) Guanfacine decreases excitatory transmission in the BNST of wild-type mice. C) Methoxamine does not significantly decrease excitatory field potential recordings done in α_{2A}-AR postsynaptic KO mice.

I hoped to be able to more specifically implicate α_{2A}-AR heteroreceptors as being responsible for the decrease in excitatory transmission observed in the BNST with guanfacine application. I attempted to do this through the use of a transgenic "α_{2A}-AR heteroreceptor KO" or "postsynaptic KO" mouse, in which α_{2A}--ARs are knocked out of the mouse, but then the α_{2A}-AR gene is overexpressed under the DBH promoter, which results in α_{2A}-AR expression specifically on norepinephrine terminals. As a result, α_{2A}-ARs are knocked out everywhere in the mouse except for on NE terminals, thus resulting in an effective "heteroreceptor KO" for α_{2A}-AR with preservation of α_{2A}-AR autoreceptors. When guanfacine was applied to whole cell electrical EPSC recordings done in postsynaptic KO mice depression of the EPSCs was not observed ($t(5)=0.9$, n.s., n=6), consistent with α_{2A}-AR heteroreceptors being responsible for the guanfacine-mediated depression of excitatory transmission. As a control, depression of excitatory transmission by guanfacine was still observed in whole cell recordings done in wild-type mice ($t(2)=4.3$, $p<0.05$, n=3). However, I wanted to ensure that overall NE signaling was restored by expression of the α_{2A}-AR on NE terminals in the transgenic mouse since we have observed previously that NE signaling is disrupted in complete α_{2A}-AR KO mice (Egli et al., 2005). When I tried to apply the α_1-AR methoxamine to field potential recordings I did not observe a significant decrease in excitatory transmission as we expected ($t(5)=2$, n.s., n=6) (McElligott and Winder, 2008). Therefore, further characterization is needed in these mice to ensure that α_{2A}-ARs are indeed expressed on NE terminals projecting from the NTS to the BNST and that there is enough

autoreceptor expression of α_{2A}-ARs in the postsynaptic KO mouse to keep NE signaling intact.

The N1 of field potential recordings in wild type mice is decreased by guanfacine

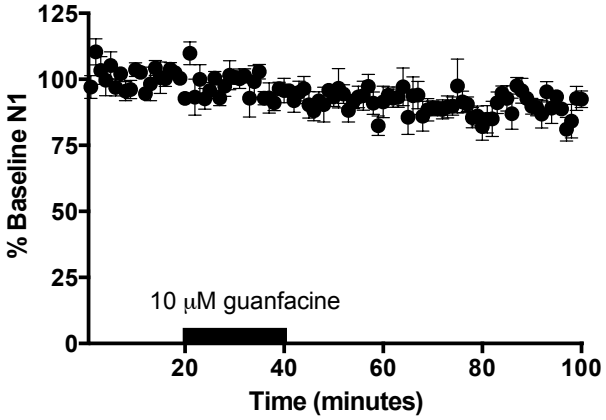

Figure 21. The N1 deflection of field potential recordings done in wild-type mice is decreased by guanfacine. There is a significant decrease in the size of the N1 recorded from wild-type mice with guanfacine application.

Application of guanfacine to the N1 deflection of the electrical field potentials recorded in wild-type mice does show a significant decrease in size ($t(4)=3.7$, $p<0.05$, $n=5$). However, there does not appear to be a major drug effect observed in graphical analysis of the data (Figure 21). Therefore, this significant decrease in size of the N1 may be slight run down of the N1 during the course of the recordings. This decrease may also be due to the off-target effects of guanfacine described in Figure 18 and 19. The N1 is thought to be due to the presynaptic fiber volley caused by the electrical stimulation. Therefore, it is also possible that guanfacine is altering the excitability of the presynaptic cell such

that it is not as responsive to electrical stimulation.

HCN1 channels in the BNST likely do not contribute to an increase postsynaptic excitability in response to guanfacine

It has been shown that post-synaptic α_{2A}-ARs in the prefrontal cortex can increase post-synaptic excitability by closing HCN channels (Wang et al., 2007). Further, it has been shown that mRNA for HCN1 channels is expressed in BNST cells (Hammack et al., 2007). Therefore, it is possible that the increase in c-fos expression that we observe with i.p. guanfacine is due to signaling through activated postsynaptic α_{2A}-ARs leading to downstream closing of HCN1 channels. In order to test this hypothesis, I made use of an HCN1 KO mouse line. The mice were handled for five days as described above and then injected with guanfacine (i.p., 1 mg/kg) ninety-minutes to two hours prior to transcardial perfusion. Slices were then prepared of the BNST and free-floated for immunohistochemical staining for c-fos with DAB. I hypothesized that if the closing of HCN1 channels by downstream signaling of activated α_{2A}-ARs was responsible for the increase in c-fos expression in the BNST following i.p. guanfacine, we would see a dramatic reduction in the amount of c-fos staining in HCN1 KO mice. Instead, I saw comparable levels of c-fos staining in HCN1 KO mice as was seen in WT mice (data not shown). Therefore, we decided not to pursue HCN1 channels as a mechanism of increased c-fos expression any further.

REFERENCES

Alden M, Besson JM, Bernard JF (1994) Organization of the efferent projections from the pontine parabrachial area to the bed nucleus of the stria terminalis and neighboring regions: a PHA-L study in the rat. The Journal of comparative neurology 341:289-314.

Alheid GF, Heimer L (1988) New perspectives in basal forebrain organization of special relevance for neuropsychiatric disorders: the striatopallidal, amygdaloid, and corticopetal components of substantia innominata. Neuroscience 27:1-39.

Arenkiel BR, Peca J, Davison IG, Feliciano C, Deisseroth K, Augustine GJ, Ehlers MD, Feng G (2007) In vivo light-induced activation of neural circuitry in transgenic mice expressing channelrhodopsin-2. Neuron 54:205-218.

Aston-Jones G, Delfs JM, Druhan J, Zhu Y (1999) The bed nucleus of the stria terminalis. A target site for noradrenergic actions in opiate withdrawal. Annals of the New York Academy of Sciences 877:486-498.

Banihashemi L, Rinaman L (2006) Noradrenergic inputs to the bed nucleus of the stria terminalis and paraventricular nucleus of the hypothalamus underlie hypothalamic-pituitary-adrenal axis but not hypophagic or conditioned avoidance responses to systemic yohimbine. The Journal of neuroscience : the official journal of the Society for Neuroscience 26:11442-11453.

Barth AL, Gerkin RC, Dean KL (2004) Alteration of neuronal firing properties after in vivo experience in a FosGFP transgenic mouse. The Journal of neuroscience : the official journal of the Society for Neuroscience 24:6466-6475.

Bienkowski MS, Rinaman L (2013) Common and distinct neural inputs to the medial central nucleus of the amygdala and anterior ventrolateral bed nucleus of stria terminalis in rats. Brain structure & function 218:187-208.

Briand LA, Vassoler FM, Pierce RC, Valentino RJ, Blendy JA (2010) Ventral tegmental afferents in stress-induced reinstatement: the role of cAMP response element-binding protein. The Journal of neuroscience : the official journal of the Society for Neuroscience 30:16149-16159.

Brown SA, Vik PW, Patterson TL, Grant I, Schuckit MA (1995) Stress, vulnerability and adult alcohol relapse. Journal of studies on alcohol 56:538-545.

Brown ZJ, Nobrega JN, Erb S (2011) Central injections of noradrenaline induce reinstatement of cocaine seeking and increase c-fos mRNA expression in the extended amygdala. Behavioural brain research 217:472-476.

Brownstein M, Saavedra JM, Palkovits M (1974) Norepinephrine and dopamine in the limbic system of the rat. Brain research 79:431-436.

Buffalari DM, See RE (2010) Amygdala mechanisms of Pavlovian psychostimulant conditioning and relapse. Current topics in behavioral neurosciences 3:73-99.

Buffalari DM, Baldwin CK, See RE (2012) Treatment of cocaine withdrawal anxiety with guanfacine: relationships to cocaine intake and reinstatement of cocaine seeking in rats. Psychopharmacology 223:179-190.
Bylund DB, Eikenberg DC, Hieble JP, Langer SZ, Lefkowitz RJ, Minneman KP, Molinoff PB, Ruffolo RR, Jr., Trendelenburg U (1994) International Union of Pharmacology nomenclature of adrenoceptors. Pharmacological reviews 46:121-136.
Carey MR, Regehr WG (2009) Noradrenergic control of associative synaptic plasticity by selective modulation of instructive signals. Neuron 62:112-122.
Carter ME, Soden ME, Zweifel LS, Palmiter RD (2013) Genetic identification of a neural circuit that suppresses appetite. Nature 503:111-114.
Cecchi M, Khoshbouei H, Morilak DA (2002a) Modulatory effects of norepinephrine, acting on alpha 1 receptors in the central nucleus of the amygdala, on behavioral and neuroendocrine responses to acute immobilization stress. Neuropharmacology 43:1139-1147.
Cecchi M, Khoshbouei H, Javors M, Morilak DA (2002b) Modulatory effects of norepinephrine in the lateral bed nucleus of the stria terminalis on behavioral and neuroendocrine responses to acute stress. Neuroscience 112:13-21.
Chiba T, Kayahara T, Nakano K (2001) Efferent projections of infralimbic and prelimbic areas of the medial prefrontal cortex in the Japanese monkey, Macaca fuscata. Brain research 888:83-101.
Choi DC, Furay AR, Evanson NK, Ostrander MM, Ulrich-Lai YM, Herman JP (2007) Bed nucleus of the stria terminalis subregions differentially regulate hypothalamic-pituitary-adrenal axis activity: implications for the integration of limbic inputs. The Journal of neuroscience : the official journal of the Society for Neuroscience 27:2025-2034.
Cullinan WE, Herman JP, Watson SJ (1993) Ventral subicular interaction with the hypothalamic paraventricular nucleus: evidence for a relay in the bed nucleus of the stria terminalis. The Journal of comparative neurology 332:1-20.
Day HE, Campeau S, Watson SJ, Jr., Akil H (1997) Distribution of alpha 1a-, alpha 1b- and alpha 1d-adrenergic receptor mRNA in the rat brain and spinal cord. Journal of chemical neuroanatomy 13:115-139.
Day HE, Curran EJ, Watson SJ, Jr., Akil H (1999) Distinct neurochemical populations in the rat central nucleus of the amygdala and bed nucleus of the stria terminalis: evidence for their selective activation by interleukin-1beta. The Journal of comparative neurology 413:113-128.
Day HE, Nebel S, Sasse S, Campeau S (2005) Inhibition of the central extended amygdala by loud noise and restraint stress. The European journal of neuroscience 21:441-454.
Day HE, Badiani A, Uslaner JM, Oates MM, Vittoz NM, Robinson TE, Watson SJ, Jr., Akil H (2001) Environmental novelty differentially affects c-fos mRNA expression induced by amphetamine or cocaine in subregions of the bed

nucleus of the stria terminalis and amygdala. The Journal of neuroscience : the official journal of the Society for Neuroscience 21:732-740.
Delaney AJ, Crane JW, Sah P (2007) Noradrenaline modulates transmission at a central synapse by a presynaptic mechanism. Neuron 56:880-892.
Delfs JM, Zhu Y, Druhan JP, Aston-Jones G (2000) Noradrenaline in the ventral forebrain is critical for opiate withdrawal-induced aversion. Nature 403:430-434.
Dobolyi A, Irwin S, Makara G, Usdin TB, Palkovits M (2005) Calcitonin gene-related peptide-containing pathways in the rat forebrain. The Journal of comparative neurology 489:92-119.
Dong HW, Petrovich GD, Watts AG, Swanson LW (2001) Basic organization of projections from the oval and fusiform nuclei of the bed nuclei of the stria terminalis in adult rat brain. The Journal of comparative neurology 436:430-455.
Dumont EC, Williams JT (2004) Noradrenaline triggers GABAA inhibition of bed nucleus of the stria terminalis neurons projecting to the ventral tegmental area. The Journal of neuroscience : the official journal of the Society for Neuroscience 24:8198-8204.
Eccles JC, Llinas R, Sasaki K (1966) The excitatory synaptic action of climbing fibres on the Purkinje cells of the cerebellum. The Journal of physiology 182:268-296.
Egli RE, Winder DG (2003) Dorsal and ventral distribution of excitable and synaptic properties of neurons of the bed nucleus of the stria terminalis. Journal of neurophysiology 90:405-414.
Egli RE, Kash TL, Choo K, Savchenko V, Matthews RT, Blakely RD, Winder DG (2005) Norepinephrine modulates glutamatergic transmission in the bed nucleus of the stria terminalis. Neuropsychopharmacology : official publication of the American College of Neuropsychopharmacology 30:657-668.
Erb S, Shaham Y, Stewart J (2001) Stress-induced relapse to drug seeking in the rat: role of the bed nucleus of the stria terminalis and amygdala. Stress 4:289-303.
Erb S, Hitchcott PK, Rajabi H, Mueller D, Shaham Y, Stewart J (2000) Alpha-2 adrenergic receptor agonists block stress-induced reinstatement of cocaine seeking. Neuropsychopharmacology : official publication of the American College of Neuropsychopharmacology 23:138-150.
Flavin SA, Winder DG (2013) Noradrenergic control of the bed nucleus of the stria terminalis in stress and reward. Neuropharmacology 70:324-330.
Flavin SA, Matthews RT, Wang Q, Muly EC, Winder DG (2014) alpha2A-Adrenergic Receptors Filter Parabrachial Inputs to the Bed Nucleus of the Stria Terminalis. The Journal of neuroscience : the official journal of the Society for Neuroscience 34:9319-9331.
Forray MI, Gysling K (2004) Role of noradrenergic projections to the bed nucleus of the stria terminalis in the regulation of the hypothalamic-pituitary-adrenal axis. Brain research Brain research reviews 47:145-160.

Fox H, Sinha R (2014) The role of guanfacine as a therapeutic agent to address stress-related pathophysiology in cocaine-dependent individuals. Advances in pharmacology 69:217-265.
Fox HC, Morgan PT, Sinha R (2014) Sex Differences in Guanfacine Effects on Drug Craving and Stress Arousal in Cocaine-Dependent Individuals. Neuropsychopharmacology : official publication of the American College of Neuropsychopharmacology.
Fox HC, Seo D, Tuit K, Hansen J, Kimmerling A, Morgan PT, Sinha R (2012) Guanfacine effects on stress, drug craving and prefrontal activation in cocaine dependent individuals: preliminary findings. Journal of psychopharmacology 26:958-972.
Fudge JL, Haber SN (2001) Bed nucleus of the stria terminalis and extended amygdala inputs to dopamine subpopulations in primates. Neuroscience 104:807-827.
Fuentealba JA, Forray MI, Gysling K (2000) Chronic morphine treatment and withdrawal increase extracellular levels of norepinephrine in the rat bed nucleus of the stria terminalis. Journal of neurochemistry 75:741-748.
Fulwiler CE, Saper CB (1984) Subnuclear organization of the efferent connections of the parabrachial nucleus in the rat. Brain research 319:229-259.
Georges F, Aston-Jones G (2001) Potent regulation of midbrain dopamine neurons by the bed nucleus of the stria terminalis. The Journal of neuroscience : the official journal of the Society for Neuroscience 21:RC160.
Georges F, Aston-Jones G (2002) Activation of ventral tegmental area cells by the bed nucleus of the stria terminalis: a novel excitatory amino acid input to midbrain dopamine neurons. The Journal of neuroscience : the official journal of the Society for Neuroscience 22:5173-5187.
Gos T, Schulkin J, Gos A, Bock J, Poeggel G, Braun K (2013) Paternal deprivation affects the functional maturation of corticotropin-releasing hormone (CRH)- and calbindin-D28k-expressing neurons in the bed nucleus of the stria terminalis (BNST) of the biparental Octodon degus. Brain structure & function.
Grueter BA, Winder DG (2005) Group II and III metabotropic glutamate receptors suppress excitatory synaptic transmission in the dorsolateral bed nucleus of the stria terminalis. Neuropsychopharmacology : official publication of the American College of Neuropsychopharmacology 30:1302-1311.
Grueter BA, Gosnell HB, Olsen CM, Schramm-Sapyta NL, Nekrasova T, Landreth GE, Winder DG (2006) Extracellular-signal regulated kinase 1-dependent metabotropic glutamate receptor 5-induced long-term depression in the bed nucleus of the stria terminalis is disrupted by cocaine administration. The Journal of neuroscience : the official journal of the Society for Neuroscience 26:3210-3219.
Gungor NZ, Pare D (2014) CGRP inhibits neurons of the bed nucleus of the stria terminalis: implications for the regulation of fear and anxiety. The Journal

of neuroscience : the official journal of the Society for Neuroscience 34:60-65.
Hammack SE, Mania I, Rainnie DG (2007) Differential expression of intrinsic membrane currents in defined cell types of the anterolateral bed nucleus of the stria terminalis. Journal of neurophysiology 98:638-656.
Han JS, Li W, Neugebauer V (2005) Critical role of calcitonin gene-related peptide 1 receptors in the amygdala in synaptic plasticity and pain behavior. The Journal of neuroscience : the official journal of the Society for Neuroscience 25:10717-10728.
Han JS, Adwanikar H, Li Z, Ji G, Neugebauer V (2010) Facilitation of synaptic transmission and pain responses by CGRP in the amygdala of normal rats. Molecular pain 6:10.
Harris GW (1948) Neural control of the pituitary gland. Physiological reviews 28:139-179.
Hazra R, Guo JD, Ryan SJ, Jasnow AM, Dabrowska J, Rainnie DG (2011) A transcriptomic analysis of type I-III neurons in the bed nucleus of the stria terminalis. Molecular and cellular neurosciences 46:699-709.
Hein L (2006) Adrenoceptors and signal transduction in neurons. Cell and tissue research 326:541-551.
Herman JP, Cullinan WE, Watson SJ (1994) Involvement of the bed nucleus of the stria terminalis in tonic regulation of paraventricular hypothalamic CRH and AVP mRNA expression. Journal of neuroendocrinology 6:433-442.
Herman JP, Figueiredo H, Mueller NK, Ulrich-Lai Y, Ostrander MM, Choi DC, Cullinan WE (2003) Central mechanisms of stress integration: hierarchical circuitry controlling hypothalamo-pituitary-adrenocortical responsiveness. Frontiers in neuroendocrinology 24:151-180.
Highfield D, Yap J, Grimm JW, Shalev U, Shaham Y (2001) Repeated lofexidine treatment attenuates stress-induced, but not drug cues-induced reinstatement of a heroin-cocaine mixture (speedball) seeking in rats. Neuropsychopharmacology : official publication of the American College of Neuropsychopharmacology 25:320-331.
Hu HJ, Carrasquillo Y, Karim F, Jung WE, Nerbonne JM, Schwarz TL, Gereau RWt (2006) The kv4.2 potassium channel subunit is required for pain plasticity. Neuron 50:89-100.
Hurley KM, Herbert H, Moga MM, Saper CB (1991) Efferent projections of the infralimbic cortex of the rat. The Journal of comparative neurology 308:249-276.
Jennings JH, Sparta DR, Stamatakis AM, Ung RL, Pleil KE, Kash TL, Stuber GD (2013) Distinct extended amygdala circuits for divergent motivational states. Nature 496:224-228.
Jobes ML, Ghitza UE, Epstein DH, Phillips KA, Heishman SJ, Preston KL (2011) Clonidine blocks stress-induced craving in cocaine users. Psychopharmacology 218:83-88.
Kash TL, Winder DG (2006) Neuropeptide Y and corticotropin-releasing factor bi-directionally modulate inhibitory synaptic transmission in the bed nucleus of the stria terminalis. Neuropharmacology 51:1013-1022.

Kaur S, Pedersen NP, Yokota S, Hur EE, Fuller PM, Lazarus M, Chamberlin NL, Saper CB (2013) Glutamatergic signaling from the parabrachial nucleus plays a critical role in hypercapnic arousal. The Journal of neuroscience : the official journal of the Society for Neuroscience 33:7627-7640.

Krawczyk M, Georges F, Sharma R, Mason X, Berthet A, Bezard E, Dumont EC (2011) Double-dissociation of the catecholaminergic modulation of synaptic transmission in the oval bed nucleus of the stria terminalis. Journal of neurophysiology 105:145-153.

Kudo T, Konno K, Uchigashima M, Yanagawa Y, Sora I, Minami M, Watanabe M (2014) GABAergic neurons in the ventral tegmental area receive dual GABA/enkephalin-mediated inhibitory inputs from the bed nucleus of the stria terminalis. The European journal of neuroscience 39:1796-1809.

Kudo T, Uchigashima M, Miyazaki T, Konno K, Yamasaki M, Yanagawa Y, Minami M, Watanabe M (2012) Three types of neurochemical projection from the bed nucleus of the stria terminalis to the ventral tegmental area in adult mice. The Journal of neuroscience : the official journal of the Society for Neuroscience 32:18035-18046.

Le AD, Funk D, Juzytsch W, Coen K, Navarre BM, Cifani C, Shaham Y (2011) Effect of prazosin and guanfacine on stress-induced reinstatement of alcohol and food seeking in rats. Psychopharmacology 218:89-99.

Lebow M, Neufeld-Cohen A, Kuperman Y, Tsoory M, Gil S, Chen A (2012) Susceptibility to PTSD-like behavior is mediated by corticotropin-releasing factor receptor type 2 levels in the bed nucleus of the stria terminalis. The Journal of neuroscience : the official journal of the Society for Neuroscience 32:6906-6916.

Lee A, Rosin DL, Van Bockstaele EJ (1998) alpha2A-adrenergic receptors in the rat nucleus locus coeruleus: subcellular localization in catecholaminergic dendrites, astrocytes, and presynaptic axon terminals. Brain research 795:157-169.

Leri F, Flores J, Rodaros D, Stewart J (2002) Blockade of stress-induced but not cocaine-induced reinstatement by infusion of noradrenergic antagonists into the bed nucleus of the stria terminalis or the central nucleus of the amygdala. The Journal of neuroscience : the official journal of the Society for Neuroscience 22:5713-5718.

Lu R, Li Y, Zhang Y, Chen Y, Shields AD, Winder DG, Angelotti T, Jiao K, Limbird LE, Zhou Y, Wang Q (2009) Epitope-tagged receptor knock-in mice reveal that differential desensitization of alpha2-adrenergic responses is because of ligand-selective internalization. The Journal of biological chemistry 284:13233-13243.

Ma S, Morilak DA (2005) Norepinephrine release in medial amygdala facilitates activation of the hypothalamic-pituitary-adrenal axis in response to acute immobilisation stress. Journal of neuroendocrinology 17:22-28.

Mantsch JR, Weyer A, Vranjkovic O, Beyer CE, Baker DA, Caretta H (2010) Involvement of noradrenergic neurotransmission in the stress- but not cocaine-induced reinstatement of extinguished cocaine-induced conditioned place preference in mice: role for beta-2 adrenergic receptors.

Neuropsychopharmacology : official publication of the American College of Neuropsychopharmacology 35:2165-2178.
Mathews PJ, Lee KH, Peng Z, Houser CR, Otis TS (2012) Effects of climbing fiber driven inhibition on Purkinje neuron spiking. The Journal of neuroscience : the official journal of the Society for Neuroscience 32:17988-17997.
McCoy ES, Taylor-Blake B, Street SE, Pribisko AL, Zheng J, Zylka MJ (2013) Peptidergic CGRPalpha primary sensory neurons encode heat and itch and tonically suppress sensitivity to cold. Neuron 78:138-151.
McDonald AJ, Shammah-Lagnado SJ, Shi C, Davis M (1999) Cortical afferents to the extended amygdala. Annals of the New York Academy of Sciences 877:309-338.
McElligott ZA, Winder DG (2008) Alpha1-adrenergic receptor-induced heterosynaptic long-term depression in the bed nucleus of the stria terminalis is disrupted in mouse models of affective disorders. Neuropsychopharmacology : official publication of the American College of Neuropsychopharmacology 33:2313-2323.
McElligott ZA, Klug JR, Nobis WP, Patel S, Grueter BA, Kash TL, Winder DG (2010) Distinct forms of Gq-receptor-dependent plasticity of excitatory transmission in the BNST are differentially affected by stress. Proceedings of the National Academy of Sciences of the United States of America 107:2271-2276.
Milner TA, Lee A, Aicher SA, Rosin DL (1998) Hippocampal alpha2a-adrenergic receptors are located predominantly presynaptically but are also found postsynaptically and in selective astrocytes. The Journal of comparative neurology 395:310-327.
Milner TA, Rosin DL, Lee A, Aicher SA (1999) Alpha2A-adrenergic receptors are primarily presynaptic heteroreceptors in the C1 area of the rat rostral ventrolateral medulla. Brain research 821:200-211.
Muly EC, Maddox M, Smith Y (2003) Distribution of mGluR1alpha and mGluR5 immunolabeling in primate prefrontal cortex. The Journal of comparative neurology 467:521-535.
Mungarndee SS, Lundy RF, Jr., Norgren R (2006) Central gustatory lesions and learned taste aversions: unconditioned stimuli. Physiology & behavior 87:542-551.
Niu JG, Yokota S, Tsumori T, Qin Y, Yasui Y (2010) Glutamatergic lateral parabrachial neurons innervate orexin-containing hypothalamic neurons in the rat. Brain research 1358:110-122.
Nobis WP, Kash TL, Silberman Y, Winder DG (2011) beta-Adrenergic receptors enhance excitatory transmission in the bed nucleus of the stria terminalis through a corticotrophin-releasing factor receptor-dependent and cocaine-regulated mechanism. Biological psychiatry 69:1083-1090.
Olsen CM, Winder DG (2010) Operant sensation seeking in the mouse. Journal of visualized experiments : JoVE.

Olson VG, Heusner CL, Bland RJ, During MJ, Weinshenker D, Palmiter RD (2006) Role of noradrenergic signaling by the nucleus tractus solitarius in mediating opiate reward. Science 311:1017-1020.
Onur OA, Walter H, Schlaepfer TE, Rehme AK, Schmidt C, Keysers C, Maier W, Hurlemann R (2009) Noradrenergic enhancement of amygdala responses to fear. Social cognitive and affective neuroscience 4:119-126.
Pacak K, McCarty R, Palkovits M, Kopin IJ, Goldstein DS (1995) Effects of immobilization on in vivo release of norepinephrine in the bed nucleus of the stria terminalis in conscious rats. Brain research 688:242-246.
Park J, Kile BM, Wightman RM (2009) In vivo voltammetric monitoring of norepinephrine release in the rat ventral bed nucleus of the stria terminalis and anteroventral thalamic nucleus. The European journal of neuroscience 30:2121-2133.
Park J, Wheeler RA, Fontillas K, Keithley RB, Carelli RM, Wightman RM (2012) Catecholamines in the bed nucleus of the stria terminalis reciprocally respond to reward and aversion. Biological psychiatry 71:327-334.
Phelix CF, Liposits Z, Paull WK (1992) Monoamine innervation of bed nucleus of stria terminalis: an electron microscopic investigation. Brain research bulletin 28:949-965.
Poulin JF, Arbour D, Laforest S, Drolet G (2009) Neuroanatomical characterization of endogenous opioids in the bed nucleus of the stria terminalis. Progress in neuro-psychopharmacology & biological psychiatry 33:1356-1365.
Rainbow TC, Parsons B, Wieczorek CM (1984) Quantitative autoradiography of [3H]hemicholinium-3 binding sites in rat brain. European journal of pharmacology 102:195-196.
Rainnie DG, Hazra R, Dabrowska J, Guo JD, Li CC, Dewitt S, Muly EC (2014) Distribution and functional expression of Kv4 family alpha subunits and associated KChIP beta subunits in the bed nucleus of the stria terminalis. The Journal of comparative neurology 522:609-625.
Ricardo JA, Koh ET (1978) Anatomical evidence of direct projections from the nucleus of the solitary tract to the hypothalamus, amygdala, and other forebrain structures in the rat. Brain research 153:1-26.
Rosenkranz JA, Buffalari DM, Grace AA (2006) Opposing influence of basolateral amygdala and footshock stimulation on neurons of the central amygdala. Biological psychiatry 59:801-811.
Sallee FR, Eaton K (2010) Guanfacine extended-release for attention-deficit/hyperactivity disorder (ADHD). Expert opinion on pharmacotherapy 11:2549-2556.
Saper CB, Loewy AD (1980) Efferent connections of the parabrachial nucleus in the rat. Brain research 197:291-317.
Savchenko VL, Boughter JD, Jr. (2011) Regulation of neuronal activation by Alpha2A adrenergic receptor agonist. Neurotoxicity research 20:226-239.
Sawada S, Yamamoto C (1981) Postsynaptic inhibitory actions of catecholamines and opioid peptides in the bed nucleus of the stria terminalis. Experimental brain research 41:264-270.

Scheinin M, Lomasney JW, Hayden-Hixson DM, Schambra UB, Caron MG, Lefkowitz RJ, Fremeau RT, Jr. (1994) Distribution of alpha 2-adrenergic receptor subtype gene expression in rat brain. Brain research Molecular brain research 21:133-149.

Shaham Y, Highfield D, Delfs J, Leung S, Stewart J (2000) Clonidine blocks stress-induced reinstatement of heroin seeking in rats: an effect independent of locus coeruleus noradrenergic neurons. The European journal of neuroscience 12:292-302.

Shammah-Lagnado SJ, Beltramino CA, McDonald AJ, Miselis RR, Yang M, de Olmos J, Heimer L, Alheid GF (2000) Supracapsular bed nucleus of the stria terminalis contains central and medial extended amygdala elements: evidence from anterograde and retrograde tracing experiments in the rat. The Journal of comparative neurology 422:533-555.

Shields AD, Wang Q, Winder DG (2009) alpha2A-adrenergic receptors heterosynaptically regulate glutamatergic transmission in the bed nucleus of the stria terminalis. Neuroscience 163:339-351.

Shimada S, Inagaki S, Kubota Y, Kito S, Funaki H, Takagi H (1989) Light and electron microscopic studies of calcitonin gene-related peptide-like immunoreactive terminals in the central nucleus of the amygdala and the bed nucleus of the stria terminalis of the rat. Experimental brain research 77:217-220.

Shimada S, Shiosaka S, Emson PC, Hillyard CJ, Girgis S, MacIntyre I, Tohyama M (1985) Calcitonin gene-related peptidergic projection from the parabrachial area to the forebrain and diencephalon in the rat: an immunohistochemical analysis. Neuroscience 16:607-616.

Shin JW, Geerling JC, Loewy AD (2008) Inputs to the ventrolateral bed nucleus of the stria terminalis. The Journal of comparative neurology 511:628-657.

Silberman Y, Winder DG (2013) Corticotropin releasing factor and catecholamines enhance glutamatergic neurotransmission in the lateral subdivision of the central amygdala. Neuropharmacology 70:316-323.

Silberman Y, Matthews RT, Winder DG (2013) A corticotropin releasing factor pathway for ethanol regulation of the ventral tegmental area in the bed nucleus of the stria terminalis. The Journal of neuroscience : the official journal of the Society for Neuroscience 33:950-960.

Sinha R, Catapano D, O'Malley S (1999) Stress-induced craving and stress response in cocaine dependent individuals. Psychopharmacology 142:343-351.

Sinha R, Shaham Y, Heilig M (2011) Translational and reverse translational research on the role of stress in drug craving and relapse. Psychopharmacology 218:69-82.

Sinha R, Kimmerling A, Doebrick C, Kosten TR (2007) Effects of lofexidine on stress-induced and cue-induced opioid craving and opioid abstinence rates: preliminary findings. Psychopharmacology 190:569-574.

Sink KS, Davis M, Walker DL (2013a) CGRP antagonist infused into the bed nucleus of the stria terminalis impairs the acquisition and expression of context but not discretely cued fear. Learning & memory 20:730-739.

Sink KS, Walker DL, Yang Y, Davis M (2011) Calcitonin gene-related peptide in the bed nucleus of the stria terminalis produces an anxiety-like pattern of behavior and increases neural activation in anxiety-related structures. The Journal of neuroscience : the official journal of the Society for Neuroscience 31:1802-1810.

Sink KS, Chung A, Ressler KJ, Davis M, Walker DL (2013b) Anxiogenic effects of CGRP within the BNST may be mediated by CRF acting at BNST CRFR1 receptors. Behavioural brain research 243:286-293.

Sweatt JD (2004) Mitogen-activated protein kinases in synaptic plasticity and memory. Current opinion in neurobiology 14:311-317.

Vaughn LK, Mantsch JR, Vranjkovic O, Stroh G, Lacourt M, Kreutter M, Hillard CJ (2012) Cannabinoid receptor involvement in stress-induced cocaine reinstatement: potential interaction with noradrenergic pathways. Neuroscience 204:117-124.

Vranjkovic O, Hang S, Baker DA, Mantsch JR (2012) beta-adrenergic receptor mediation of stress-induced reinstatement of extinguished cocaine-induced conditioned place preference in mice: roles for beta1 and beta2 adrenergic receptors. The Journal of pharmacology and experimental therapeutics 342:541-551.

Wang M, Ramos BP, Paspalas CD, Shu Y, Simen A, Duque A, Vijayraghavan S, Brennan A, Dudley A, Nou E, Mazer JA, McCormick DA, Arnsten AF (2007) Alpha2A-adrenoceptors strengthen working memory networks by inhibiting cAMP-HCN channel signaling in prefrontal cortex. Cell 129:397-410.

Wang X, Cen X, Lu L (2001) Noradrenaline in the bed nucleus of the stria terminalis is critical for stress-induced reactivation of morphine-conditioned place preference in rats. European journal of pharmacology 432:153-161.

Weiss F, Koob GF (2001) Drug addiction: functional neurotoxicity of the brain reward systems. Neurotoxicity research 3:145-156.

Weitlauf C, Egli RE, Grueter BA, Winder DG (2004) High-frequency stimulation induces ethanol-sensitive long-term potentiation at glutamatergic synapses in the dorsolateral bed nucleus of the stria terminalis. The Journal of neuroscience : the official journal of the Society for Neuroscience 24:5741-5747.

Weller KL, Smith DA (1982) Afferent connections to the bed nucleus of the stria terminalis. Brain research 232:255-270.

Woulfe JM, Hrycyshyn AW, Flumerfelt BA (1988) Collateral axonal projections from the A1 noradrenergic cell group to the paraventricular nucleus and bed nucleus of the stria terminalis in the rat. Experimental neurology 102:121-124.

Yuan LL, Adams JP, Swank M, Sweatt JD, Johnston D (2002) Protein kinase modulation of dendritic K+ channels in hippocampus involves a mitogen-activated protein kinase pathway. The Journal of neuroscience : the official journal of the Society for Neuroscience 22:4860-4868.